2019

Application of Quality by Design and Process Analytical Technology towards Hot-Melt Extrusion Processes

Priyanka Thipsay
University of Mississippi

APPLICATION OF QUALITY BY DESIGN AND PROCESS ANALYTICAL TECHNOLOGY TOWARDS HOT-MELT EXTRUSION PROCESSES

A Dissertation presented in partial fulfillment of requirements for the Doctoral of Philosophy in Pharmaceutical Sciences with an emphasis in Pharmaceutics and Drug Delivery
The University of Mississippi

PRIYANKA THIPSAY

May 2019

ABSTRACT

In the area of Quality-by-Design (QbD), the determination of process parameters or quality attributes of a product using sufficient process analytical technology (PAT) is a crucial for the establishment of continuous processes as a standard pharmaceutical technology, such as hot-melt extrusion. For the purpose of the study, three different formulations were developed and design space was evaluated with the aid of PAT, while a design of experiment (DoE) was implemented to assess the effect of the process critical parameters and to identify the critical quality attributes (CQA) of the extrusion processing.

Solid self-emulsifying drug delivery systems were developed instead of a conventional liquid system. Solid surfactants was chosen to emulsify lipids with different HLB properties. Type of surfactant, type of lipid, Lipid/surfactant L/S ratio, feed rate, screw speed and screw configuration, were the formulation and process parameters evaluated. Solid self-emulsifying drug delivery systems were successfully developed on the hot-melt extruder for the first time which is a continuous processing technology.

Blends of theophylline, (HMPC K4M, Affinisol 100LV) were processed using a twin screw extruder to investigate the effect of temperature and screw configuration on the various granule properties. Particle size distribution was measured using Parsum probe in-line particle size analysis. The effect of the critical process parameters to optimize the conditions or design space to achieve the tablet with greater sustained release properties. Affinisol 100LV was proven to have better sustained release properties and was robust with respect to the change in process parameters.

Continuous salt preparation was achieved of a poorly water soluble compound Indomethacin with a highly water soluble co-former tromethamine. Design of experiments was used to evaluate the effect of feed rate, screw speed, temperature on the salt properties. The effect of the different process parameters on the extent of formation of the crystalline salt was determined using in-line FTNIR analysis. Furthermore, the integration of the DoE experiments demonstrated that

temperature and screw configuration, had a significant effect on the quality attributes. This QbD approach was successfully employed as a paradigm for the development of pharmaceutical formulations via HME processing.

DEDICATION

This work is dedicated to my parents, sister, husband and all my teachers who helped me grow in my life personally and professionally

ACKNOWLEDGEMENT

I would like to express my deep and sincere gratitude to my advisor, Dr. Michael Repka for his support, patience and encouragement throughout my research work. His belief in me and support at all the time during my research helped me achieve greater understanding in research. I am ever grateful for all his kind support.

I would like to take this opportunity to express my sincere thanks to Dr. S.N. Murthy, Dr. Soumyajit Majumdar, and Dr. Samir Ross for accepting my request, spending their valuable time and providing valuable suggestions during my prospectus that I believe have improved my overall work. It was kind of Ms. Deborah King for helping me with all the departmental procedures and providing all the supplies required on time.

I owe a great thanks to my lab members (Dr. Manjeet Pimparade, Dr. Hemlata Patil, Joe Morott, Dr. Ajinkya Bhagurkar) for helping me in performing my research successfully. I would also like to thank my current labmates for all their help and support and all the graduate students of pharmaceutics and drug delivery department for their support in various projects.

I would like to acknowledge the help of Dr. Ross and Herman He for their support in interpretation of NMR and performing FT-NIR studies respectively.

I owe my greatest thanks to my mother (Prachi Thipsay) and father (Pradeep Thipsay) for all the support and encouragement. A special thanks to my sister (Prajakta Thipsay), my husband (Saurabh Vispute) for their loving support. I sincerely acknowledge the support from department

of Pharmaceutics, Pii Center of Pharmaceutical Technology, Graduate School and other funding sources which aided strongly to carry out my Ph.D. work.

TABLE OF CONTENTS

LIST OF TABLES

LIST OF FIGURES

I. CHAPTER

INTRODUCTION

With the advent of combinatorial chemistry and high-throughput screening, the drug discovery pipelines have witnessed extremely insoluble molecules (Lee et al., 2017). This results in low dissolution rate and variations in the bioavailability when administered orally. Many formulation technologies such as salt formation, cocrystallization, lipid based delivery, solid dispersion, particle size reduction, have been used to enhance dissolution rate and oral bioavailability of such compounds. However, there are limitations associated with respect to each of the methods. For example in lipid based drug delivery system, there is critical balance required to be achieved to attain complete drug solubility in formulation as well as maintain the drug in solubilized state during dilution while dissolution in gastro-intestinal tract. Also there is a need for more reliable rapid characterization techniques to enable early phase screening. In addition, the amount of drug delivered in lipid based drug delivery system is limited by the solubility of the drug in that lipid, surfactant system. With respect to salt or co-crystal formulations there is a tendency for the individual components to be dissociated into their counter-parts (Nie et al., 2016; Qiao, Wang, Schlindwein, Davies, & Li, 2013). Amorphous solid dispersion has been of increasing importance in the recent years. For early development, formulation of amorphous solid dispersion is performed using spray drying, this results in requirement of large quantity of organic solvent for dissolution of drug and carrier. The need for solvent handling during manufacturing is increased for such

applications. Drug precipitation due to instability and re-crystallization from the polymer matrix is a major hurdle in the development of stable amorphous solid dispersions. (Serajuddin, 1999).

In addition to the techniques mentioned above, salt formation of acidic and basic drugs is most common strategy for enhancement of dissolution and widely used in the pharmaceutical industry. Salt formation is the primary method used to enhance the dissolution rate and oral bioavailability. When salt formation is not a feasible or does not provide desired solubility then other techniques for bioavailability enhancement are applied. Approximately, 50% of marketed drugs are formulated as salt forms of ionizable active pharmaceutical ingredients (APIs) having acidic or basic moieties (Berge, Bighley, & Monkhouse, 1977; Pudipeddi, Serajuddin, Grant, & Stahl, 2002).

There has also been an interest in forming Formulation of cocrystals of APIs, has also gained significant attention in the past decade, especially when the salt formation is not feasible. However, cocrystals do not form for most APIs. As salts could be considered as new APIs and thus have the advantage of patent protection, hence are considered more valuable than cocrystals in development of pharmaceuticals (Rajput, 2014; Stephenson, Aburub, & Woods, 2011).

In this study, the limitations of the formulations such as self-emulsifying drug delivery system, sustained release tablets, salt formation by solvent driven process has been addressed. Firstly, Attempts were made to develop a solid self-emulsifying drug delivery system which eliminates the issues of a liquid in capsule type of a system. Secondly, with the sustained release tablet formulations, it was proposed to develop a high drug load of melt granules which aids in suitable lowering of tablet weight and provide sustained release for upto 18 hours. In addition, salt formation of a poorly water soluble API was carried out in a continuous processing technique. All

the formulations were developed on a twin screw extruder which eliminates the need of using organic solvent for processing.

In the current research, Quality by design (QbD) and the elements of QbD are applied and its implementation in pharmaceutics field is highlighed, including design of experiment, and process analytical technology (PAT), are introduced for development of three different formulations. Moreover, applications of QbD in various pharmaceutical related unit operations are summarized and presented. A quality-by-design (QbD) approach was used to optimize the development of three different formulations such as solid self-emulsifying drug delivery system, sustained-release tablet and in-situ salt formation of poorly water soluble API manufactured by hot-melt extrusion (HME). For the purpose of the study, off-line FTIR chemical imaging, in-line particle size analysis, in-line near-infrared (NIR) spectroscopy as a process analytical technology (PAT) was explored while a design of experiment (DoE) was implemented to assess the effect of the process critical parameters and to identify the critical quality attributes (CQA) of the extrusion processing.

II. CHAPTER

Applying design of experiments for investigating the impact of formulation and processing parameters on solid self-emulsifying drug delivery systems prepared via hot-melt extrusion technology

1. Introduction

Lipid-based formulations (LBF) have emerged as a useful formulation strategy to increase the bioavailability of poorly water soluble drugs. Around 40% of new chemical entities present solubility and bioavailability-related problems.

Unfortunately development of lipid-based products has been slow, which is probably due to the perceived problems of physical and chemical instability, as well as unpredictable bioavailability and in vivo performance of these dosage forms.

Literature presents techniques like solid dispersion, surface modification, cyclodextrin complexation,and micellar solutions that have been developed to improve aqueous solubility of poorly water-soluble drugs. One such technique used to improve the dispersion and enhance solubility of lipophilic drugs is nano-emulsification (Saxena & Hussain, 2012). Nano-emulsions (NEs) are clear, stable, isotropic mixtures of oil, water, surfactants and co surfactants. NEs provide wide application in the area of drug delivery. Nanoemulsion have gained importance as a platform technology is because of their high solubilization capacity for various drugs, nanosize, PGP inhibitory effects, stability over wide range of pH and ionic media

(Gupta, Hwang, Doshi, & Mitragotri, 2013; Sha, Yan, Wu, Li, & Fang, 2005). This results in reproducible plasma concentration profiles and improved bioavailability of various drugs. Delivering the NE in the form of pre-concentrates or self-nanoemulsifying drug delivery systems (SNEDDS) in hard or soft gelatin capsules is the traditional approach. There is a tendency for the surfactants, co-surfactants and oils present in the NE system to interact with the capsule shell and affect its integrity (Kim, Kang, Oh, Yong, & Choi, 2012). Hence formulation of emulsions as free flowing powders or granules is a better approach. These dry powders can be processed by solvent evaporation, spray drying and lyophilization. However, the disadvantage with these process is that they are batch processes and involve use of organic solvents. When administered orally these dry emulsion powders or solid emulsions will get converted back to the emulsions in gastric fluid. Solid nano-emulsions (SMEs) can be formulated by adsorption of SNEDDS on one or more carriers (Gumaste et al., 2013). Solid carrier provides the surface area for adsorption of the oil and surfactant droplets and also contributes the bulk to the SMEs. Due to the advantage of solid SMEDDS ability to be blended with excipients or converted into tablets, pellets and filled in capsules they are preferred choice (Balakrishnan et al., 2009; Bari, Doijad, More, & Disouza, 2011). The rational design of lipid formulations requires a better understanding of formulation and manufacturing variables that may affect the quality of the products. Meeting specific objectives of the product and process performance characteristics have to be designed scientifically and not merely empirically derived from performance of test batches. The rational co-incides with the 'quality-by-design' principle that has been promoted by the FDA. Ideally, from the selection of drug substance, polymorphic form, and excipients, to the design, manufacturing and controls of the produc, the approaches can be applied to all phases of pharmaceutical development.

This research work has focused on evaluating the feasibility of formulating solid SNEDDS using hot melt extrusion technology and focus on the details of the formulation and manufacturing variables of solid self-nanoemulsifying drug delivery system (Bahloul, Lassoued, & Sfar, 2014). Previous research has demonstrated the use of conventional formulation techniques of SNEDDS which has inherent shortcomings such as batch size manufacturing, non-uniformity of content, liquid form of SNEDDS, stability, leakage from capsule shell (Dixit & Nagarsenker, 2010) (Cole, Cadé, & Benameur, 2008). The present work has addressed these challenges by careful selection of solid surfactants which act as the emulsifier as well as solid carrier thereby negating additional burden of polymer as carrier. Also a systematic study (response surface model) has been designed to evaluate the effect of formulation variables and process variables of hot-melt extrusion processing.

2. Materials

Fenofibrate was purchased from Ria International (East Hanover, NJ, USA) chemicals and was used as model BCS class II drug. Different lipids and surfactants such as Labrafac®PG, Capryo®90, Labrasol®, Gellucire®44/14 were generously gifted by Gattefosse (USA) and Lutrol®F68, Lutrol®F127, Kolliphor®TPGS by BASF chemicals (New Jersey, USA). HPLC-grade organic solvents such as methanol was obtained from Fisher Scientific (USA).

3. Methods

3.1 Screening of lipids and surfactants

3.1.1 Solubility of fenofibrate in lipid and surfactant

Lipids were selected from different chemical class with wide range of HLB values (Figure 1,2). Excess fenofibrate was weighed and added to 5ml of lipids and 500mg surfactants. Solubility

studies were conducted by placing an excess amount of fenofibrate in scintillation vials containing approximately 5–7 g of vehicles independently. The mixture was then shaken in a water bath at 25°C for 24 h. The shaking time of 24 h was set because preliminary experiments showed that the solutions reached equilibrium within 12 h and there was no further change in concentration when shaking was continued for 24 h and longer. The supernatant was withdrawn, filtered through 0.45-μm polypropylene membrane filter and diluted with acetonitrile for HPLC analysis. A Waters High performance liquid chromatography (HPLC) system equipped with a Water 600 binary pump, Waters 2489 UV/detector, and Waters 717 plus auto-sampler (Waters Technologies Corporation, Milford, USA) and a Phenomenex Luna 5um C18 (2) 250 x 4.6 mm column (Torrance, CA, USA) were used at a detection wavelength of 288 nm. The mobile phase consisted of acetonitrile and water at a ratio of 80:20% (v/v). The mobile phase flow rate was maintained at 1.0mL/min. and an injection volume of was 10 μL was used HPLC data was analyzed using Empower V. software (Milford, MA, USA)(Patel, Li, & Serajuddin, 2016; Shah & Serajuddin, 2012).

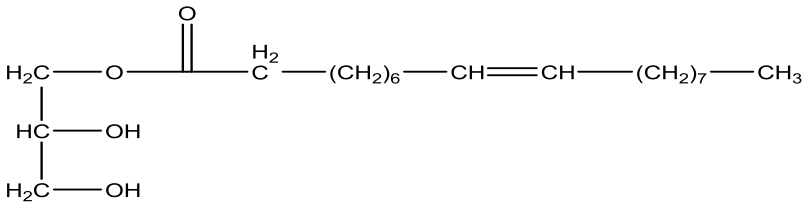

Labrafil®M1944 (HLB 9) Oleoyl polyoxyl-6-glycerides

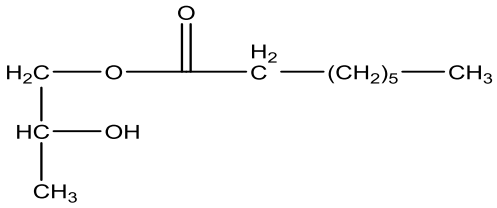

Capryol®90 (HLB 5) Propylene glycol monocaprylate

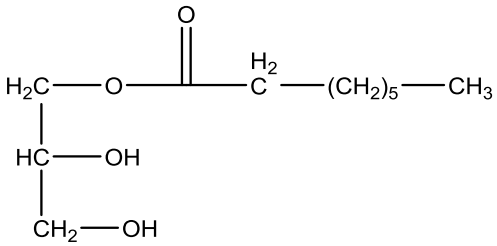

Labrasol® (HLB 12) Caprylocaproyl polyoxyl-8-glycerides

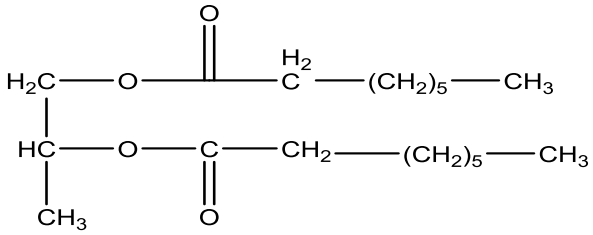

Labrafac®PG (HLB 1) Propylene glycol dicaprylate

Figure 1: Structure of Lipids used in the formulations

Surfactant name	**Surfactant chemical name**	**HLB**
Lutrol F68	Poloxamer 188 Polyoxyethylene-polyoxypropylene block copolymer (Ratio 80:27)	24
Lutrol F127	Poloxamer 407 Polyoxyethylene-polyoxypropylene block copolymer (Ratio 101:56)	18
Gellucire®44/14	Lauroyl polyoxyl-32 glycerides	11
Kolliphor®TPGS	(D-α- Tocopherol polyethylene glycol)	13

Figure 2: Surfactants used in the formulation

3.1.2 Dispersion study

Solid SNEDDS were evaluated for their ability to disperse into globules of size <200nm in suitable dissolution medium. Labrafac®PG (HLB 1) and Capryol®90(HLB 5) were chosen as the lipids due to higher solubility of fenofibrate in the lipids and Lutrol F68 and Lutrol F127 were selected as the solid surfactant system. Fenofibrate was loaded in the lipids upto 90% of its solubility in order to avoid precipitation due to saturation. Two different lipid:surfactant ratios were chosen of 50:50 and 60:40 to test the dispersion efficiency in Fasted state Simulated Gastric Fluid (FaSSGF).

4.1.3 In-vitro dissolution

The in-vitro dissolution of the both the ratios formulated with the lipids and surfactants were evaluated using USP type II apparatus in 250ml of simulated FaSSGF at 37°C. The formulations were incorporated into a dialysis bag and placing 5ml of media into the dialysis unit and clipped using dialysis bag sealer. Samples were withdrawn at 5, 15, 30, 60, 120mins.

3.2 Feasibility of preparation of solid SNEDDS

3.2.1 Preparation of solid SNEDDS by conventional technique- Melt sonication

Fenofibrate loaded solid SNEDDS were prepared conventionally by melt probe sonication technique. Liquid lipid such as Labrafac®PG, Capryol®90 were chosen as the desired lipid for the formulation. Two different solid surfactant such as Lutrol®F68 and Lutrol®F127 were selected for the formulation. Fenofibrate was pre-dissolved in the lipid upto 90% its solubility. The lipid and solid surfactant were mixed in different ratios of 50:50 and 60:40 respectively as shown in table 2 and 3. The drug loaded lipid solution was mixed with the solid surfactant and heated upto 70°C so that solid surfactants were completed melted. At this temperature the mixture was sonicated on an Ultrasonicator for 5mins.

3.2.2 Preparation of modified Labrafac®PG Solid SNEDDS

The previous mentioned formulation of Labrafac®PG formulation was modified where 50% of the total incorporated solid surfactant was replaced with Kolliphor®TPGS and Gellucire®44/14 as co-surfactants (Table 4).

3.2.3 Preparation of solid SNEDDS by hot melt extrusion

Solid self nano-emulsifying drug delivery (S-SNEDDS) systems of fenofibrate were formulated by twin screw extrusion process using Process 11, Thermo Fisher Scientific®. The solid surfactants were fed from the hopper, whereas the lipid was added from third zone of extruder. The extrusion was carried out at 100 rpm and 7% feed rate (1.9 g/min) (Table 6). The temperature of extrusion process was kept as 65°C (Zone1-4), 45°C (zone 5-6) and 30°C (zone 7-8). Initial temperature of operation assured complete melting of the solid surfactants, while gradual cooling towards the end was carried to avoid separation of surfactant and lipid matrix once the product exits the extruder. Two different screw configurations were evaluated for its effect on obtaining the desired product characteristics whose schematic representation is shown in Figure 3 (A) (B).

3.3 Design of experiments

A response surface (optimal) design was adopted to study the effect of critical process parameters and formulation variables on the product characteristics. Optimal design is one of the most commonly used designs of the experiment. They are the resolution five designs, so they can be used to study the main effects and interactions between variables to be investigated. The processing input variables studied were feed rate (4-8 g/min), screw speed (100- 200 rpm), screw configuration (impact of one kneading block v/s two) (Figure 3A and 8B); while the formulation variables were Ratio of Lipid to Surfactant (0.5-1 L/S ratio), type of lipid (HLB 5, 9, 12), type of surfactant used (HLB 18, 24). A total of 41 experimental trials with a response surface design were

constructed using design expert stat-ease software version 9 to study the six variables (Table 1). Multilinear regression analysis was performed to test the significance of the model and the factor coefficients. The experimental runs (formulations) were prepared in triplicate. The dependent variables were In-vitro dissolution (Y1), average particle size (Y3), poly-dispersity index (Y4).

The linear equation of the model is as follows:

$$Y = b0 + b1X1 + b2X2 + b3X3 + b4X4 + b5X5 + bnXn\ldots$$

where Y is the response, b0 is the constant, and b1,..bn is the coefficient of factor X1,…Xn.

Run No.	A: Feed rate g/min	B: Screw speed rpm	C: Ratio of L/S	D: Screw configuration	E: Type of lipid (L) HLB	F: Type of surfactant (S) HLB
1	5.11	115	0.68	1	5	24
2	6.02	200	0.85	1	5	24
3	8.00	100	0.80	1	5	24
4	5.40	169	0.96	1	5	24
5	6.61	110	0.50	1	5	18
6	5.60	166	0.72	1	5	18
7	8.00	176	0.50	1	9	24
8	8.00	176	1.00	1	9	24
9	5.40	100	0.96	1	9	24
10	5.11	100	0.68	1	9	24
11	4.00	200	0.50	1	9	18
12	7.32	145	0.50	1	9	18
13	7.73	100	0.96	1	9	18
14	4.00	121	0.50	1	12	24
15	8.00	200	0.64	1	12	24

16	5.60	174	0.72	1	12	24
17	4.00	156	0.80	1	12	24
18	6.25	200	0.58	1	12	18
19	6.02	121	0.85	1	12	24
20	4.00	165	1.00	1	12	18
21	8.00	200	0.78	1	12	18
22	6.00	100	0.95	1	12	18
23	4.75	183	1.00	2	5	24
24	8.00	133	1.00	2	5	24
25	4.00	200	1.00	2	5	18
26	4.88	100	0.50	2	5	18
27	6.48	200	0.51	2	5	18
28	4.00	200	0.50	2	5	18
29	8.00	183	1.00	2	5	24
30	7.98	117	0.53	2	9	24
31	4.00	200	0.50	2	9	24
32	8.00	154	0.50	2	9	24
33	4.55	145	1.00	2	9	18
34	5.51	200	1.00	2	9	18
35	4.00	145	0.62	2	9	18
36	8.00	100	0.88	2	9	18
37	4.22	100	0.50	2	12	24
38	6.25	198	0.58	2	12	24
39	7.14	145	0.63	2	12	18
40	4.00	150	0.79	2	12	18
41	8.00	100	0.99	2	12	18

Table 1: Response surface design of experiments (Design Expert®)

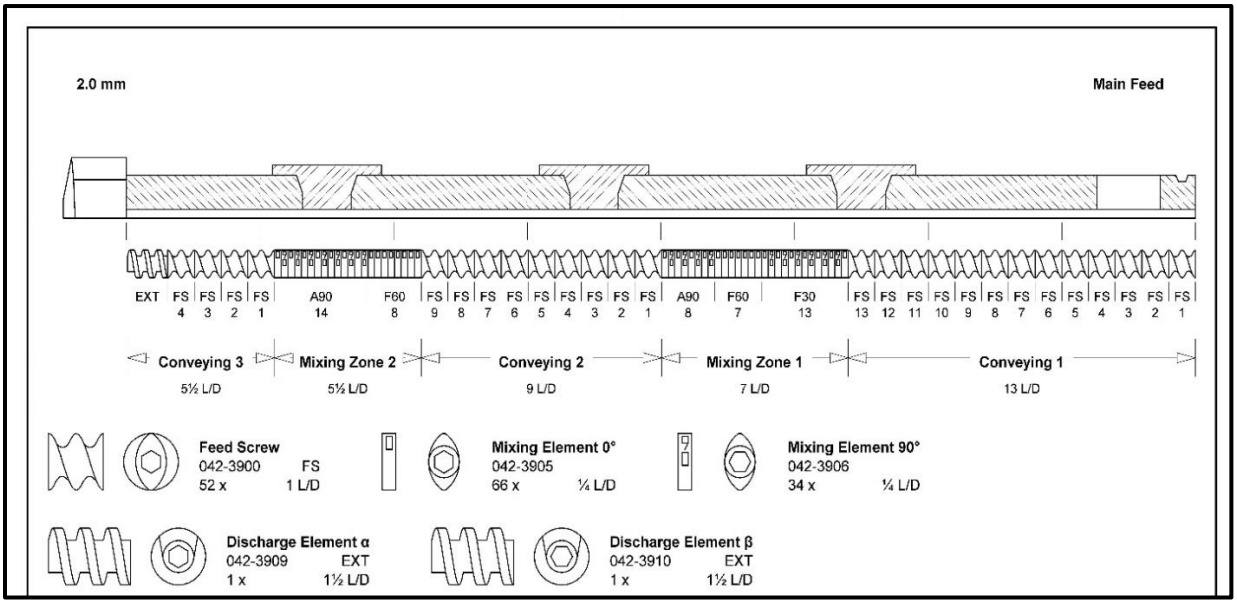

Figure 3 (A): Screw configuration 1 (2kneading blocks), 11mm twin screw extruder Thermo Scientific®

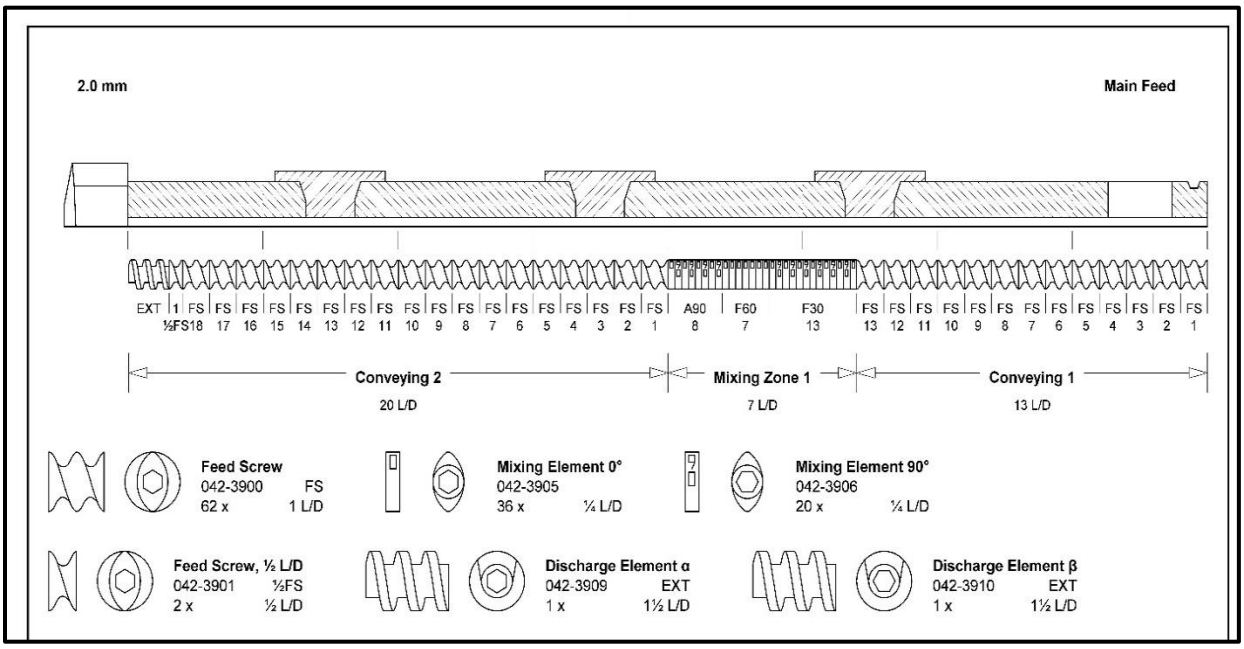

Figure 3 (B): Screw configuration 2 (1kneading block), 11mm twin screw extruder Thermo Scientific®

3.4 Characterization of conventional and hot-melt extruded formulations

The extruded formulations were compared to the conventionally prepared ones by melt sonication technique. The S-SNEDDS prepared were analyzed for percent drug dissolved in media by Dissolution testing using dialysis bag, physical state of drug in formulation by Differential Scanning Calorimetry, Content Uniformity by FTIR Chemical Imaging, Globule size of dispersed emulsion.

3.4.1 Differential Scanning Calorimetry

DSC studies were performed with a Perkin Elmer Diamond differential scanning calorimeter (DSC) equipped with Pyris software (Shelton, CT, USA). Samples were prepared by sealing 3-5 mg of pure API, physical mixtures, blank formulations, drug loaded extrudates in hermetically sealed aluminum pans and heated from the temperature range of 30°C to 100°C at the heating rate of 20°C/min under an inert nitrogen atmosphere at a flow rate of 20 mL/min.

3.4.2 Fourier transforms infrared spectroscopy (FTIR)

FTIR spectra of the API, lipids, surfactants and milled extrudates were recorded using an Agilent Cary 660 FTIR spectrophotometer (Santa Clara, CA, USA) to investigate any possible interactions between the drug, polymer and other excipients. The infrared images were produced by taking spectral derivatives of the obtained spectra and isolating spectral bands representative of fenofibrate alone**.** Images were taken to study the uniformity of distribution of fenofibrate in the formulation.

3.4.3 Content Uniformity

In addition to evaluating the content uniformity via chemical imaging, the content of fenofibrate in formulation was analyzed by assaying a measured quantity using HPLC reverse phase analysis. About 50mg of the formulations were weighed and dissolved in methanol to dissolve the API. The extracted methanolic solution was suitably diluted to be analyzed via reverse phase HPLC. The content uniformity was evaluated using Waters HPLC-UV system (Water Corporation) and a Luna 5µm C18 column at 285nm.

Content Uniformity ratio = Actual drug loading/ Expected drug loading.

When the content uniformity ratio was close to 1 implied that the actual and expected drug loading was similar. When content uniformity ratio was >1 it implied that the actual drug loading was higher than expected, whereas when it was <1 it implied that the actual drug loading was lesser than expected.

3.4.4 Dispersion testing and globule size analysis

To simulate the degree and efficiency of emulsification of lipids in GI fluids after oral administration of the solid systems developed, the dispersion test was conducted by using the USP apparatus II (paddle method; Distek Inc., NJ, USA) at 50 RPM and 37°C with 250 ml of simulated FaSSGF as the dispersion medium. Since the aqueous solubility of the drug fenofibrate was pH-independent and all lipids and solid systems were non-ionic, the medium did not affect the release of the drug. Since the solid dosage form after oral administration encounters an acidic environment in the stomach FaSSGF was chosen as the medium.

A volume of 250 ml was selected for the dispersion test to mimic the gastric fluid volume as per the Biopharmaceutical Classification System after oral administration of solid dosage unit.

Approximately 200mg of the formulation was directly added to the dispersion vessel using weighing boats. To evaluate the effect of drug loading, if any, on emulsification properties of solid systems, controls without drugs were also subjected to dispersion test. Thus, the dispersion test for a particular formulation was conducted six times, three with drug and three without drug. Both drug concentration and particle size of dispersion fluids were analyzed for formulations with drugs, while only particle sizes of oil globules were measured for drug-free systems. Aliquots from dispersion vessels were withdrawn at 5, 15, 30, 45, 60, 90, 120 min time points. Particle sizes were measured without any dilution. The mean particle size and polydispersity index (PDI) of the developed solid SNEDDS were determined by using Zetasizer Nano ZS (Malvern, USA). Dynamic light scattering technique was used to measure particle size. This technique measures the diffusion of particles moving under Brownian motion and converts this to size and a size distribution using the Stokes-Einstein relationship.

3.4.5 In-vitro dissolution

All the formulations (conventional and hot-melt extruded) were evaluated for the in-vitro drug dissolution profile. 100mg of formulation was weighed and filled into dialysis bag (MWCO 100,000 daltons, pore size 4nm). About 5ml of dissolution medium was added to the dialysis bag. The dialysis bag was placed in the dissolution medium containing FaSSGF. The dissolution testing was performed using type II dissolution apparatus. The use of dialysis method ensured that only fenofibrate solubilizing in the gastric fluid was analyzed and not the lipid micelle globules. The samples were taken at different time intervals of 5, 15, 30, 60, 120mins and analyzed for fenofibrate content using reverse phase HPLC.

4. Results and Discussion

4.1 Screening study to evaluate SNEDDS formation

4.1.1 Dispersion study

Solid SNEDDS were evaluated for their ability to disperse into globules of size <200nm. Labrafac® PG (HLB 1) and Capryol®90(HLB 5) were chosen as the lipids due to higher solubility of fenofibrate in the lipids (Table 2) and Lutrol®F68 and Lutrol®F127 were selected as the solid surfactant system. Fenofibrate was loaded in the lipids upto 90% of its solubility in order to avoid precipitation due to saturation. Two different lipid: surfactant ratios were chosen (50:50 and 60:40) to test the dispersion efficiency.

Lipid and surfactant	HLB	Solubility (mg/ml)
Capryol®90	5	112.93
Labrafac®PG	1	94.34
Labrafil®M1944	9	57.2
Labrasol®	12	92.01
Lutrol ®F68	24	< 50 µg/ml
Lutrol ®F127	18	
Kolliphor® TPGS	13	
Gellucire® 44/14	11	

Table 2: Solubility data for fenofibrate in different lipids

All the evaluated ratios of the different lipid and surfactant (conventional) formulations were found to have particle size of <200nm. From Table 3, 4 it can be seen that Capryol®90 has particle size lesser than Labrafac®PG. Labrafac®PG has greater hydrophobic groups as compared to Capryol®

90, hence stabilizing the lipid micelle is a challenge. Due to this, certain co-surfactants such as Kolliphor®TPGS and Gellucire®44/14 with lower HLB compared to the existing Lutrol® surfactants. were added at a concentration of 50% of the initial surfactant which is depicted in Table 5. As seen in figure 4 the particle size of modified Labrafac®PG solid SNEDDS dispersed in the gastro intestinal fluids displayed smaller globule size than the original solid SNEDDS formulation. This can possibly be due to stabilization of the globule with additional hydrophobic chains of the co-surfactant. Kolliphor®TPGS provided the better stability to the formulation as compared to Gellucire®44/14.

Formulation	Lipid	Surfactant	(Ratio of lipid: surfactant)	Average particle size (nm)
L-1	Labrafac®PG	Lutrol® F68	(50:50)	150
L-2	Labrafac®PG	Lutrol® F68	(60:40)	161
L-3	Labrafac®PG	Lutrol® F127	(50:50)	186
L-4	Labrafac®PG	Lutrol® F127	(60:40)	174

Table 3: Dispersion test and particle size measurement of conventionally prepared SNEDDS of Capryol® 90

Formulation	Lipid	Surfactant	(Ratio of lipid: surfactant)	Average particle size (nm)
C-1	Capryol®90	Lutrol® F68	(50:50)	108
C-2	Capryol®90	Lutrol® F68	(60:40)	102
C-3	Capryol®90	Lutrol® F127	(50:50)	147
C-4	Capryol®90	Lutrol® F127	(60:40)	118

Table 4: Dispersion test and particle size measurement on conventionally prepared SNEDDS of Labrafac®PG

Formulation	Lipid (50%)	Co-Surfactant (25%)	Surfactant (25%)
SNEDDS-1	Labrafac®PG	Kolliphor®TPGS	Lutrol®F68
SNEDDS-2	Labrafac®PG	Gellucire®44/14	Lutrol®F68

Table 5: Labrafac®PG SNEDDS modified formulation with co-surfactant

Conventional Formulation	HME formulation
SNEDDS- 1	HME- 1
SNEDDS- 2	HME- 2
C1	HME- 3
C2	HME- 4
C3	HME- 5
C4	HME- 6

Table 6: Conventional formulation and their respective hot-melt extruded formulation denotation

The particle size of hot-melt extruded modified Labrafac®PG formulations (Figure 5) compared to the conventional formulations was significantly lesser due to increased shear intensive mixing that could be achieved during extrusion and better molecular miscibility between the solid surfactants, co-surfactants and lipids. Also better content uniformity of the hot melt extruded formulations was one of the reasons. This was also shown with respect to Capryol®90 solid SNEDDS extruded formulations (Figure 6).

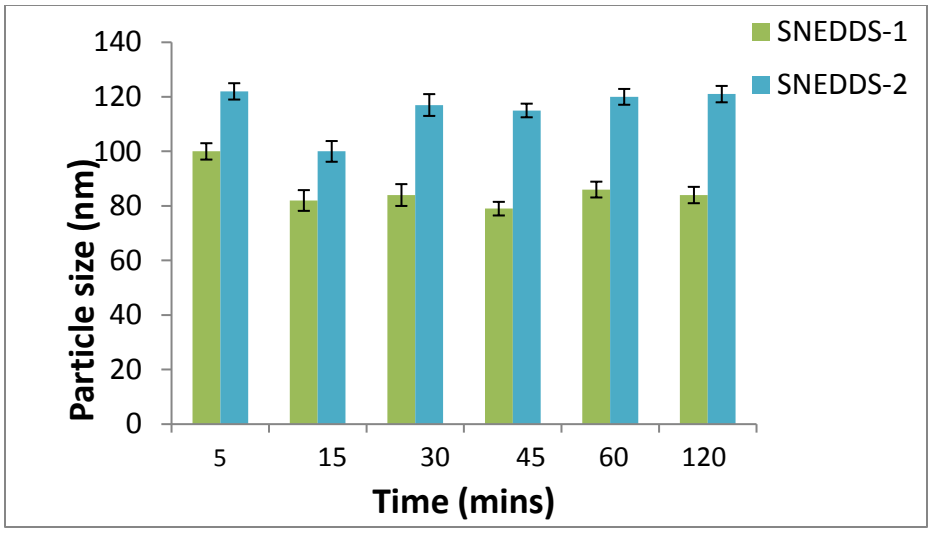

Figure 4: Particle size of modified Labrafac®PG SNEDDS (conventional method)

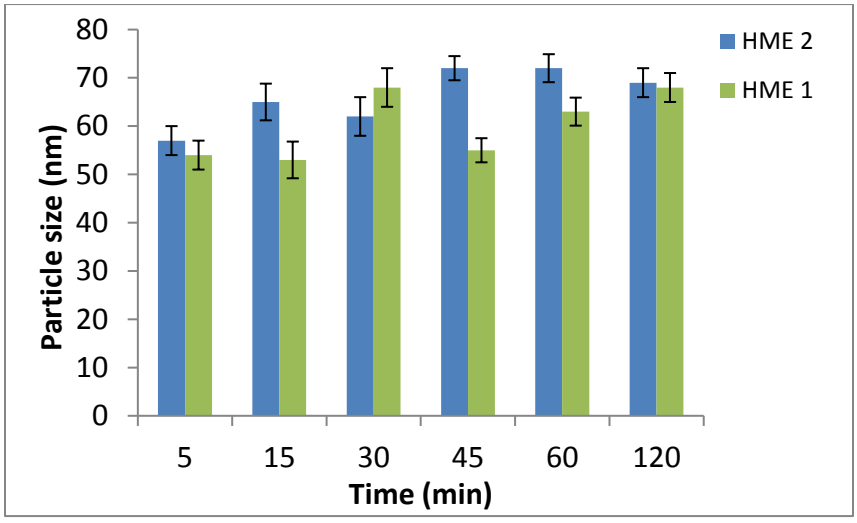

Figure 5: Particle size of modified Labrafac®PG SNEDDS (hot-melt extrusion method)

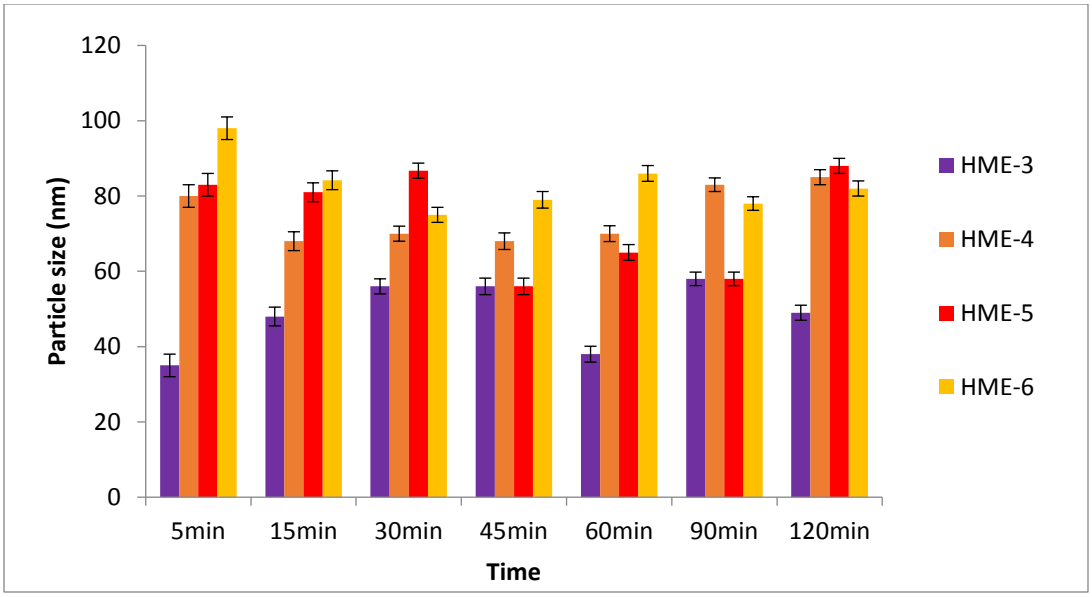

Figure 6: Particle size of Capryol®90 SNEDDS dispersed formulations (hot –melt extruded)

4.1.2 In-vitro dissolution

In-vitro dissolution of Labrafac®PG SNEDDS formulation (Figure 7), did not result in complete dissolution of API into the FaSSGF medium. All the ratios of 50:50 and 60:40 only resulted in the 25-35% drug dissolved at the end of 2 hours. Due to larger particle size of the Labrafac®PG globules, the total specific surface area available was smaller. Hence, the formulation was modified to incorporate co-surfactants to decrease the globule size and hence increase the area available for dissolution.

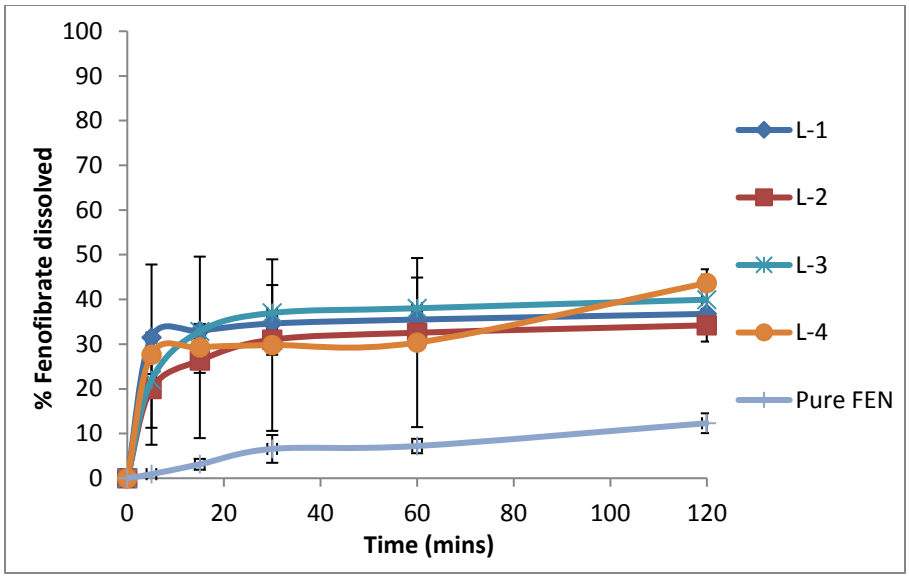

Figure 7: In-vitro dissolution test for Labrafac®PG SNEDDS (conventional method)

From the plot of %in-vitro dissolution of modified Labrafac®PG, it was seen that the release increased upto 45% for Gellucire®44/14 formulations and 68% for Kolliphor® TPGS at the end of 2 hours. Inspite of the change in formulation composition, significant increase in dissolution was not achieved with conventional melt sonicated solid SNEDDS formulations (Figure 8).

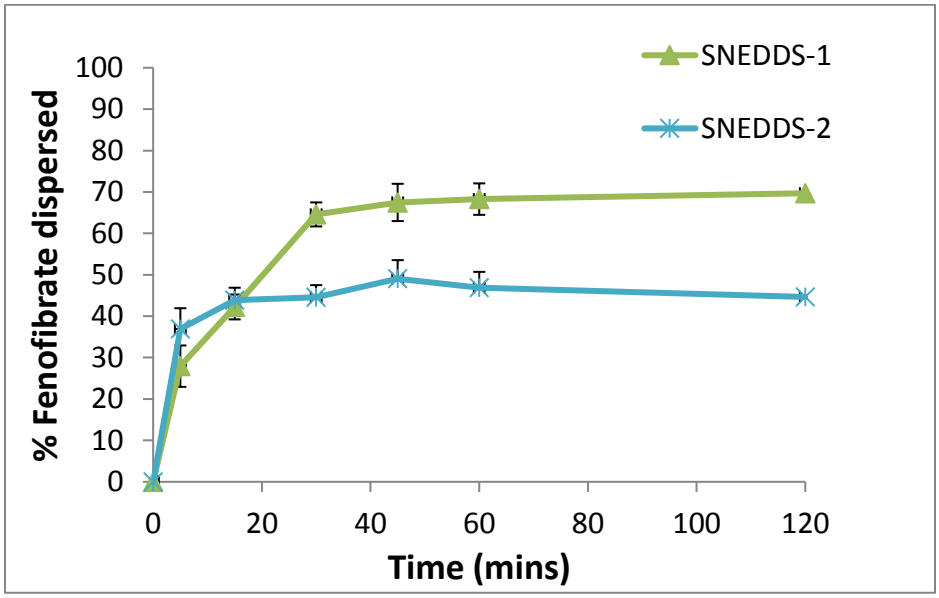

Figure 8: In-vitro dissolution test for modified Labrafac®PG SNEDDS (conventional method)

The hot-melt extruded formulations achieved significantly higher drug release (65% and 85%) as compared to the conventional ones as noted from Figure 9. Although Labrafac®PG extruded formulations attained greater release as compared to conventional ones, complete 100% release was not attained. This can be due to higher affinity of drug for the hydrophobic lipid and poor release from the lipid into the dissolution medium.

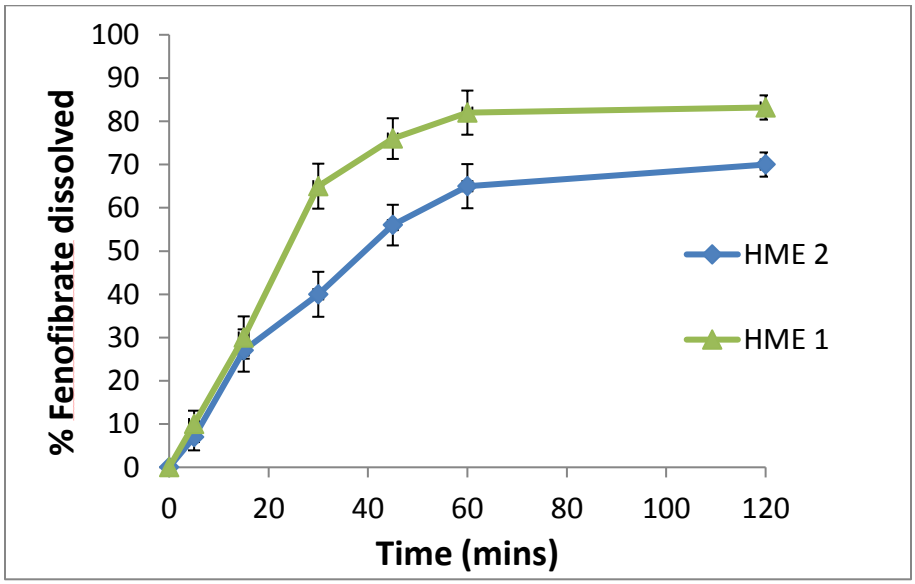

Figure 9: In-vitro dissolution test for modified Labrafac®PG SNEDDS (hot-melt extrusion method)

Hence, Capryol®90 a lipid with higher hydrophilicity (HLB) was chosen for the formulation. From Figure 10, it can be seen that greater than 85% drug release was obtained in the first 15min of the study. This was attributed to lesser affinity of the drug to the lipid and better diffusion into the medium.

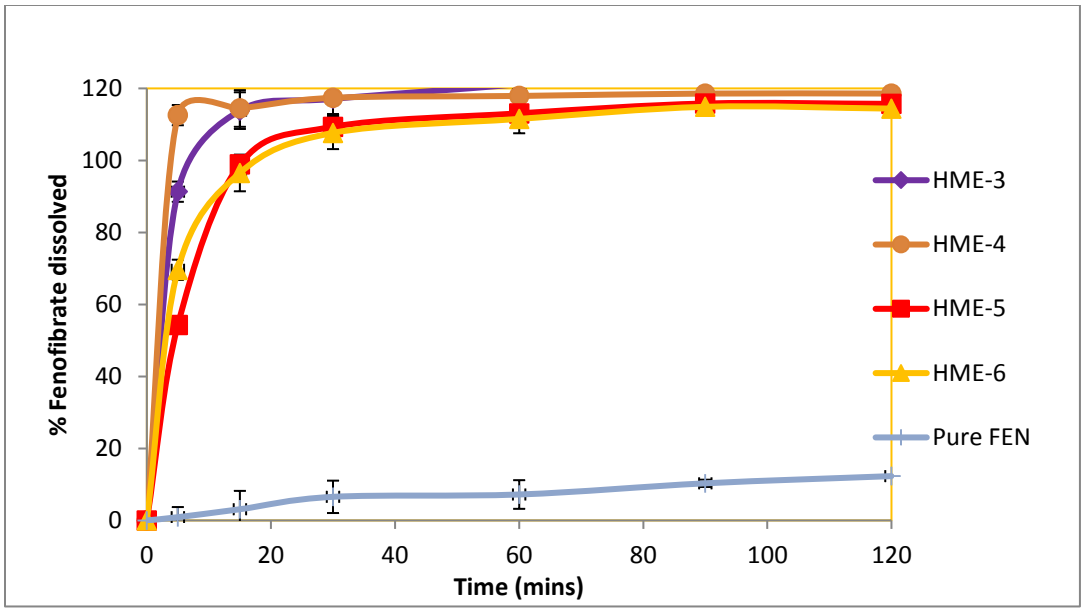

Figure 10: In-vitro dissolution test for modified Capryol®90 SNEDDS (hot-melt extrusion method)

4.1.3 Differential Scanning Calorimetry

The physical state of fenofibrate in the formulation was evaluated using a differential scanning calorimeter (Pyris®DSC) to evaluate re-crystallization. Figure 11 (A), (B), (C) demonstrates the Differential Scanning thermograms of physical mixture of formulation components; blank and fenofibrate loaded hot-melt extruded formulations. Fenofibrate has a melting point of 87°C and the solid surfactants used in the formulations melt between 45-55°C. It could be inferred that fenofibrate was in amorphous or solubilized state in the hot melt extruded formulations. From Figure 11 A the physically mixed formulations demonstrate the crystalline state of fenofibrate.

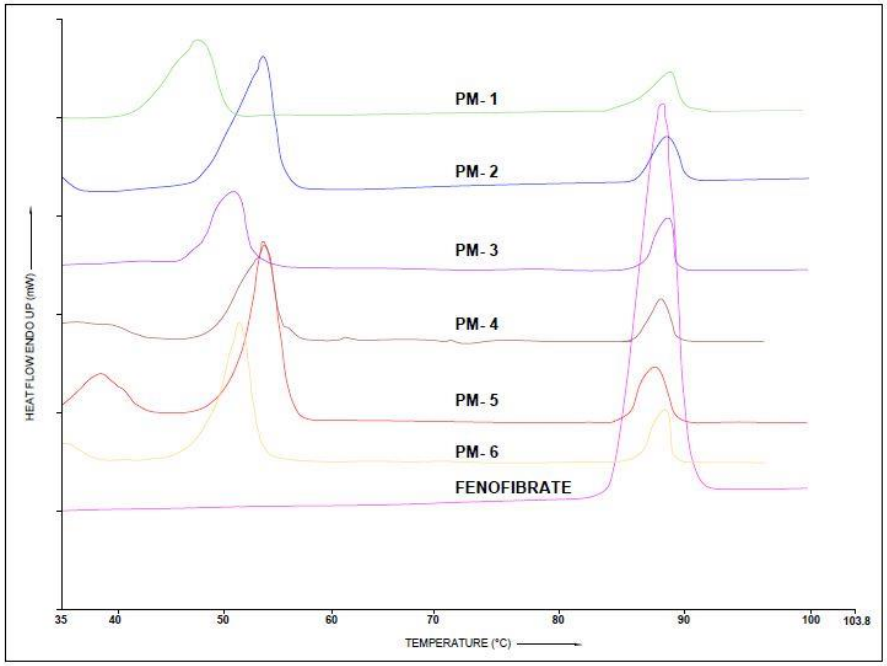

Figure 11 (A): DSC thermograms of physical mixtures of fenofibrate, lipid and surfactant

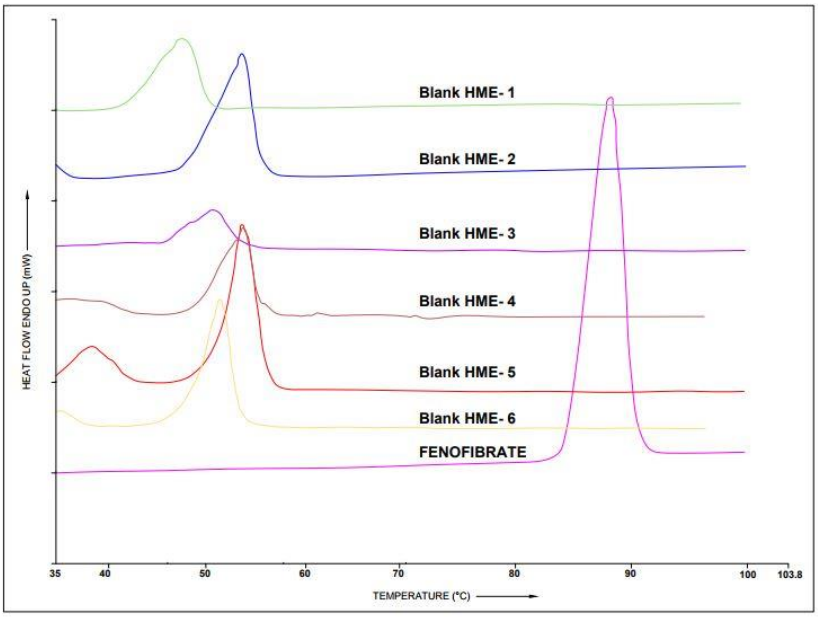

Figure 11 (B): DSC thermograms of hot-melt extruded blank formulations

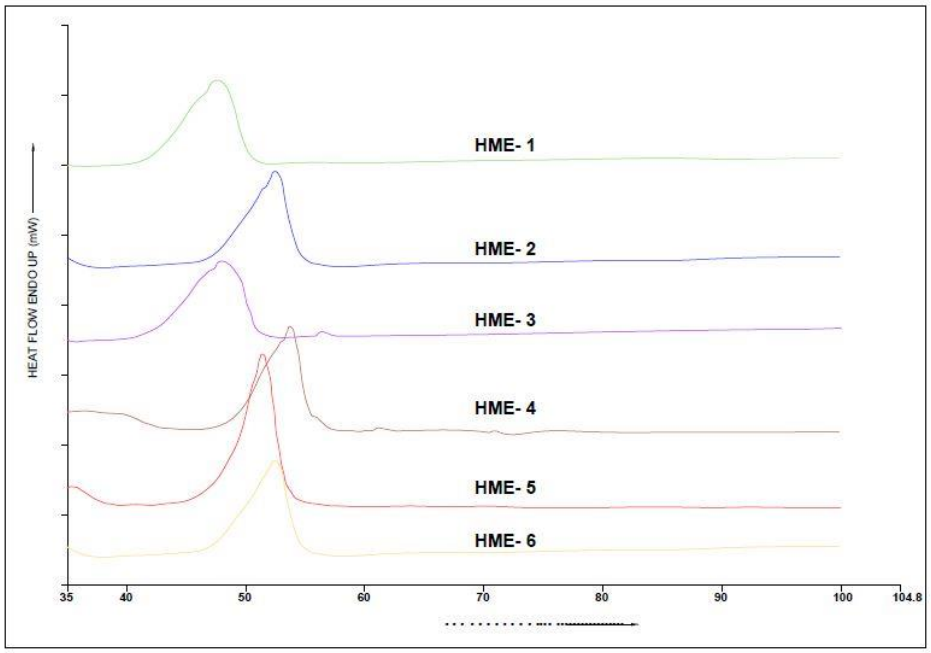

Figure 11 (C): DSC thermograms of hot-melt extruded fenofibrate loaded formulations

4.1.4 Fourier Transform Infra-red Spectroscopy and Imaging

Figure 12 shows the FTIR spectra's of pure components incorporated into the modified Labrafac® PG formulations. At a wavenumber (1650 cm^{-1}) corresponding to only fenofibrate complete 3D imaging was performed to evaluate content uniformity of the drug in conventional and hot-melt extruded formulations. From Figure 13 (A) (B) corresponding to SNEDDS-1 and SNEDDS-2 (conventional) it can be seen that the distribution was very non-uniform where high concentrations of drug (red area) was seen at the edges of the sample as opposed to Figure 14 (A) (B) corresponding to HME-1 and HME-2. In the latter case fenofibrate was seen uniformly distributed throughout the sample specimen. Uniform distribution of the API can be attributed to homogenous distribution of lipid inside the solid surfactant matrix, as the drug has solubility only in the lipid and negligible solubility if the surfactant. During the second half of the hot-melt extrusion process where the temperature was gradually reduced below the melting temperature of the solid

surfactants, solidification was observed. During this solidification, homogenous blending between lipid and surfactant was provided by the kneading blocks of the extruder, which was not available in the conventional method. In the conventional method, as the formulation cooled, there was separation due to solidification of surfactant.

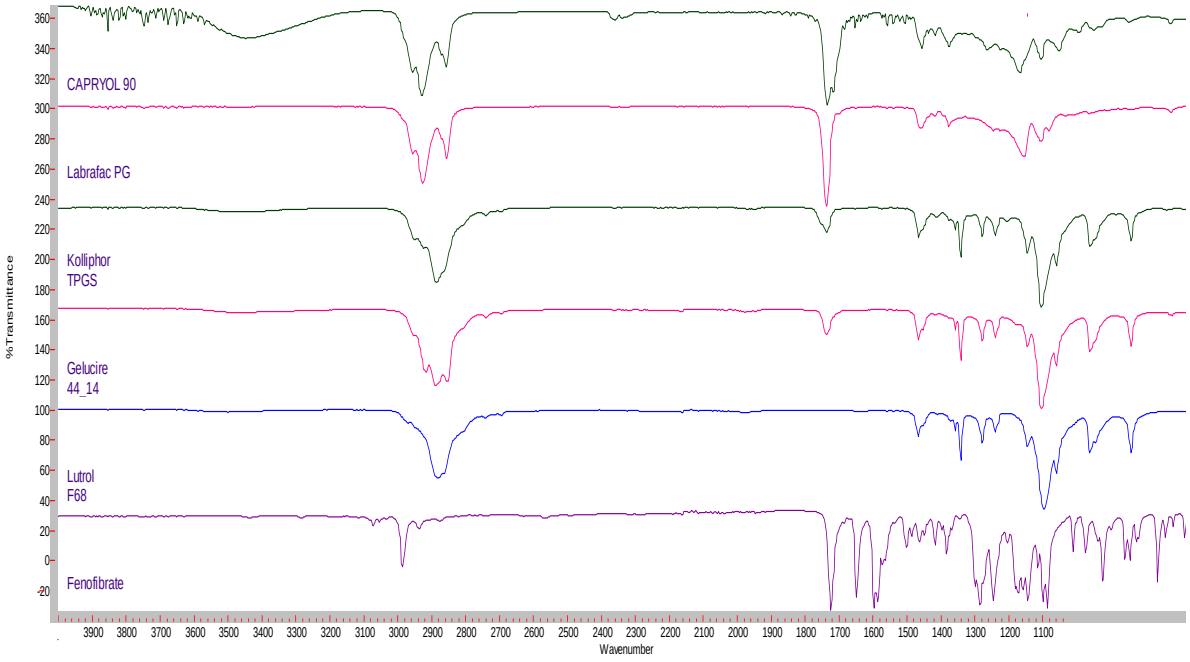

Figure 12: FTIR spectra of formulation excipients

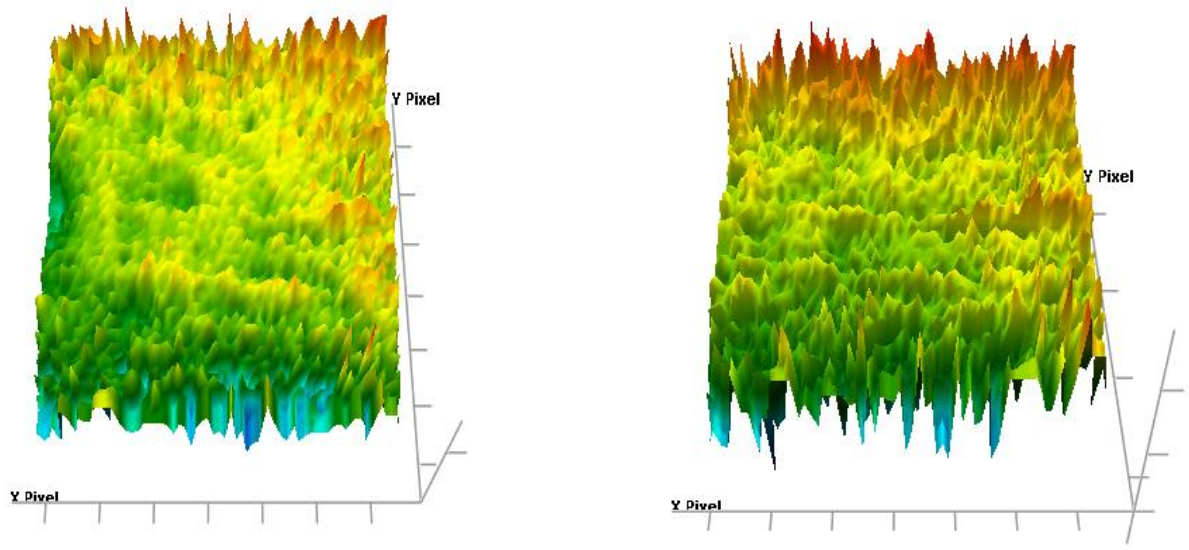

(A) SNEDDS-1 (B) SNEDDS-2

Figure 13: FTIR Chemical Images of modified Labrafac®PG SNEDDS (conventional)

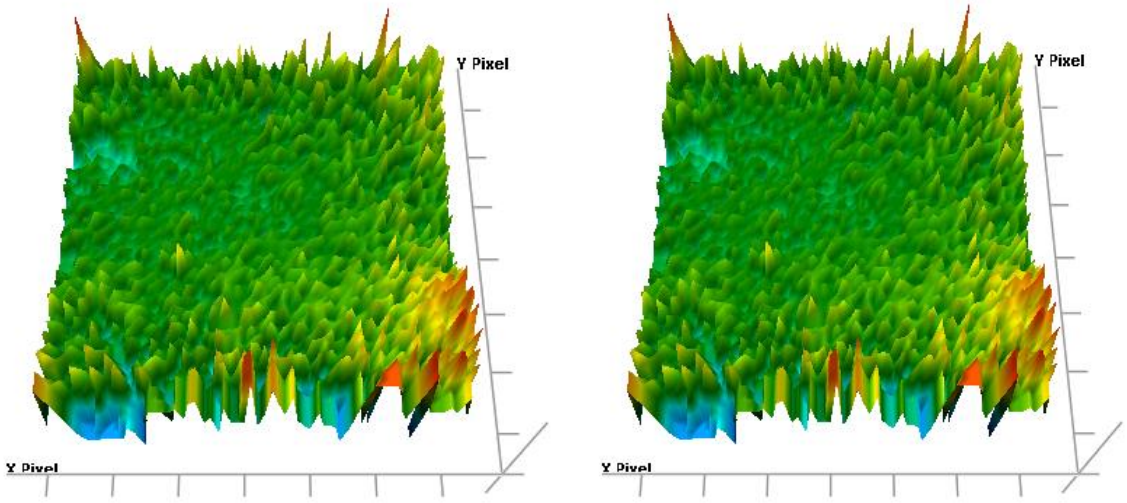

(A) HME-1 (B) HME-2

Figure 14: FTIR Chemical Imaging Spectra of modified Labrafac®PG SNEDDS (hot-melt extruded)

4.2 Evaluation of DOE response surface model

4.2.1 Effect on in-vitro dissolution rate

The type of lipid and surfactant chosen for formulation significantly impacted the dissolution rate of the formulations as shown in Figure 15, 16. Formulations with Lutrol®F68 suggested higher dissolution rate compared to those with Lutrol®F127. This can be attributed to higher hydrophilic groups in Lutrol®F68 which can efficiently form micelles of a smaller size compared to those with Lutrol®F127 and result in greater surface area available for dissolution into the media. All three lipids had greater than 85% drug dissolved within 15mins. Relatively Labrafil® M1944 had higher dissolution rate compared to both Capryol®90 and Labrasol®. This was possibly due to lower drug loading of 1.7-2.5%w/w that could be achieved in Labrafil®M1944 compared to 3.5-5.06%w/w in Capryol®90 and 2.7-4.15% w/w in Labrasol®. Hence, there was twice the amount of surfactant available for solid SNEDDS formulation in Labrafil®M1944 as compared to those in Capryol®90 and Labrasol®. The Pareto chart plot for effect of different variables on the in-vitro dissolution is shown in figure 15. The type of lipid and surfactant were the two main factors which influenced dissolution rate significantly ($p<0.05$). The interactions between the parameters did not significantly influence the in-vitro dissolution rate.

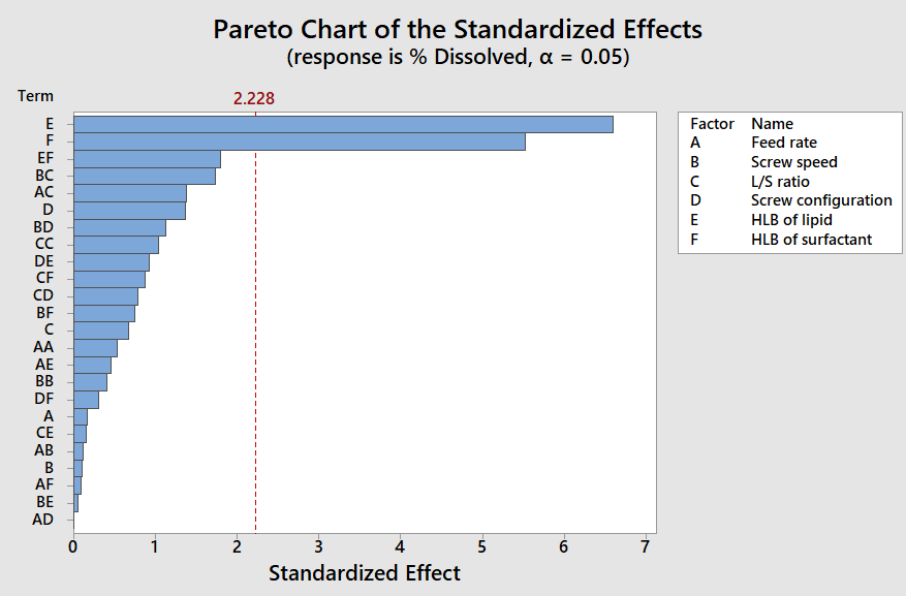

Figure 15: Pareto Chart to study the impact of input variables on In-vitro dissolution rate

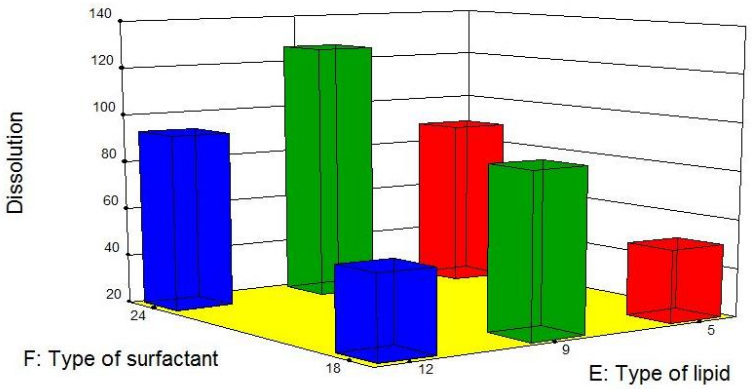

Figure 16: 3D plot for influence of input variables on In-vitro dissolution rate

4.2.2 Effect on Content Uniformity

The type of surfactant significantly impacted the uniformity of distribution of API. Lutrol®F127 is reported to have higher melt viscosity as compared to Lutrol®F68 (Kocbek, Baumgartner, & Kristl, 2006; Schilling & McGinity, 2010; Schmolka, 1977). Hence formulations with Lutrol®F68 had good content uniformity as compared to those with Lutrol®F127 due to better dispersion effect

in the kneading zone. Figure 18 (A) and (B) it can be noted that formulation with screw configuration 1 and Lutrol®F68 had the content uniformity ratio approximately 1 and those with screw configuration 2 and Lutrol®F68 was significantly greater than 1. This implies that a minimum of two kneading blocks (screw configuration 1) was essential in the formulation of uniform dispersion of lipid into the surfactant matrix. From the pareto chart (Figure 17) it is noted that the type of lipid also significantly impacted the content uniformity. Formulations with Capryol®90 and Labrasol® had content uniformity ratio close to 1 (1.002, 1.06) whereas for Labrafil®M1944 it was significantly different (0.7).

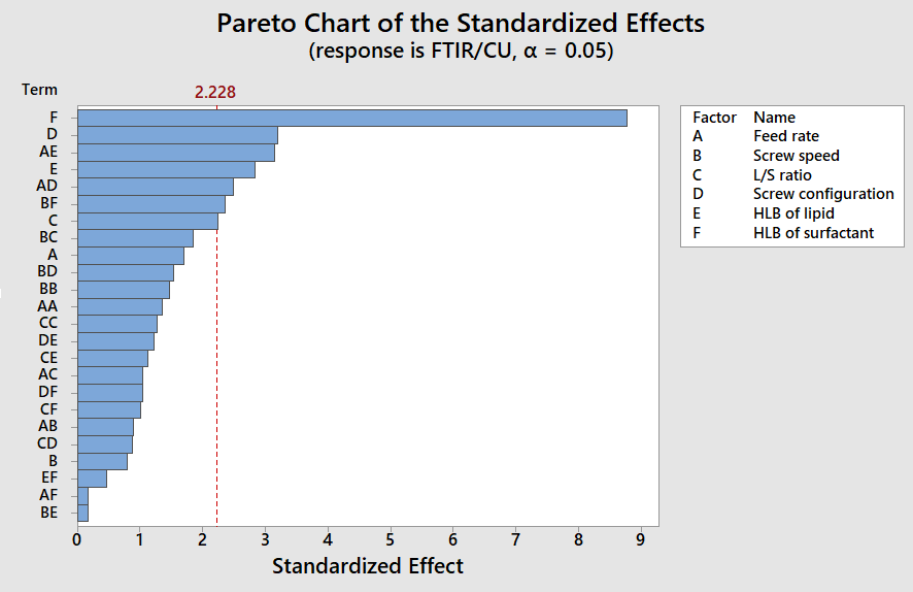

Figure 17: Pareto Chart to study the impact of input variables on content uniformity of extrudates

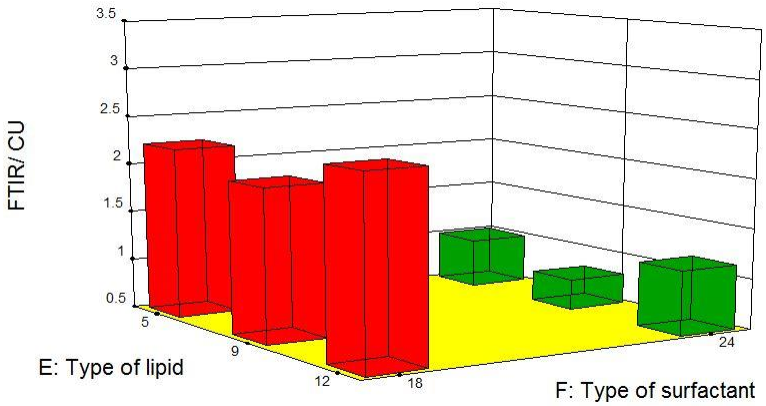

Figure 18 (A): 3D plot for influence of input variables on content uniformity (Feed rate 4g/min, Screw speed 200rpm, L/S ratio 0.60, Screw configuration 1)

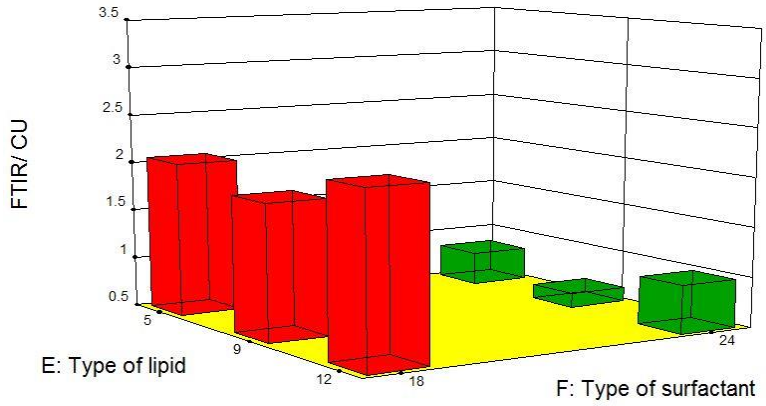

Figure 18 (B): 3D plot for influence of input variables on content uniformity (Feed rate 4g/min, Screw speed 200rpm, L/S ratio 0.60, Screw configuration 2)

4.2.3 Effect on Particle size

The particle size of the globules was significantly impacted by the type of the lipid and screw configuration. Formulations manufactured with screw configuration 1 had significantly smaller particle size as compared to the ones with screw configuration (Figure 20). The greater the intensity of shear incorporated due to screw configuration 1 aided in greater molecular dispersion of the surfactant with the lipid and hence resulted in a finer globule size. The pareto chart (Figure 19)

indicates the type of lipid to have significant influence on the globule size. The smallest globule size was achieved by formulations with Capryol®90.

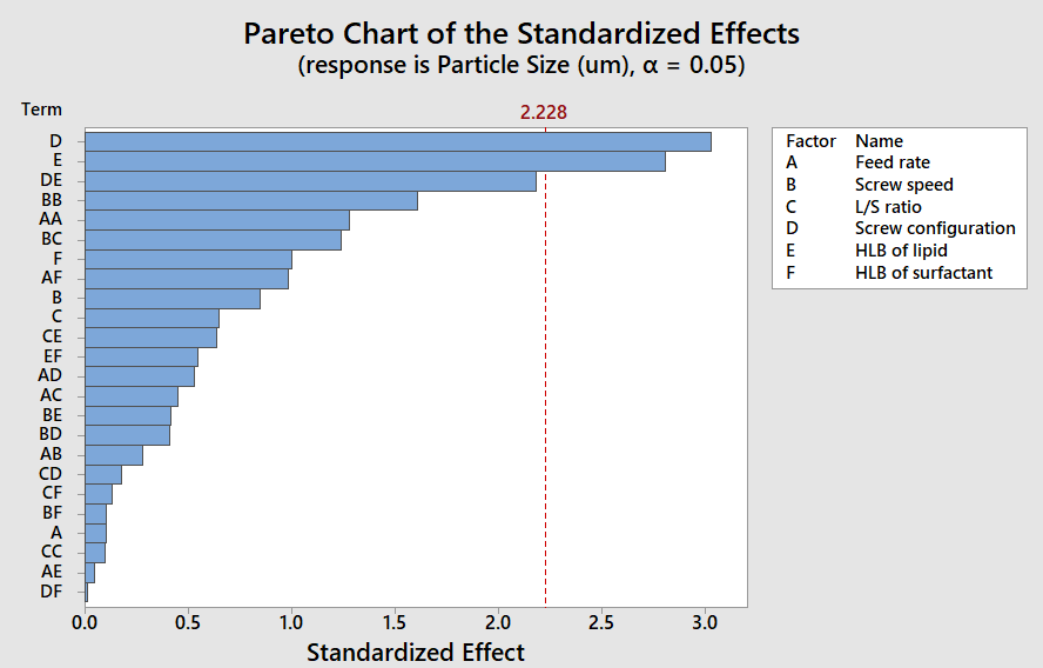

Figure 19: Pareto Chart to study the impact of input variables on particle size of SNEDDS dispersion

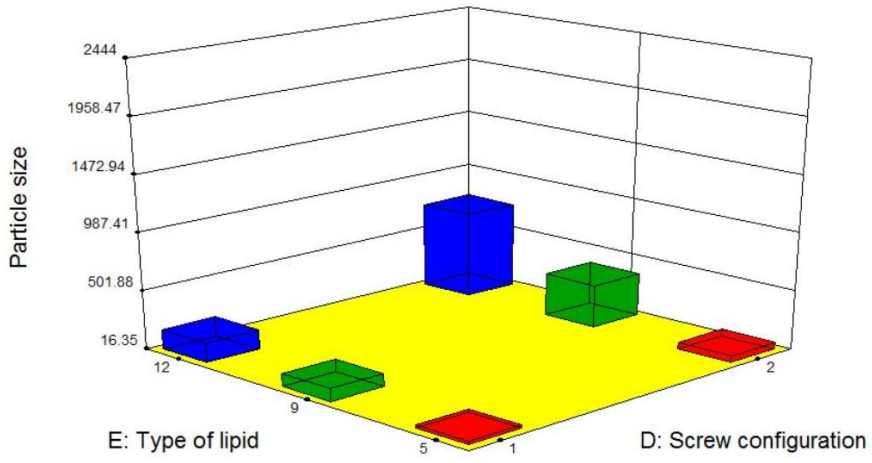

Figure 20: 3D plot for influence of input variables on particle size (Feed rate 4g/min, Screw speed 200rpm, L/S ratio 0.60, Type of surfactant Lutrol®F68)

4.2.4 Effect on Poly-dispersity index

The polydispersity index (PDI) of the dispersed globules of the solid self nano-emulsifying systems was significantly impacted by the type of lipid incorporated in the formulation (Figure 21). The PDI was lower for formulations with Capryol®90 due to its lower HLB value as compared to Labrafil®M1944 and Labrasol® (Figure 22). The optimum HLB of Capryol®90 ensured the solubility of fenofibrate in the lipid globule and after dispersion in the media ensured gradual dissolution of API from the relatively smaller and stable micelle. In case of Labrafil®M1944 and Labrasol® lipids, due to their higher HLB, had greater preferred miscibility in water which resulted in unstable micellar structure.

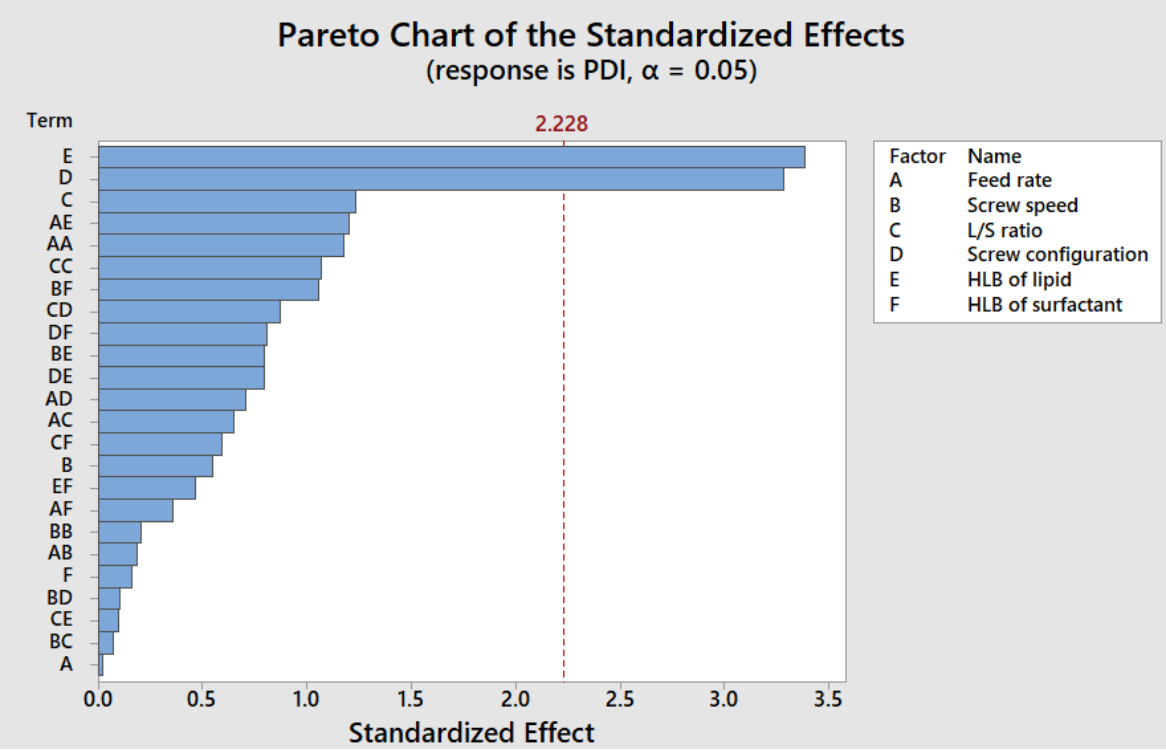

Figure 21: Pareto Chart to study the impact of input variables on PDI of particles from SNEDDS dispersion

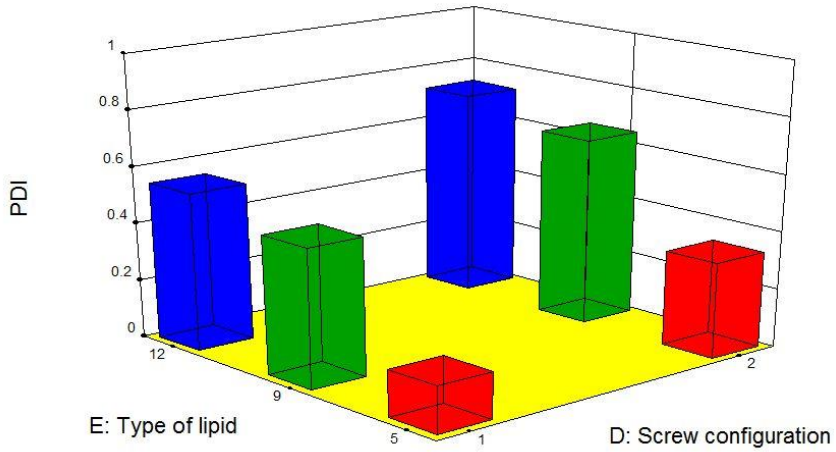

Figure 22: 3D plot for influence of input variables on PDI of particles from SNEDDS dispersion

4.2.5 Desirability index

The desired or optimum process and formulation parameters were plotted from Design Expert software (Figure 23) which resulted in higher value of in-vitro dissolution (Y1), content uniformity ratio equivalent to 1 (Y2), lowest possible globule size (Y3) and Lowest poly-dispersity index (Y4). The optimum process conditions (desirability of 0.9) were 4g/min feed rate, 200rpm screw speed, Screw configuration 1, Lipid/Surfactant (L/S) 0.6, Capryol®90 as the lipid and Lutrol®F68 as the surfactant to attain >90% in-vitro dissolution, Content Uniformity ratio of 1.02, Particle size of 44nm and PDI of 0.189.

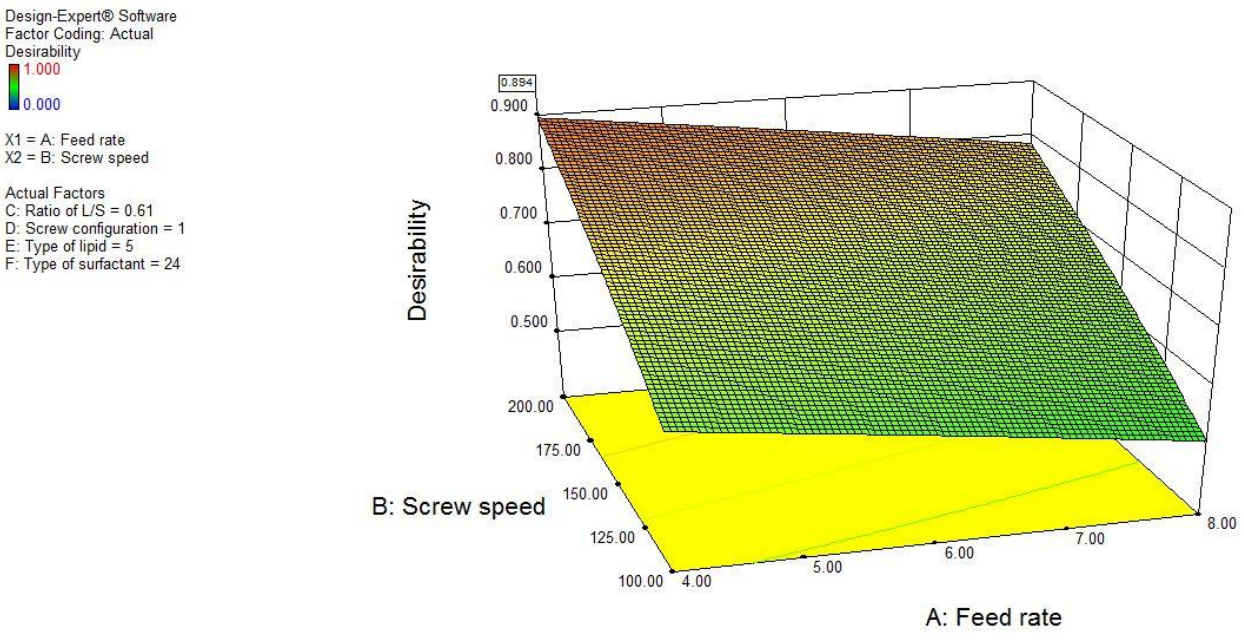

Figure 23: Desirability Index 3D plot for optimized formulation and processing conditions

5. Conclusion

Hot-melt extrusion was shown as a feasible and preferred process for manufacturing solid SNEDDS. Increased residence time of formulation due to low feed rate, higher shearing action imparted by the screw configuration and high screw speed was desired to manufacture solid SNEDDS with desired product characteristics. Lipid such as Capryol®90 with the appropriate balance of hydrophilic and hydrophobic groups was desired to be formulated into solid SNEDDS. Lutrol®F68 was suitable over Lutrol®F127 due to less melt viscosity of Lutrol®F68.

III. CHAPTER

Impact of formulation and process parameters in twin screw hot-melt granulation coupled with in-line particle size analysis of sustained release HPMC granules

1. Introduction

Twin screw granulation is currently being explored as a continuous manufacturing technology over batch type processes such as high shear granulation and fluid bed granulation. Development of sustained-release oral formulations over period of 12 h usually requires release-modifying polymers at the level of above 50% of the total weight (Vasanthavada et al., 2011). The aim of the current investigation was to reduce the use of release modifying polymer content in production of melt granules. This was done by focusing on the manufacturing aspects of processes to generate desirable quality of product. The processing conditions of the polymers (Affinisol®100LV and Methocel®100 LV) were established using hydrophilic (Xylitol) and hydrophobic (stearic acid) plasticizing agents. Theophylline was chosen as the model API having high water solubility (7.36mg/ml) and high melting point (273°C). Very few reports are available in the literature describing screw configuration for hot melt granules. In this study the different screw configurations to provide melt granules were systematically investigated (Mu & Thompson, 2012). For a continuous processing technology such as twin screw melt granulation, establishing quality by design is important to evaluate the impact that the process change has on the granule properties such as in-line particle size.

The Parsum probe IPP80® (Malverrn Instruments) was used to measures particle size distributions of the granules coming from the extruder (Figure 28).

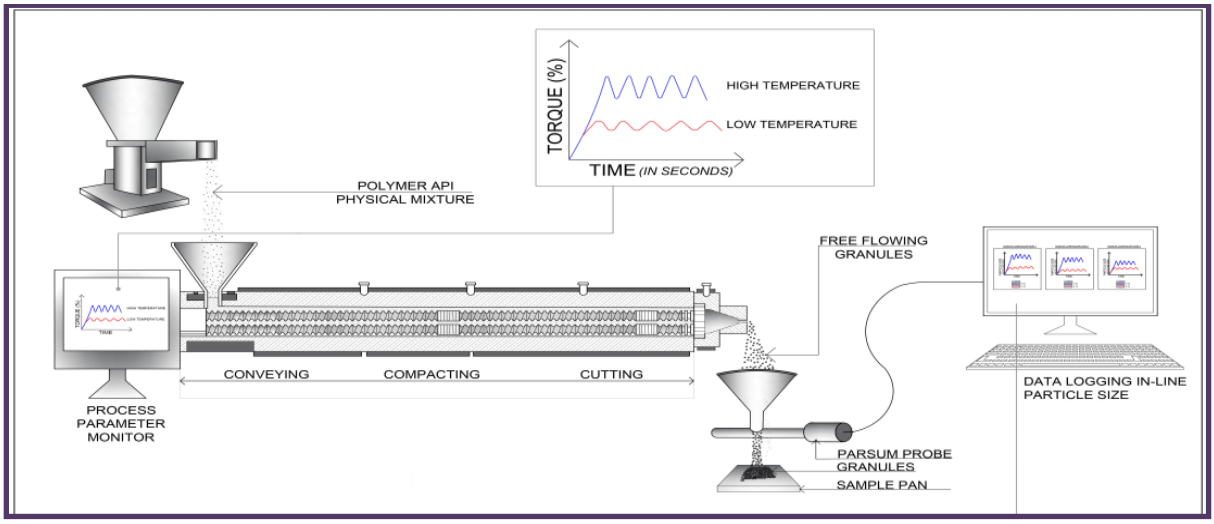

Figure 24: Schematic of melt granulation process coupled with Parsum Probe IPP80® for granule size distribution measurement

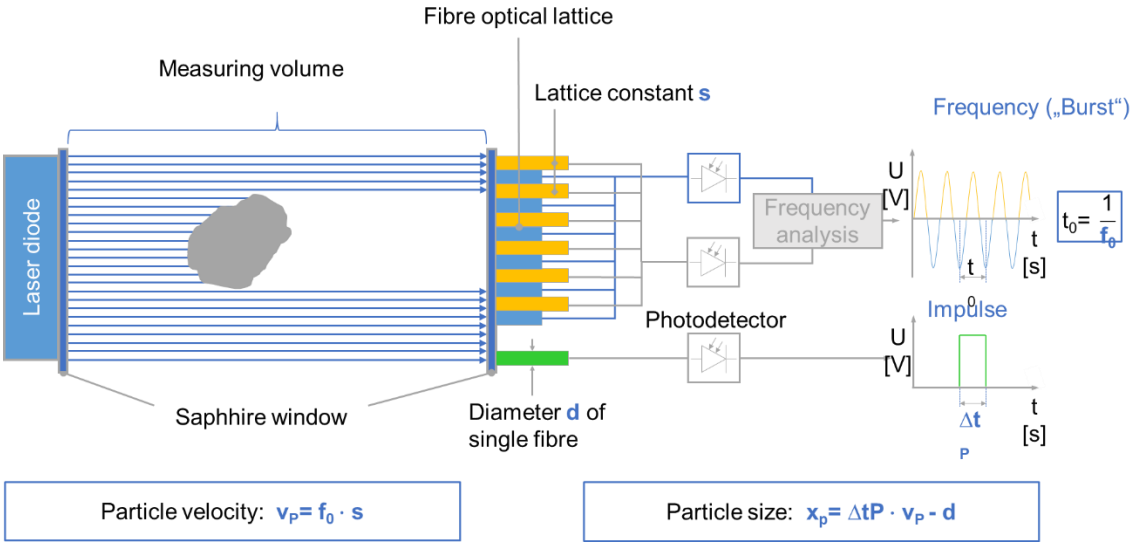

Figure 25: Schematic representation of Parsum Probe IPP80® for granule size measurements

The probe uses a patented spatial filter technique which as been developed and enhanced by Parsum (Figure 29). The Parsum probe contains an array of light-sensitive detectors which are illuminated by a laser. This array can detect single particles as they pass through the laser beam within the probe measurement zone. The shadow produced by each particle can be used to calculate the particle velocity and its chord length (particle size). The probe is capable of measuring the particles in the size range of 50µm- 6000 µm. The detector signals are sampled very rapidly, with sampling rates reaching several thousand particles per second. This ensures that a realistic number of particles is measured, giving confidence that the results reported are representative of the material within the process. The results from each particle are collected into a first-infirst-out buffer and are used for calculating a particle size distribution. The particle size distribution data is continuously updated during operation of the probe, providing a real time particle size trend. This provides direct insight into the performance of the process. The technique would present significant advantage over the conventional seive analysis which is limited by sampling a limited quantity from the entire extruded granule batch. Hence analysis is dependent on sampling technique.

The purpose of our work is listed in brief below:

Aim 1: Development of sustained release melt granules with a high drug load of 77%, by melt granulation using a twin-screw extruder.

Aim 2: Investigate the effect of processing temperature and screw configurations on the development of sustained-release melt granules.

Aim 3: Utilize an in-line particle size probe as a PAT tool to monitor the particle size distribution.

2. Materials

Methocel 100LV, Affinisol were received as gift samples from Colorcon (PA, USA), Stearic acid xylitol, HPLC solvents and vials were purchased from Fisher Scientific (USA).

3. Methods

Theophylline granules with high drug loading (77%) were prepared using a twin screw melt granulation process in a 16mm (Thermo Scientific® Prism Eurolab) extruder. Design Expert® was used to develop a response surface model ($p< 0.05$) and evaluate the effects of both processing and formulation variables of HPMC grades. Affinisol® 100LV and Methocel®100 LV (HPMC 100LV) having a t_g of 130°C and 180°C, respectively, were employed as release modifying polymers. Table 7 depicts the formulation details of the extruded granule and tablets.

Role of ingredient	**Name**	**Concentration %**	**Amount (mg)**
F1 *Granules*			
API	Theophylline	77	
Release modifying polymer	Affinisol ®100LV	23	
F2 *Granules*			
API	Theophylline	77	
Release modifying polymer	Methocel® 100LV	20.7	
Melt binder	Stearic acid	2.3	
F3 *Granules*			
API	Theophylline	77	
Release modifying polymer	Methocel® 100LV	20.7	
Melt binder	Xylitol	2.3	
Tablets			
Granules	F1/F2/F3 granules	70	175
Lubricant	Magnesium stearate	1	2.5
Tablet filler	Microcrystalline cellulose	29	72.5
Total		100	250

Table 7: Details of granule and tablet formulation

Three different screw configurations (SC) were used to study the impact of the number of kneading blocks and the presence of distributive mixing elements (DME) on the particle size distribution (PSD) of granules; where SC1 (2 kneading blocks), SC2 (2 kneading blocks + 1 DME) and SC3 (1 kneading block + 1 DME) are depicted in Figure 30.

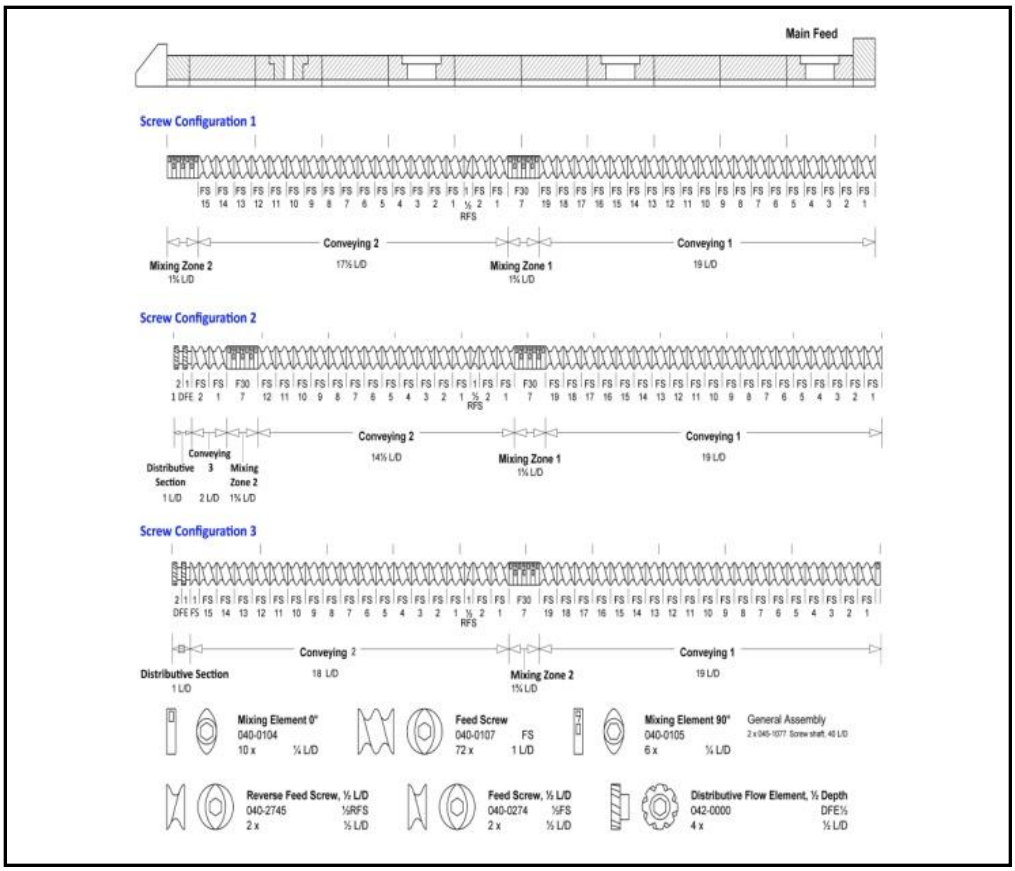

Figure 26: Schematic representation of different screw configurations 16mm Prism Eurolab® twin screw extruder Thermo Scientific®

DSC analysis was performed to screen stearic acid and xylitol as plasticizers to process Methocel®100LV. Affinisol®100LV a highly substituted form of HPMC 100LV and manufactured to reduce the operating extrusion temperature. Theophylline (77% w/w) was blended with Affinisol®100LV or Methocel®100LV with melt binders as shown in Table 7 using a V-shell blender (Globe- Pharma, Maxi blend™ New Brunswick, NJ) for 20 min at 25 rpm, after passing through US# 35 mesh screen to remove any aggregates that may have formed. Response surface design (optimal) was used for generating the design points (Table 8) and Design Expert software was used for analyzing the data. Thus, the three different variables studied were temperature of extrusion, screw configuration, Formulation (Affinisol®100LV/Methocel®100LV with 10%

stearic acid/ Methocel®100LV with 10% xylitol as release modifying polymer). The obtained granules were milled using a Fitz mill sieve size 40 at 4000rpm. Extra-granular excipients such as magnesium stearate (1%) and Microcrystalline cellulose were added to the milled granules and blended using a V-blender for 10mins. This blend was then compressed into tablets of 250mg using a 10mm circular die and punch on a single station tablet press (tablet drug loading 70%).

Run no.	Factor 1 A:Temperature	Factor 2 B: Screw configuration	Factor 3 C: Formulation
1	1	1	Affinisol® 100LV
2	-1	1	Methocel 100 LV ® 10% Xylitol
3	-1	2	Methocel 100 LV ® 10% Xylitol
4	-1	1	Methocel 100 LV ® 10% Stearic acid
5	1	2	Affinisol® 100LV
6	1	2	Methocel 100 LV ® 10% Stearic acid
7	1	2	Methocel 100 LV ® 10% Xylitol
8	-1	3	Methocel 100 LV ® 10% Xylitol
9	1	3	Methocel 100 LV ® 10% Stearic acid
10	-1	1	Affinisol® 100LV
11	1	3	Methocel 100 LV ® 10% Xylitol
12	1	3	Affinisol® 100LV
13	-1	3	Affinisol® 100LV
14	-1	2	Affinisol® 100LV
15	-1	3	Methocel 100 LV ® 10% Stearic acid
16	-1	2	Methocel 100 LV ® 10% Stearic acid
17	1	1	Methocel 100 LV ® 10% Stearic acid
18	1	1	Methocel 100 LV ® 10% Xylitol

Table 8: Response surface design of experiments (Design Expert®)

3.1 Granule and tablet Characterization

3.1.1 Differential Scanning Calorimetry

Pre-formulation evaluation was performed using Differential Scanning calorimetry (TA DSC25) testing of physical blend of 10% stearic acid and 10% xylitol with Methocel®100LV. About 5-8mg of samples were weighed into aluminum T-zero® pans and heat cycle was run from 30°C-200°C at a rate of 20°C/min. The glass transition temperature of these physical blends was calculated using Trios 4.2.1 software.

3.1.2 Milled granule flowability

The granules were characterized for flowability, strength, in-line particle size, and surface morphology.

Carr's index and Hausner's ratio were calculated to estimate the flowability of the granules. Bulk density was calculated by measuring the volume of 5 g granules in a 10 ml graduated cylinder. The cylinder was tapped 100 times until no further reduction in the volume of the granules was observed. Tapped density was calculated using the volume of the granules after tapping (Patil, Tiwari, Upadhye, Vladyka, & Repka, 2015).

Carr's Index = Tap density – Bulk density/ Tap density X 100

Hausner's ratio = Tap density/ Bulk density

3.1.3 Scanning Electron Microscopy

The intact granules were evaluated for their surface texture using Scanning Electron microscopy. The surface morphology was investigated using a JEOL 6300F scanning electron microscope (JEOL, Tokyo, Japan) operated at 5 keV. The samples were mounted on an aluminum board using a double-sided adhesive tape and sputter coated with gold using a sputter coater. A scanning electron microscope operated at various magnifications was used for samples analysis.

3.1.4 Particle Size Analysis (In-line Parsum Probe®)

Parsum Probe IPP®80 (Malvern Instruments) was used to analyze particle size in real time and data was processed using a Log Analyzer macro. Buffer size of 500 was selected from optimization of probe for particle size measurement. Particle probe loading was 30% and data was logged in every 2 secs. Real time particle size distribution data were collected by the Parsum Runtime V8.01 software processed by the Log Analyzer Macro.

3.1.5 Granule Porosity

The milled granules were characterized for the percentage porosity using Micromeritics GeoPyc Envelope density analyzer. The weighed sample was placed in a bed of DryFlo, and the DryFlo is agitated and gently consolidated about the sample. The GeoPyc collected the displacement data, performed the calculations and reported the percentage porosity. The true density value obtained from the Accu-pyc helium pycnometer (Micromeritrics) was entered into Geopyc for percentage porosity calculation.

3.1.6 Granule Strength

In addition, milled granule strength was evaluated using TA2i Texture Analyzer (Texture Technologies) in compression mode between parallel platens. Prior to measurement, granules were maintained in a humidity-controlled box at room temperature and 25% RH for 48 h. The granules size range that formed the maximum (>80%) portion of the sample were crushed using the Texture Analyzer. Each granule was positioned in the center of a flat testing platform, and a flat-tipped cylindrical stainless steel probe of 3 mm in diameter and 28.26 mm^2 (A) in area was used to apply the load. The probe traveled at 0.1 mm/s and penetrated a distance of approximately 0.5 mm in the sample. Once the predetermined distance was reached, the probe was automatically withdrawn at 0.1 mm/s. Data (force vs. displacement) were collected at a rate of 250 points per second by Texture Expert Exceed software for further analysis. The measurement was repeated 10 times for each set of granules. During each measurement, the total force F at breakage and the diameter of the granule dg were determined. Assuming the granule cross-sectional area to be circular in the plane of the punch, the compression strength (σ) was calculated (Bika, Tardos, Panmai, Farber, & Michaels, 2005).

$$\sigma = F/A$$

3.1.7 Tablet Hardness

Tablets were characterized for hardness and in-vitro dissolution. Ten tablets were randomly selected and tested for their hardness (Hardness tester, Schleuniger). An additional ten tablets were randomly selected and tested for their thickness using a digital Vernier caliper (Montana).

3.1.8 Tablet In-vitro dissolution

In- vitro drug release was measured using USP dissolution apparatus II set at 50 rpm and 37°C. The test dissolution media were 700 ml of 0.1N HCl (pH 1.2) for the first 2 h, then 200 ml of 0.2 M tribasic sodium phosphate (pH 12.5) to provide a final pH of 6.8 for 24 h (media were maintained at 37 °C) to simulate the tablet transit from stomach (pH 1.2) to the intestine (pH 6.8). The drug release studies were conducted in triplicates and the mean values were plotted versus time. A Waters High performance liquid chromatography (HPLC) system equipped with a Water 600 binary pump, Waters 2489 UV/detector, and Waters 717 plus auto-sampler (Waters Technologies Corporation, Milford, USA) and a Phenomenex Luna 5um C18 (2) 250 x 4.6 mm column (Torrance, CA, USA) were used at a detection wavelength of 254 nm. The mobile phase consisted of Methanol and water at a ratio of 35:64:1 (v/v). The mobile phase flow rate was maintained at 1.0mL/min. and an injection volume of was 10 µL was used HPLC data was analyzed using Empower V. software (Milford, MA, USA) (Park, Lee, Kang, Tiwari, & Repka, 2017).

4. Results and Discussion

4.1 Differential Scanning Calorimetry

Figure 31 depicts the t_g of Affinisol®100 LV to be 120°C. Also, stearic acid and xylitol melted at 60°C and 70°C respectively and reduced the t_g of Methocel®100LV to 140°C. Hence Affinisol®100 LV was granulated at temperatures below 120°C, whereas a plasticizing melt granulating agent such as stearic acid and xylitol were used to process Methocel®100LV at a temperature below 180°C (t_g). The melt binders acted as plasticizing agents to reduce the t_g of Methocel®100LV to 140°C.

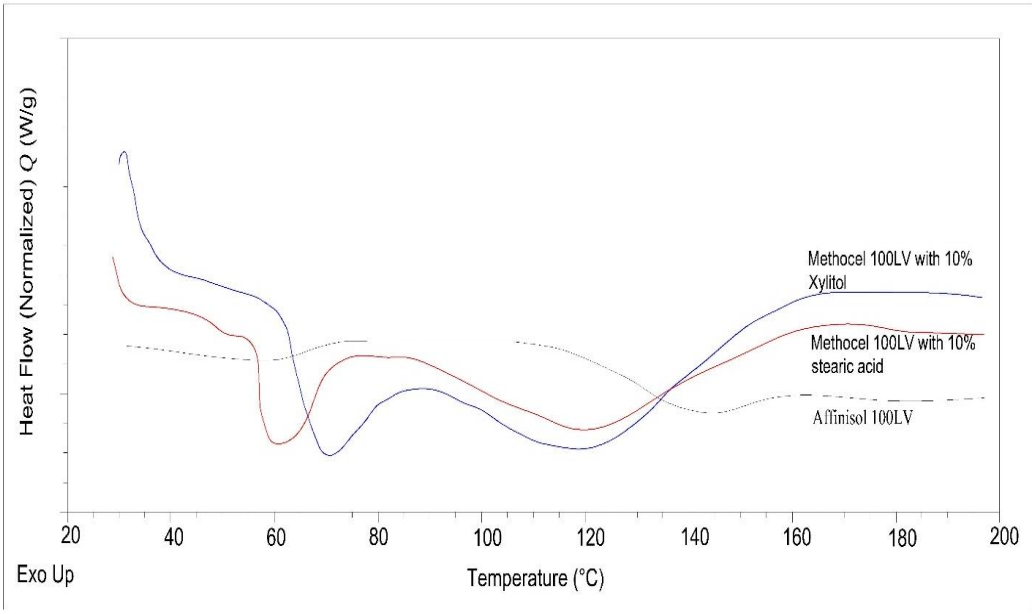

Figure 27: Differential Sanning Calorimetry thermograms of the extruded polymers with melt binders

4.2 Particle Size Analysis (In-line Parsum Probe®)

Parsum Probe IPP®80 data suggested that particle size of granules prepared using Affinisol®100LV was more uniform than those prepared with Methocel®100LV. From Figure 32 (A) (B) (C), the D10, D50 and D90 3D plots, it can be inferred that the granules formed with SC3>SC1>SC2.

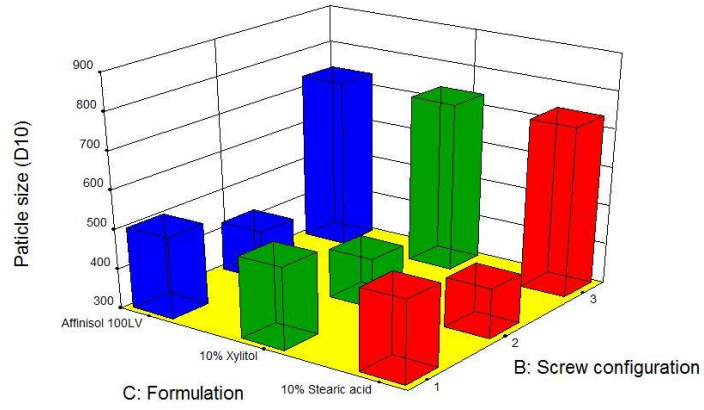

(A)

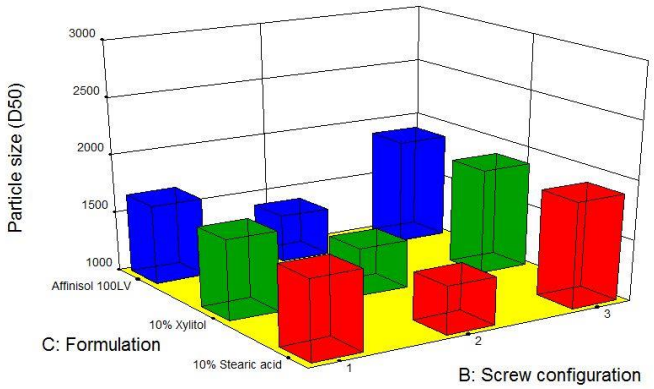

(B)

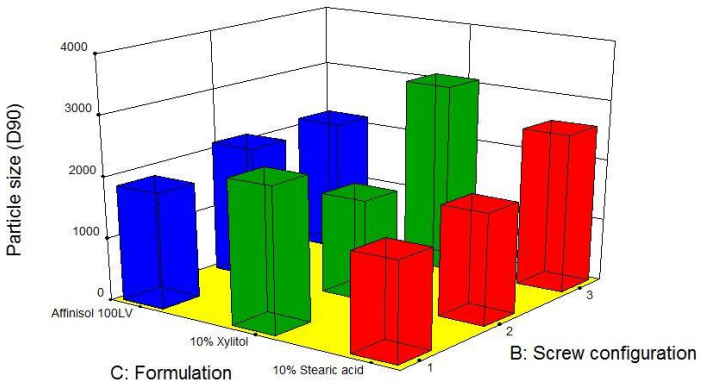

(C)

Figure 28: 3D plot for influence of screw configuration and formulation variable on particle size (A) D10 (B) D50 (C) D90

This can also be represented by the number of kneading blocks and the presence of distributive elements (DME). The addition of the second mixing block towards the end in SC1 and SC2 resulted in particle size breakage as opposed to the presence of the first kneading block in the start in all of the screw design which was critical in formation of granules. On comparison of the order of particle size, the presence of second kneading block was more critical to particle size reduction than the presence of distributive element (DME) as D50 from SC1<SC3. The granules prepared from SC3 were more uniform or homogenous due to breakage due to deformation of the pellet from all sides whereas the materials extruded with SC1, SC2 demonstrate a larger mass loss during crushing and chipping occurring in between the kneading elements and between the kneading element and the barrel wall. From Figure 33 (A) (B) (C) it can be confirmed that the screw configuration variable was of most significant impact ($p<0.05$).

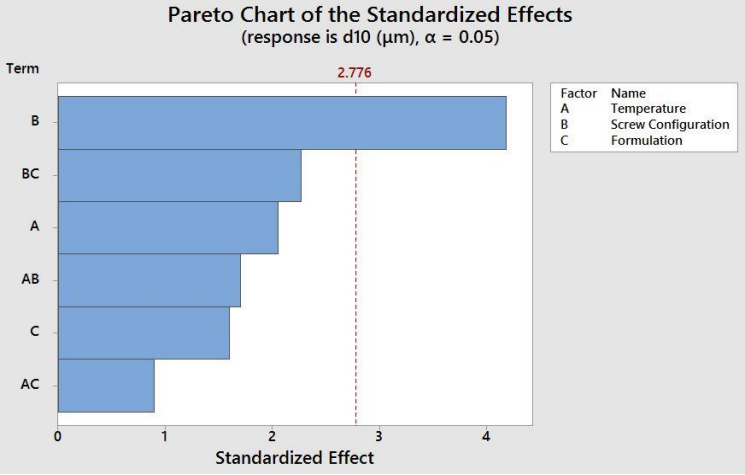

(A)

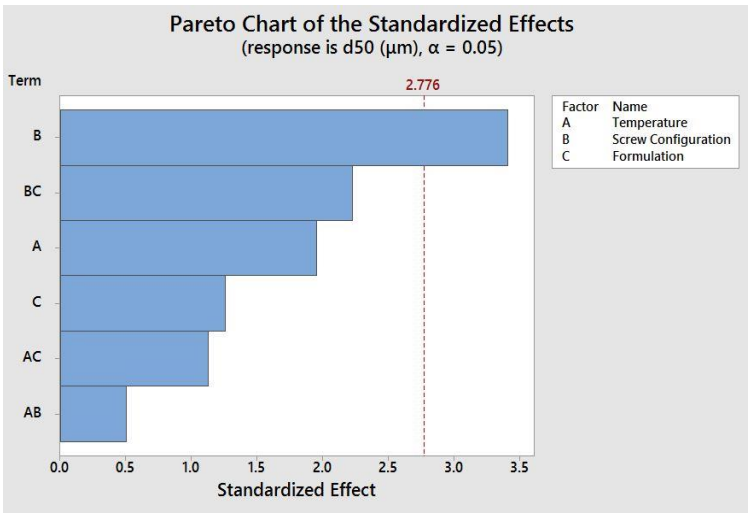

(B)

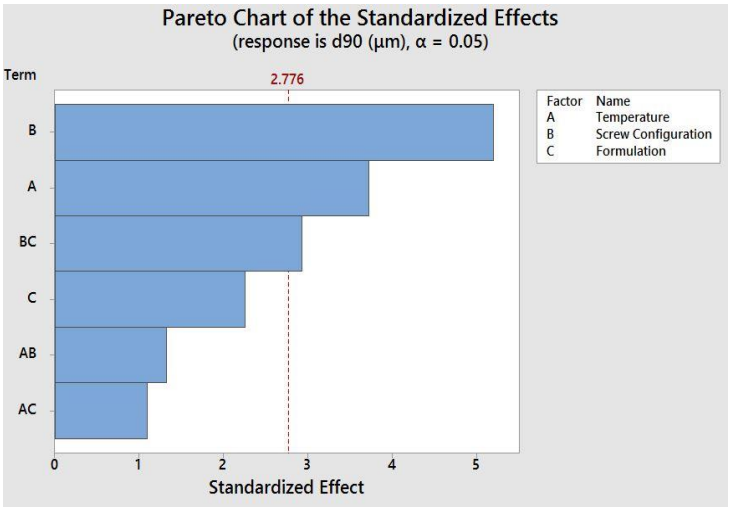

(C)

Figure 29: Pareto chart for influence of input variables on particle size

(A) D10 (B) D50 (C) D90

4.3 Scanning Electron Microscopy

The particle morphology observed from SEM analysis showed uniform, compact and smooth surface granules for Affinisol®100LV in Figure 34 (A) (B), compared to non-uniform, rough surface granules for Methocel®100LV in Figure 34 (C) (D). The surface of compact

Affinisol®100LV granules will lower the diffusion of water into the matrix structure as opposed to rough and size reduced granule structure of Methocel®100LV granules which might aid in diffusion of water into the matrix of polymer. Figure 34 (E), (F), (G) show the structure of pure polymers and theophylline. Affinisol®100LV had more rounded particles, which are better to compress as opposed to crystalline particles of Methocel®100LV.

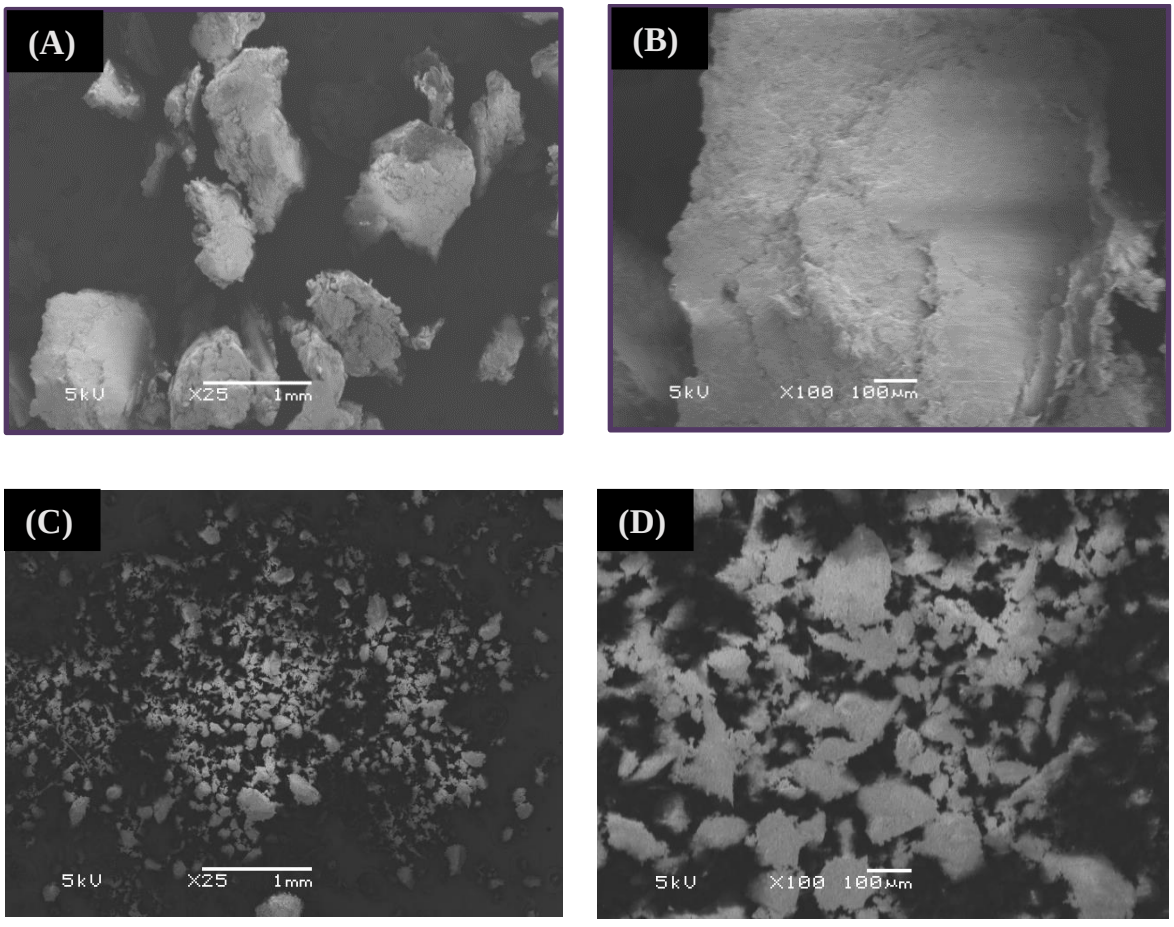

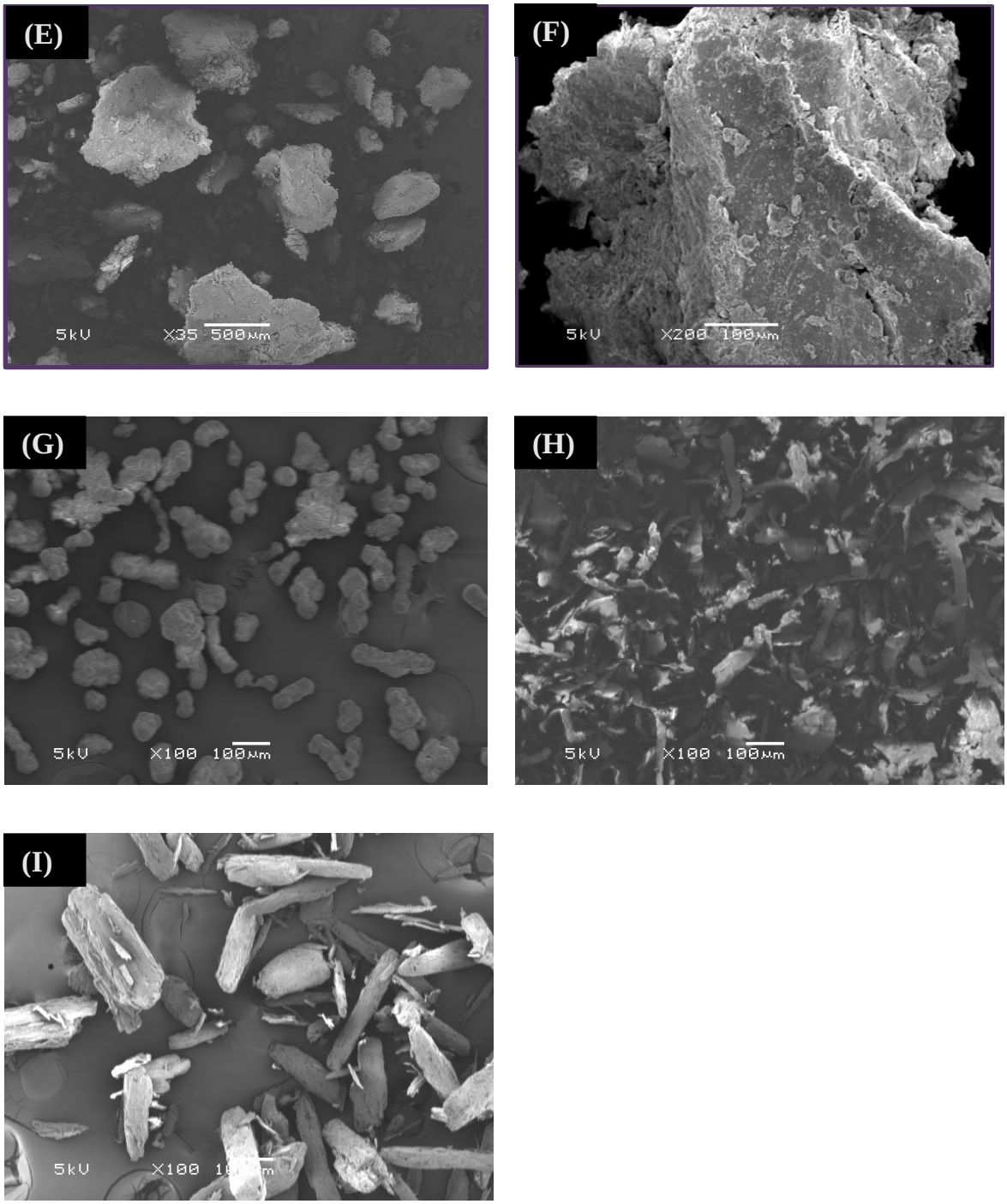

Figure 30: SEM Images of granules processed at higher temperature and SC3 formulation (A)&(B) Affinisol® 100LV theophylline granules (x25, x100); (C) & (D) Methocel®100LV with 10% stearic acid theophylline granules (x25, x100) (E)& (F) Methocel®100LV with 10% xylitol theophylline granules (x25, x100) (G) Pure Affinisol® 100LV (H) Pure Methocel®100LV (I) Pure theophylline

4.4 Milled granule flowability

Granule flowability and compactability affects the die filling and tablet mechanical characteristics; therefore, it is essential to study the granule flow properties. Various tests have been performed on all formulations such as bulk density, tapped density, Carr's index and Hausner's ratio. According to the flow property classification of USP, granules should have a Carr's index between 10.0 and 18.0%, whereas Hausner's ratio should be less than 1.25. When the Carr's index and Hausner's ratio are adequate, the powder flows at minimum bulk density and consolidates to maximum density inside the die, prior to compression. Carr's index was observed to be higher for unprocessed physical blends of HPMC and theophylline (45%) compared to the HME processed granules (12.7%), which indicated better flowability of the granules. Specifically, from figure 38 Carr's index was seen to be impacted due to the formulation type and the temperature of operation. Methocel®100LV granules had higher Carr's index at lower temperature and lower Carr's index at higher temperature Figure 37 (A) (B) (C). Carr's index of Affinisol®100LV granules did not vary significantly with the change of extrusion temperature. In general, formulations made with SC3 did not vary with the formulation type or temperature, except Methocel®100LV stearic acid granules which had higher Carr's index at lower temperature due lesser strength and size of granules due to cutting action of the DME. The Hausner's ratio also followed the same trend as the Carr's index (Figure 35, 36).

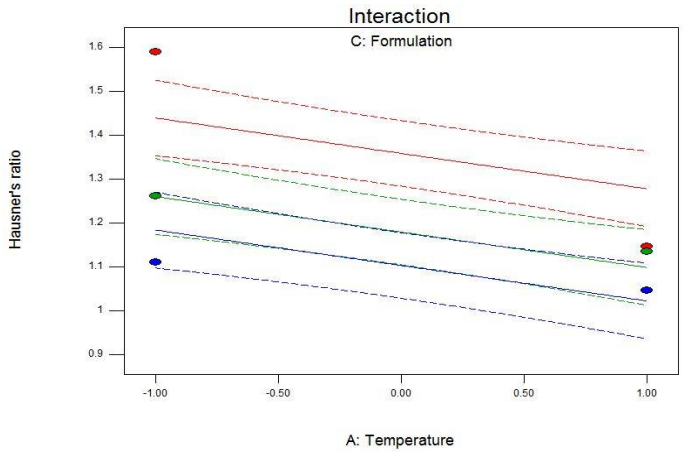
Interaction
C: Formulation
Hausner's ratio
1.6
1.5
1.4
1.3
1.2
1.1
1
0.9
-1.00
-0.50
0.00
0.50
1.00
A: Temperature

(A)

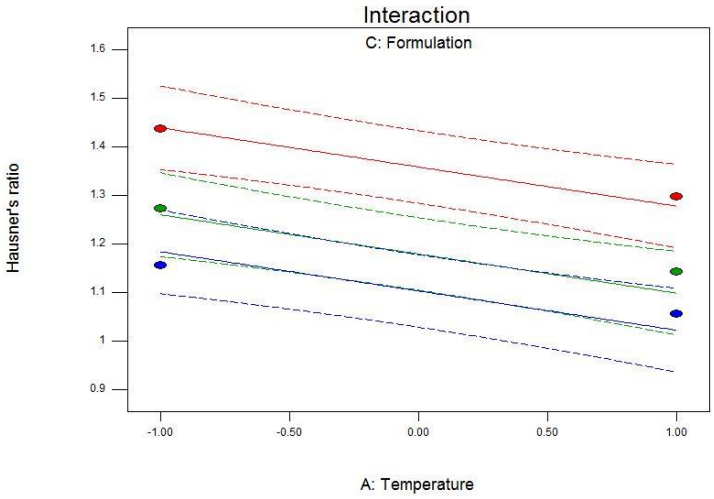
Interaction
C: Formulation
Hausner's ratio
1.6
1.5
1.4
1.3
1.2
1.1
1
0.9
-1.00
-0.50
0.00
0.50
1.00
A: Temperature

(B)

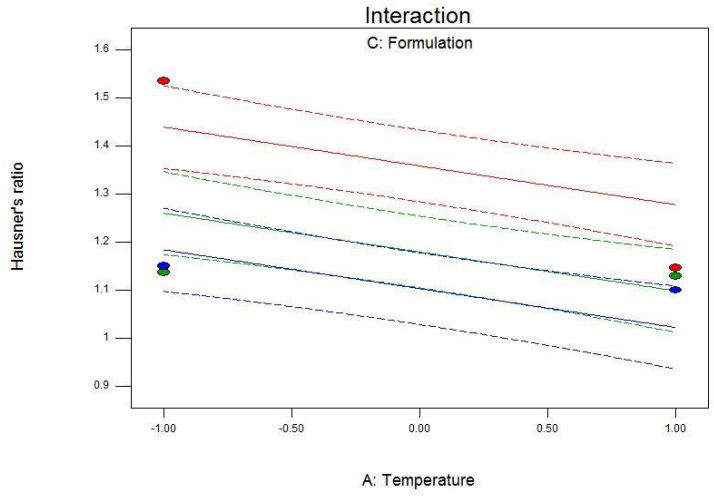
Interaction
C: Formulation
Hausner's ratio
1.6
1.5
1.4
1.3
1.2
1.1
1
0.9
-1.00
-0.50
0.00
0.50
1.00
A: Temperature

(C)

Figure 31: Impact of process and formulation variables on Hausner's ratio (A) Screw confguration 1 (B) Screw configuration 2 (C) Screw configuration 3 (Methocel® 100LV with 10% stearic acid●, Methocel® 100LV with 10% xylitol ●, Affinisol® 100LV ●)

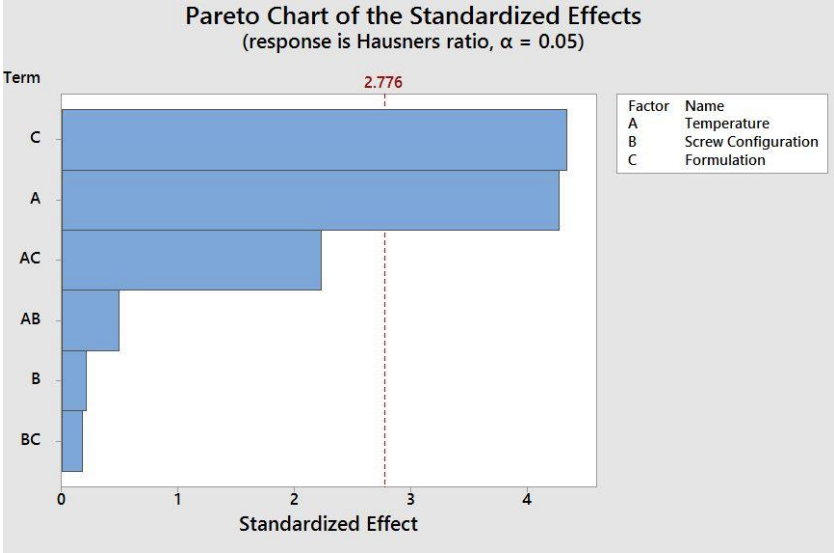

Figure 32: Pareto chart for influence of input variables on Hausner's ratio

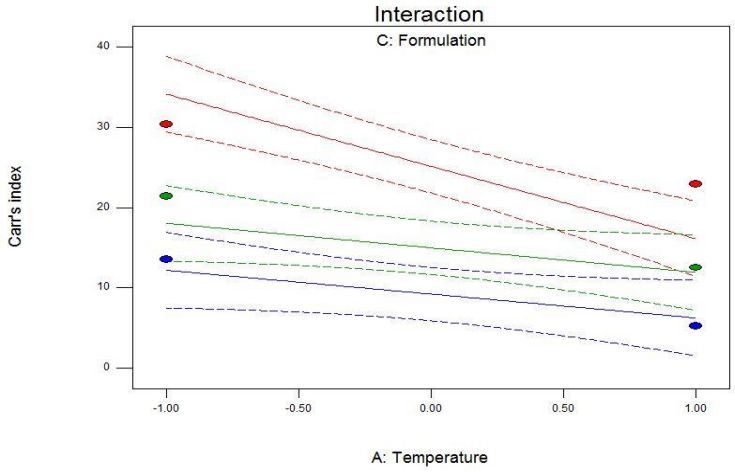

(A)

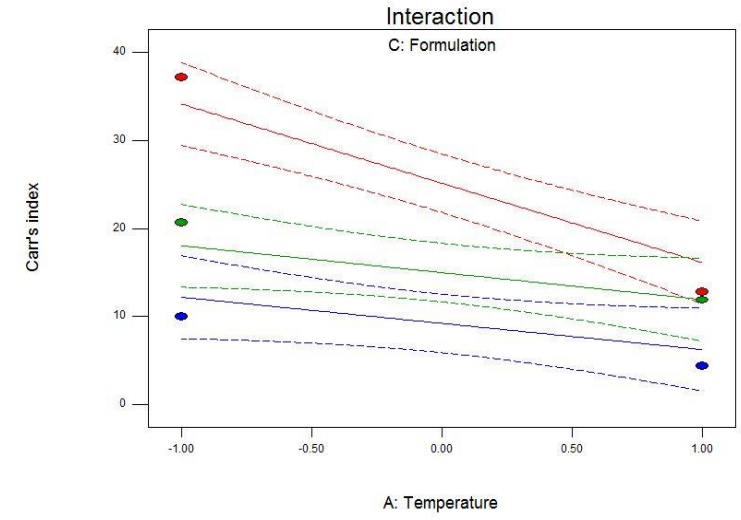

(B)

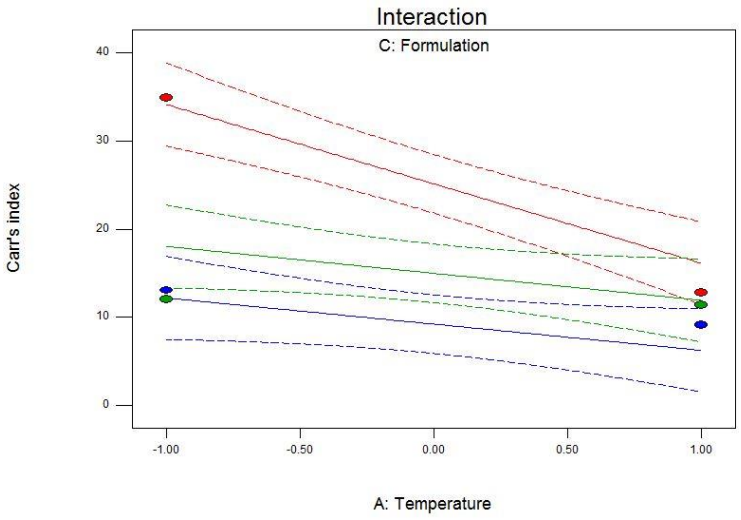

(C)

Figure 33: Impact of temperature on Carr's index of different formulations

(A) Screw confguration 1 (B) Screw configuration 2 (C) Screw configuration 3 (Methocel®100LV with 10% stearic acid ●, Methocel®100LV with 10% xylitol ●, Affinisol®100LV ●)

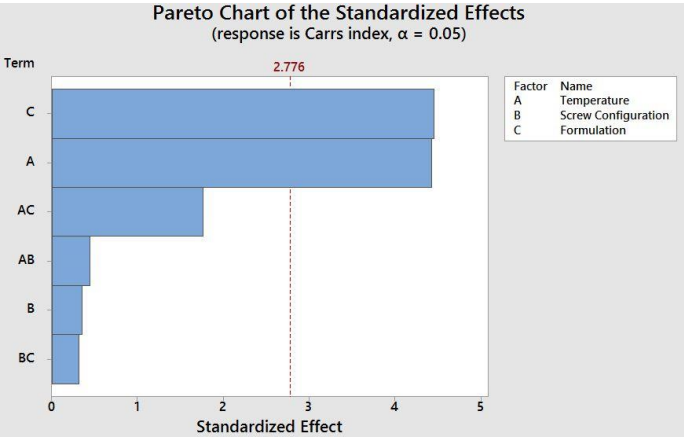

Figure 34: Pareto chart for influence of input variables on Carr's index

4.5 Compression strength

The granule strength was impacted significantly ($p<0.05$) by formulation type (Figure 40). The granules prepared with Methocel®100LV and xylitol had significantly greater strength compared to Methocel®100LV and stearic acid (Figure 39). This was due to lesser viscosity of xylitol compared to stearic acid and hence better spreadability over greater surface area and form greater bridges between powder particles. The properties of granules prepared from higher temperature of operation (tg of polymer) within the same formulation had higher strength compared to lower temperature (melt temperature of melt binder) as greater amount of granulation was observed in the former case, which increased the strength of solid bridges formed. Affinisol®100LV polymer was rubbery at both the temperatures where all the polymer particles were activated as opposed to Methocel®100LV at lower temperature only the melt binder attracts additional polymer and API powder. Hence Affinisol®100LV had higher strength than Methocel®100LV formulations.

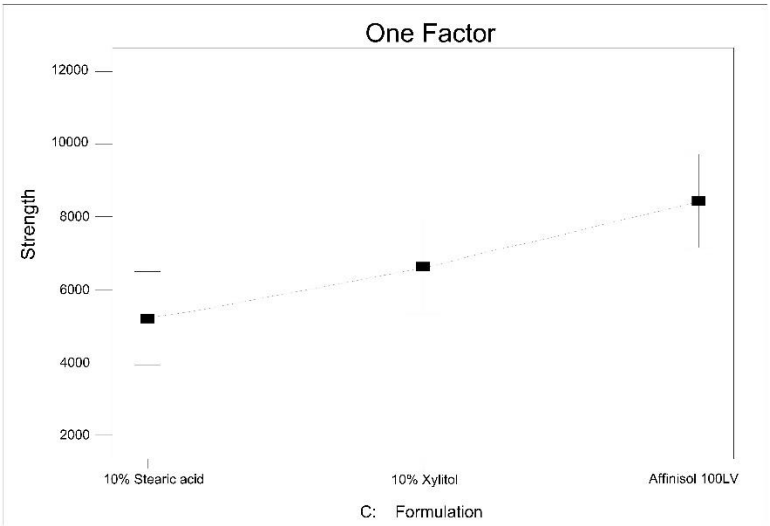

Figure 35: One factor- Plot of influence of formuation variables on strength (N/mm^2) of granules

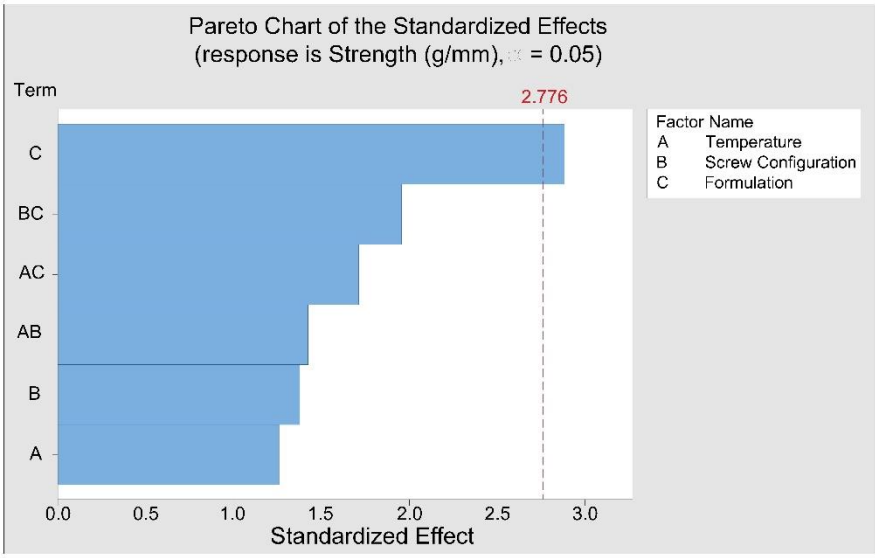

Figure 36: Pareto chart for influence of input variables on strength of granules (N/mm^2)

4.6 Percentage porosity

The formulation, temperature and screw configuration, all had significant impact on the percentage porosity as seen in the Pareto chart in Figure 42. Affinisol®100LV formulation, did not have significant difference in percent porosity at different temperature or different screw configuration (Figure 41A). Methocel®100 LV with stearic acid had lower percent porosity as compared to Affinisol®100 LV as the granules with Methocel®100 LV were easily size reduced due to low strength in the processing whereas Affinisol®100 LV had higher granule size due to greater strength and retained their basic structure. The pores inside the Affinisol®100 LV granules were hence retained while the Methocel®100 LV granules due to size reduction and particle breakage had reduced pores (Figure 41 B). All of the Methocel®100 LV with xylitol formulation had similar porosity as Methocel®100 LV with stearic acid except the one with SC3 due to least reduction of particle size and hence the pores in that formulation (Figure 41 C).

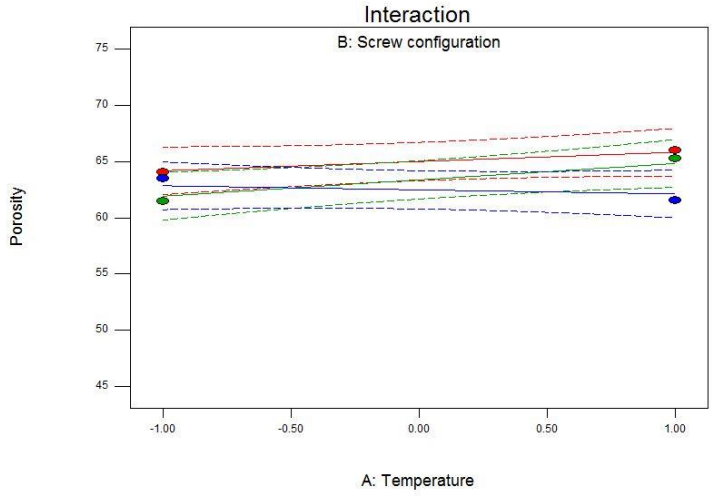

(A)

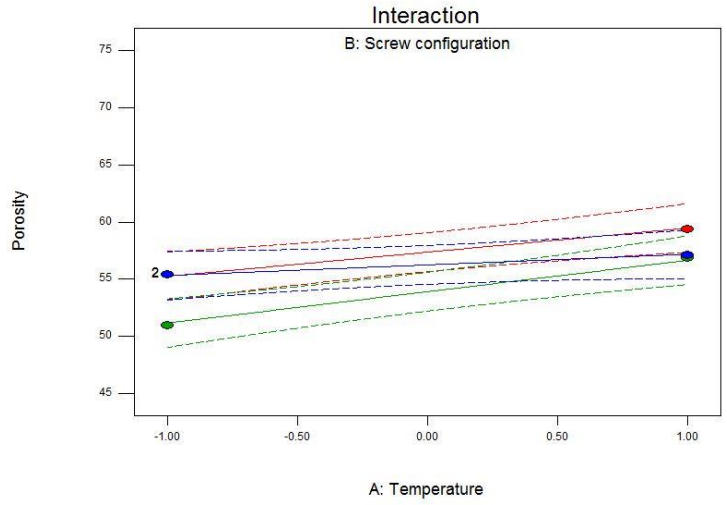

(B)

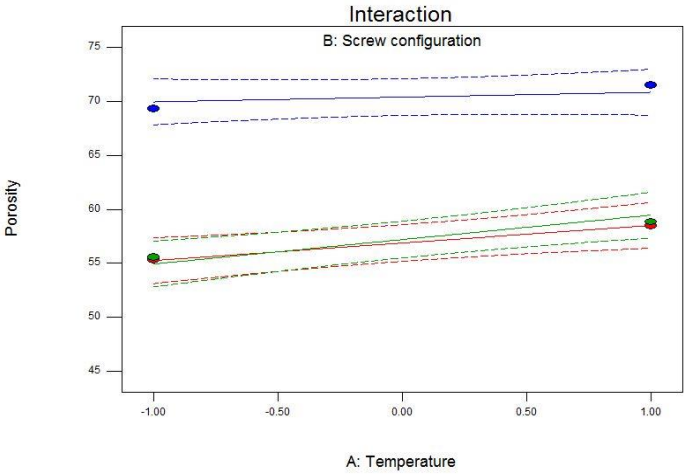

(C)

Figure 37: % Porosity of the granules (A) Affinisol®100LV (B) Methocel®100LV with 10% stearic acid (C) Methocel®100LV with 10% xylitol (SC1●, SC2●, SC3●)

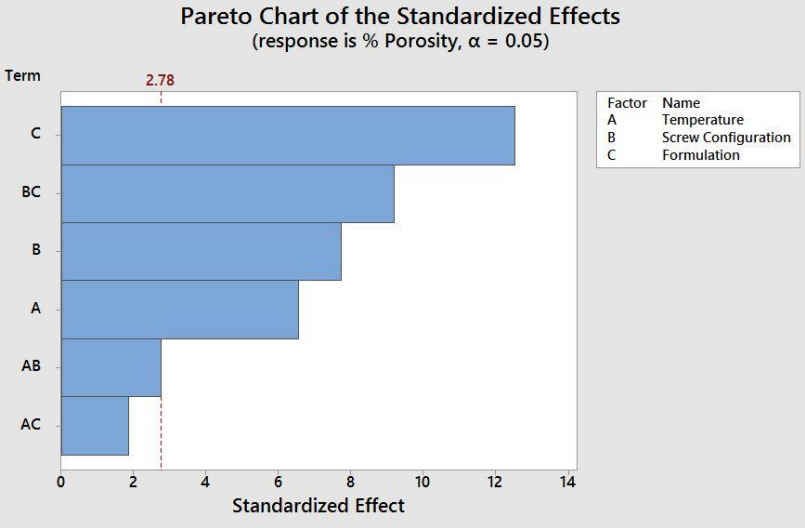

Figure 38: Pareto chart for influence of input variables on percent porosity

4.7 Tablet hardness

The hardness of tablets prepared from Methocel®100LV granules was dependent on the extrusion temperature and formulation type (Figure 44). The tablets prepared from Methocel®100LV granules using stearic acid had higher hardness at lower temperature and lower hardness at higher temperature (Figure 43A). The hardness of tablets prepared from Affinisol®100LV granules were independent of temperature and screw configuration (Figure 43C).

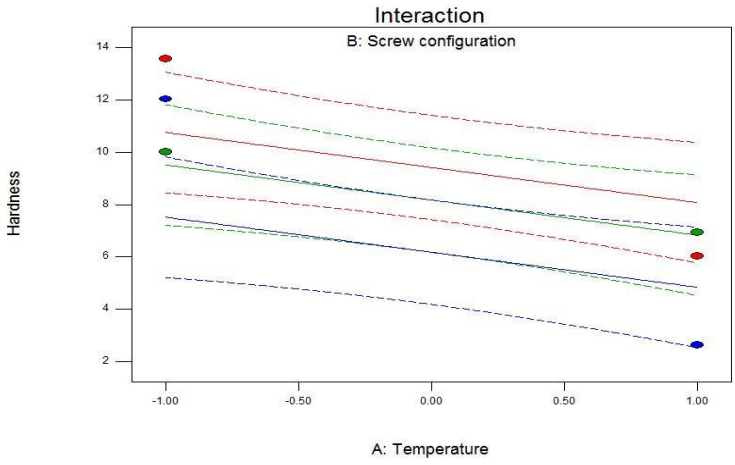

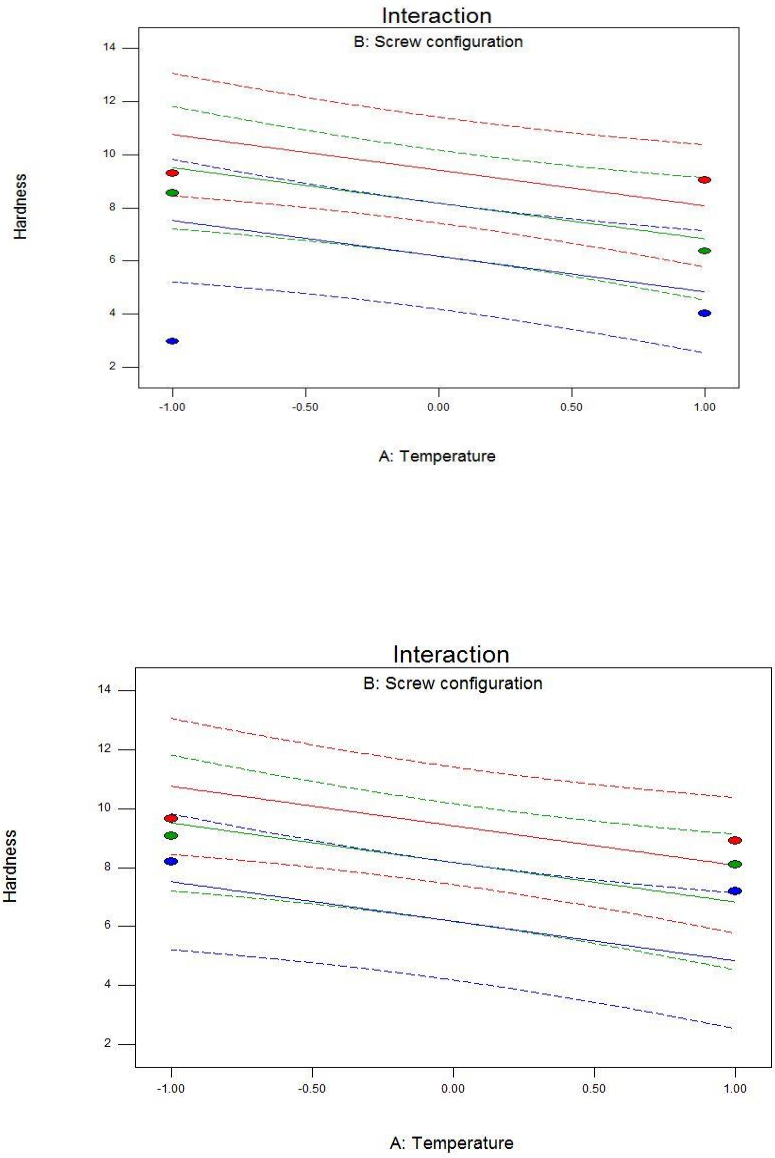

Figure 39: Effect of process variables on Hardness of tablet (SC1●, SC2●, SC3●)

(A) Methocel®100LV with 10% stearic acid (B) Methocel®100LV with 10% xylitol (C) Affinisol®100LV

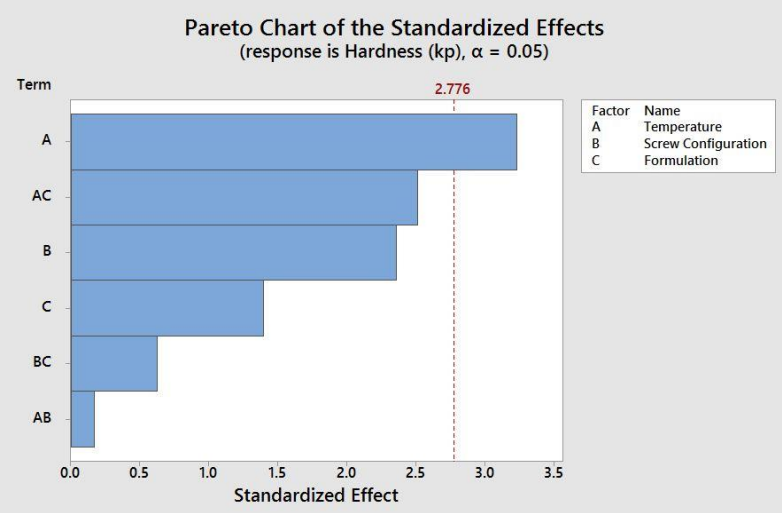

Figure 40: Pareto chart for evaluation of main effects and interaction between input variables on hardness of tablet

4.8 In-vitro Tablet dissolution

Percent drug dissolved was one of the output parameters investigated, where percent of drug dissolved at the end of 12 hours was plotted. Dissolution profiles revealed sustained release behavior for 12-16 h, which was dependent on formulation significantly (Figure 47). Affinisol®100LV granules exhibited the highest sustained release profile followed by Methocel®100LV granules using stearic acid and Methocel®100LV granules with xylitol (Figure 45). It was observed all granule formulations (except Methocel®100LV + xylitol) extruded at lower temperatures using SC3, exhibited lower in-vitro release in 12h (73%) (Figure 46). Xylitol acted as a pore former which increased the diffusion of drug into the dissolution matrix. The dissolution profile was pH independent for all formulations.

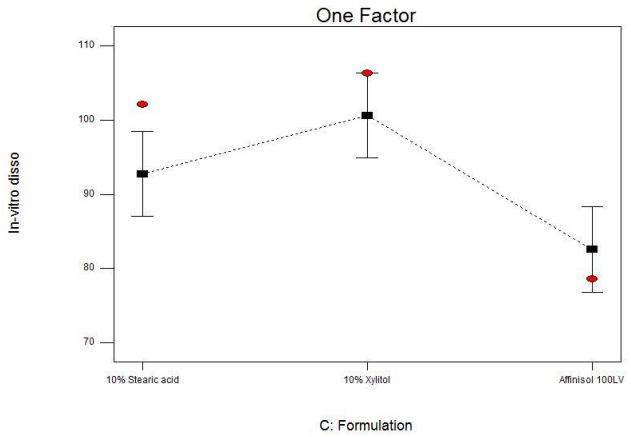

Figure 41: One factor- Impact of formulation variables on the in-vitro dissolution rate

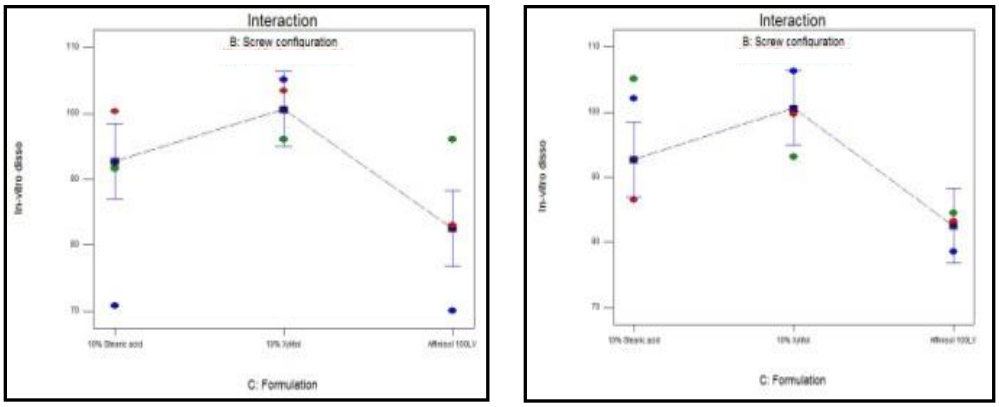

Figure 42: Interaction plot- Impact of formulation variables and screw configuration on the in-vitro dissolution rate (SC1●, SC2●, SC3●) (A) Low temperature (B) High temperature

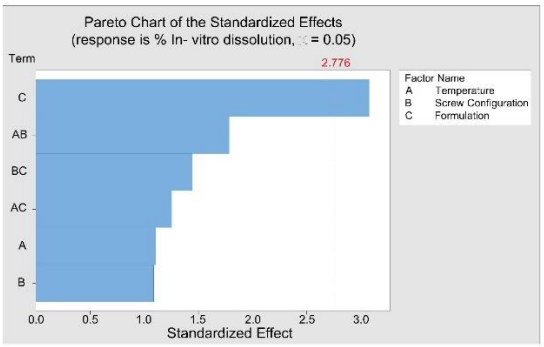

Figure 43: Pareto chart for evaluation of main effects and interaction between input variables on in-vitro dissolution of tablet

4.9 Desirability index

The desired or optimum process and formulation parameters were plotted (Figure 48) from Design Expert® software which resulted in lowest value of in-vitro dissolution (Y1), low Carr's index and Hausner's ratio (Y2), high granule strength (Y3), unimodal granule size distribution (Y4), high hardness (Y5). The optimum process conditions (desirability of 0.75) were Screw configuration 3, Affinisol®100LV as release modifying polymer, higher (120°C) temperature of extrusion to achieve <80% in-vitro dissolution in 12 hours, Carr's index of 9, Hausner's ratio of 1.1, granule size distribution of 800-2000 µm, granule strength of 10478 N/mm^2 and tablet hardness of 8.

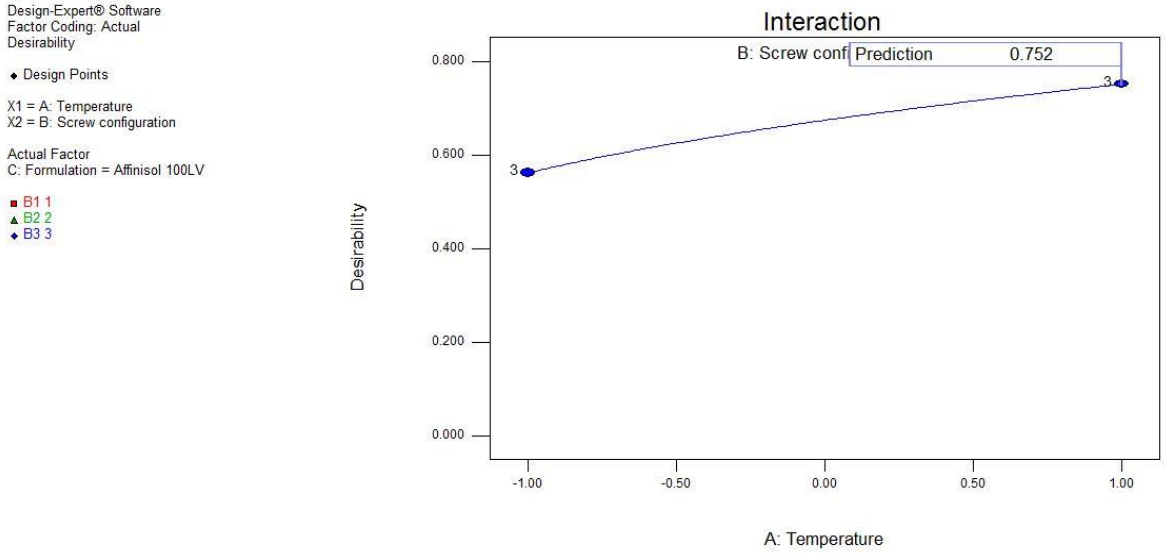

Figure 44: Desirability index plot for optimal processing

5. Conclusion

Particle size of granules depended on screw configuration ($p<0.05$) and reduced with addition of 2nd mixing block and DME. SC3 resulted in producing uniform and larger granules. Parsum probe IPP®80 in-line particle size analyzer was successfully applied as a PAT tool to study the impact of processing and formulation parameters on twin screw melt granulation processes. The understanding of the geometric aspects of the screw elements and their effect on the maximum size of granules from a real time particle size analysis probe in a twin Screw Granulator is a step towards tailored granule size distributions. By choosing a certain type and design of the screw elements, the breakage mechanisms in the granulator can be modified resulting in broad mono-modal or bimodal granule size distributions. Affinisol®100LV holds greater promise to serve as a sustained release polymer matrix with 70% drug loading to achieve release over 18hrs. Also, the granule properties of the Affinisol®100LV granules did not vary significantly with changing process parameters and delivered the desired output.

IV. CHAPTER

Monitoring the molecular interaction of Indomethacin with co-former during hot-melt extrusion using in-line FT-NIR for enhancing dissolution rate of poorly water soluble compound

1. Introduction

With the advent of combinatorial chemistry and high throughput screening, most of the newly synthesized small molecules in the drug discovery pipelines have been extremely insoluble in aqueous media. As a consequence, they have low dissolution rates and exhibit poor and variable bioavailability after oral administration to animals and humans. Many enabling methodologies, including salt formation, co-crystallization, particle size reduction, lipid-based delivery, and amorphous solid dispersion, have been employed to enhance dissolution rate and oral bioavailability of such compounds (Aakeröy, Fasulo, & Desper, 2007; Pudlas et al., 2015). However, each of these methodologies has its own limitations. In recent years, there has also been much interest in amorphous solid dispersions. At the early stage of drug development, amorphous solid dispersions are usually prepared by spray drying, which requires large volumes of organic solvents to simultaneously dissolve drug and carrier, thus creating solvent handling issues during manufacturing. The physical instability due to recrystallization of the drug from, solubilized or amorphous state, is also a major issue for the amorphous solid dispersion (Qian, Huang, & Hussain, 2010). Salt formation of these poorly water soluble moieties is an excellent method to overcome such disadvantages. However, the manufacture of salts on relatively large scales remains a

complex process. Commonly used manufacturing techniques for salt formation require very large volumes of organic solvents and high temperatures to dissolve drugs and salt forming agents, enable chemical reaction, and obtain salts in crystalline states. Moreover, these are batch processes rather than continuous ones. Since salts may be considered as new APIs and thus enjoy patent protection, they are considered more valuable than co-crystals in pharmaceutical development. Salts are generally prepared by acid–base reaction in relatively large volumes of organic solvents, followed by crystallization (Lee et al., 2017). In this study, the potential for preparing a pharmaceutical salt between Indomethacin (Indo) (water solubility 0.9 µg/ml, pKa 4.5) and Tromethamine (Tro) (highly water soluble, pKa 8.1) by a novel solvent-free method using a twin-screw melt extruder was investigated. In-addition, the continuous preparation of the salt was monitored via an in-line FT-NIR probe to determine the extrusion conditions that result in complete interaction between the weakly acidic API and basic co-former to obtain a crystalline salt. The pH–solubility relationship between Indo and Tro in aqueous medium was first determined, which demonstrated that 1:1 salt formation between them was feasible (pH_{max} 8.1; salt solubility 19.3 mg/mL). Salts were also prepared by solution crystallization from 200 proof ethanol and compared with those obtained by melt extrusion.

2. Materials

Indomethacin ($C_{19}H_{16}ClNO_4$, ≥ 98% purity, MW: 357.79 g/mol, M.P. 162°C, pKa 4.5) was purchased from Combi-Blocks, Inc. (San Diego, California). Tromethamine ($C_4H_{11}NO_3$, ≥99% purity, MW: 121.136g/mol, M.P. 142°C (metastable polymorph) 171°C (stable polymorph), pKa 8.07) was obtained from AK Scientific, Inc. (Union City, California). All organic solvents and other chemicals used were of analytical reagent grade from Fisher Scientific (Waltham, Massachusetts).

3. Methods

3.1 FTIR spectroscopy

Spectra were obtained using an attenuated total reflectance (ATR) accessory (single reflection germanium crystal) and a DLaTGS detector. The resolution was 4 cm−1, and 32 scans were acquired in the range of 4000–400 cm^{-1}. The peak positions were determined using Resolutions Pro software peak picking function.

3.2 X-ray Diffraction

Morphology of the powder samples was investigated using a Benchtop X-ray diffraction instrument; Model Miniflex 600 (Rigaku, Woodlands, TX) with primary monochromated radiation (CuK radiation source, λ = 1.54056 A°). The instrument was operated at an accelerating voltage of 40 kV and 15 mA. All samples were subjected to the same program; scanned over a 2h range of 5–40° 2θ at a step size of 0.04° 2θ/s, a dwell time of 2 s and scan speed of 1°/min.

3.3 Differential Scanning Calorimetry (DSC)

DSC studies were performed with a TA Instruments (Q25) differential scanning calorimeter (DSC) equipped with Trios software. Samples were prepared by sealing 5-7 mg of pure API, physical mixtures, blank formulations, drug loaded extrudates in non- hermetically sealed aluminum pans and heated from the temperature range of 30°C to 100°C at the heating rate of 20°C/min under an inert nitrogen atmosphere at a flow rate of 20 mL/min.

3.4 In-vitro dissolution

In-vitro dissolution was carried out using USP (Type I – Basket apparatus) using pH 7.2 phosphate buffer medium under sink conditions maintained at 37°C according to the USP guidelines. The

milled extrudates were filled into capsules where a dose equivalent to 50mg of Indo was accurately weighed into one capsule. The in-vitro dissolution samples were taken at 5, 15, 30, 45, 60, 120 mins and analyzed using reverse phase HPLC method. Analysis was performed using C-18 column (150mm×4.6 mm, 5 µm), mobile phase of 50:50 acetonitrile and water containing 0.2% phosphoric acid at 0.8 ml/min flow rate at 254 nm detection wavelength (Nováková, Matysová, Havlíková, & Solich, 2005).

3.5 Proton and Carbon Nuclear Magnetic Resonance (^{1}H and ^{13}C NMR)

Solution Proton and Carbon Nuclear Magnetic Resonance (^{1}H and ^{13}C NMR) was performed in an NMR spectrometer (Bruker AM-400 Spectrometer) and used to determine the identity of a substance and formation of salt by determining the number of hydrogen atoms. Samples in the present study were dissolved in deuterated DMSO for measurement. NMR spectra were acquired using a BBI 1H/D-BB Z-GRD probe with a scan number of 16 at 298 K, and the acquisition time was 1 min and 32 s. In addition, Dept 135 analysis was performed to confirm the salt formation.

3.6 Indomethacin and tromethamine salt preparation

3.6.1 Hot-melt extrusion

The physical blend of Indo and Tro in a 1:1 molar ratio was prepared in a V-Blender for uniform mixing, and the blend was then fed into a twin screw extruder with screw Configurations depicted in Figure 49. The operating parameters and conditions were listed in Table 9. During extrusion, the physical blend converted to the tacky semisolid melt and then formed a thin layer on the inner contact surface of the extruder barrel. Consequently, much viscous dissipation was created among the tacky melt, the co-rotating twin screws, and the inner surface of the extruder barrel. Due to the

conversion of the blend to tacky material during extrusion, it took from 3-7 mins between the feeding of the blend into the extruder and the exit of the product (residence time).

Formulation	Temperature (°C)	Screw speed (rpm)	Feed rate (%)	Feed rate (g/min)	Screw configuration
F-1	135	200	15	3.2	1
F-2	135	200	7	1.6	1
F-3	145	200	7	1.6	1
F-4	135	100	7	1.6	1
F-5	135	100	15	3.2	1
F-6	145	100	7	1.6	1
F-7	145	100	15	3.2	1
F-8	155	100	7	1.6	1
F-9	155	100	15	3.2	1
F-10	135	100	15	3.2	2

Table 9: Extrusion conditions used for preparation of Indo: Tro salts on 11mm Thermo Scientific®

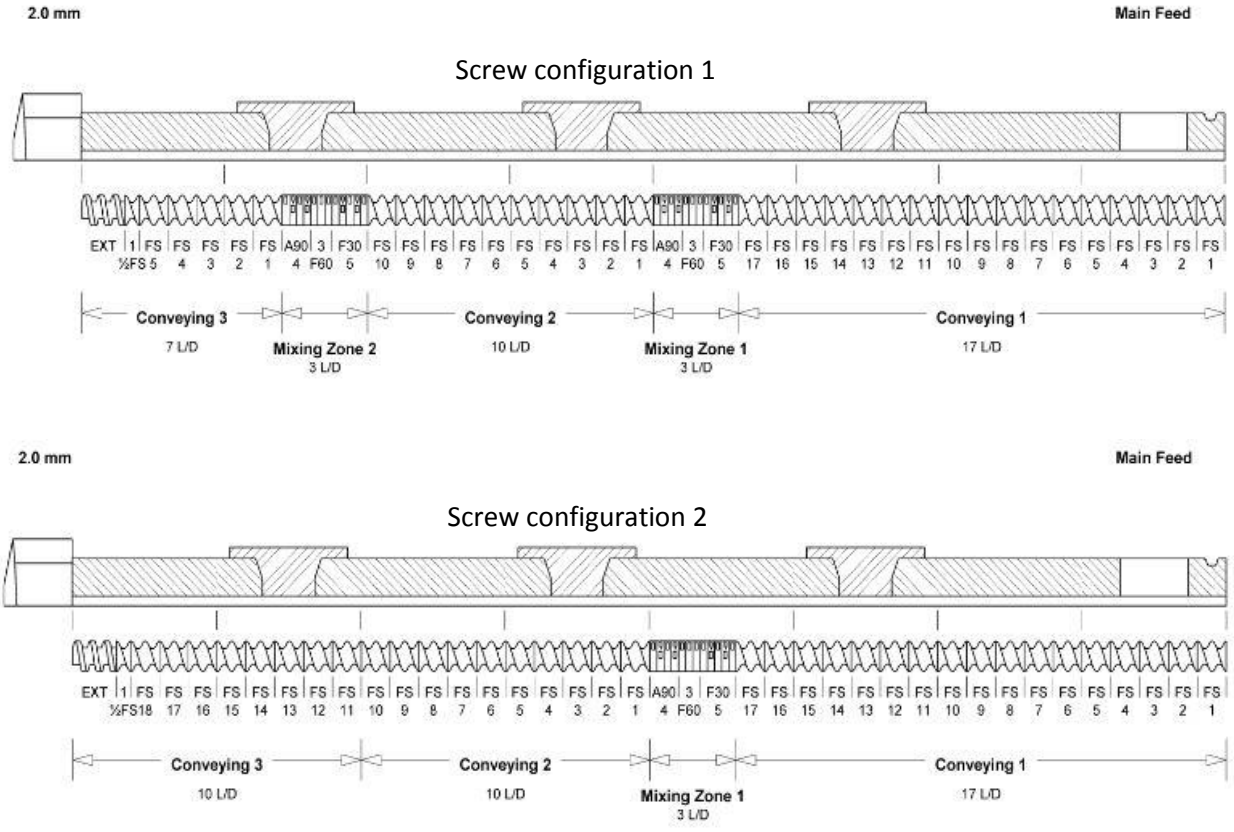

Figure 45 (A): Screw configuration 1 and 2 used for formulation of Indo-Tro salt

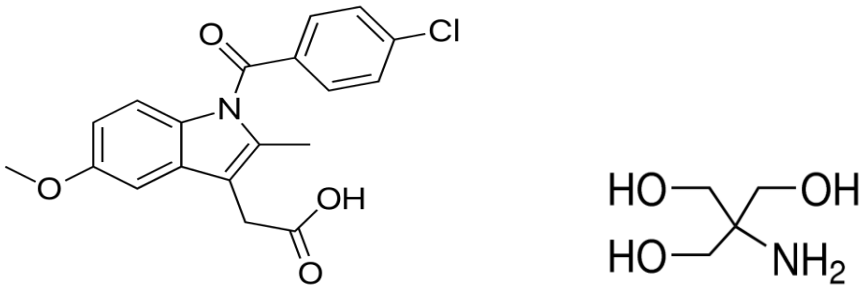

(i) Indomethacin (ii) Tromethamine

Figure 49 (B): Molecular structure of indomethacin and Tromethamine

3.6.2 Solvent evaporation

1:1 molar ratio of Indo and Tro were accurately weighed and blended using a V-Blender for 15 mins. The physical mixture was added to 200 proof ethanol (not saturated) and stirred using a magnetic stir bar until complete clear solution was achieved. This solution was rotary evaporated at 60°C at 200 rpm for 2 hours and dried using a vacuum desiccator until constant weight was achieved. 1:1 salt of Indo:Tro was thus achieved using solvent evaporation technique.

3.7 FT-NIR study

Diffuse reflectance NIR spectra were continuously collected inline and non-invasively during hot-melt extrusion using a Fourier- Transform NIR spectrometer (Thermo Fisher Scientific, Antaris II near-IR analyzer) equipped with an InGaAs detector, a quartz halogen lamp, and a fibre-optic probe which was mounted in the extrusion die. Spectra were collected every 16 s in the 9000–4500 cm^{-1} region with a resolution of 16 cm^{-1} and averaged over 8 scans (Wahl et al., 2013).

4. Results and Discussion

A general idea of the possible mechanism of salt formation by TSE may be obtained from previous investigations in preparing known co-crystals via TSE, which revealed that co-crystals may be mediated through eutectic formation. In general, the eutectic melt undergoes super-saturation that results in crystallization from the melt to form a co-crystal, whose melting is higher than the eutectic temperature. The phenomenon of eutectic formation can be observed by hot-stage microscopy.

4.1 FTIR spectroscopy

From Figure 50 (A), the overlay plot of FTIR spectra of pure indomethacin, pure tromethamine, Indo:Tro 1:1 and Indo:Tro 2:1 blends, obtained by solvent evaporation. Salt formation was confirmed by the disappearance of the C=O carboxyl functional group at around 1710 cm^{-1} and appearance of COO^- at 1550 cm^{-1} in Indo: Tro 1:1, which was not seen in Indo: Tro 2:1 (Coates, 2000). In addition, from figure 50 (B) (C) (D) (E) which corresponds to F-1, F-2, F-3, F-10 hot melt extrudates, shift of the asymmetric ionized COO^- was seen in formulations F-1, F-2, F-10 but not in F-3. F-3 showed a broad shoulder at 1710 cm^{-1} indicating presence of crystalline Indo precipitated from amorphous salt. Thus optimum salt formation was seen when extrusion was carried out at 135°C.

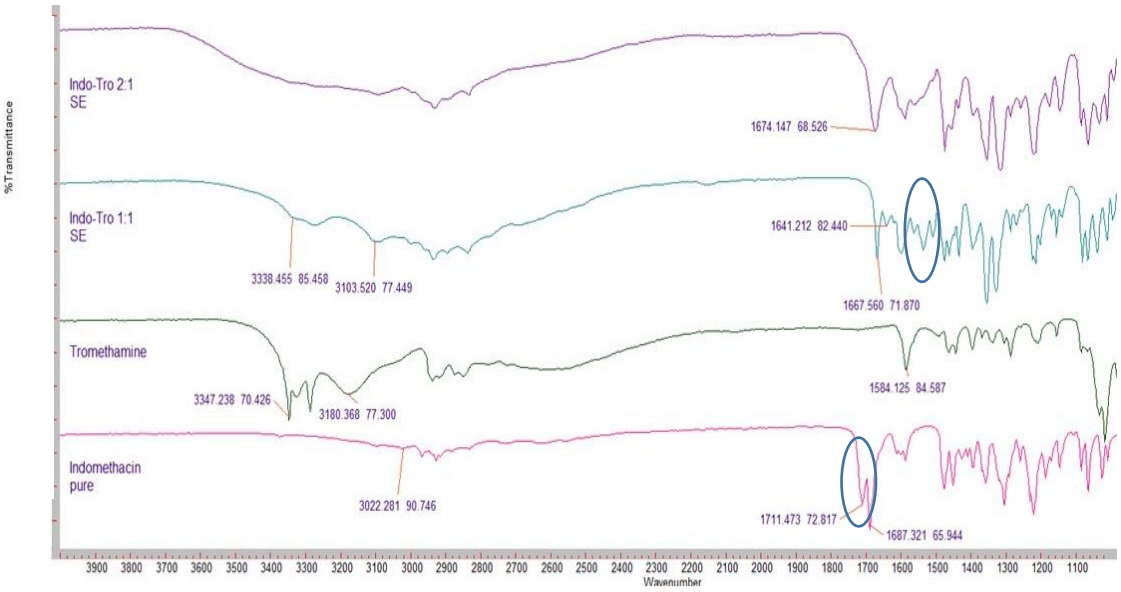

Figure 46 (A): Overlay spectra of pure indomethacin, tromethamine, Indo:Tro 1:1 and 2:1 SE (solvent evaporation) formulation

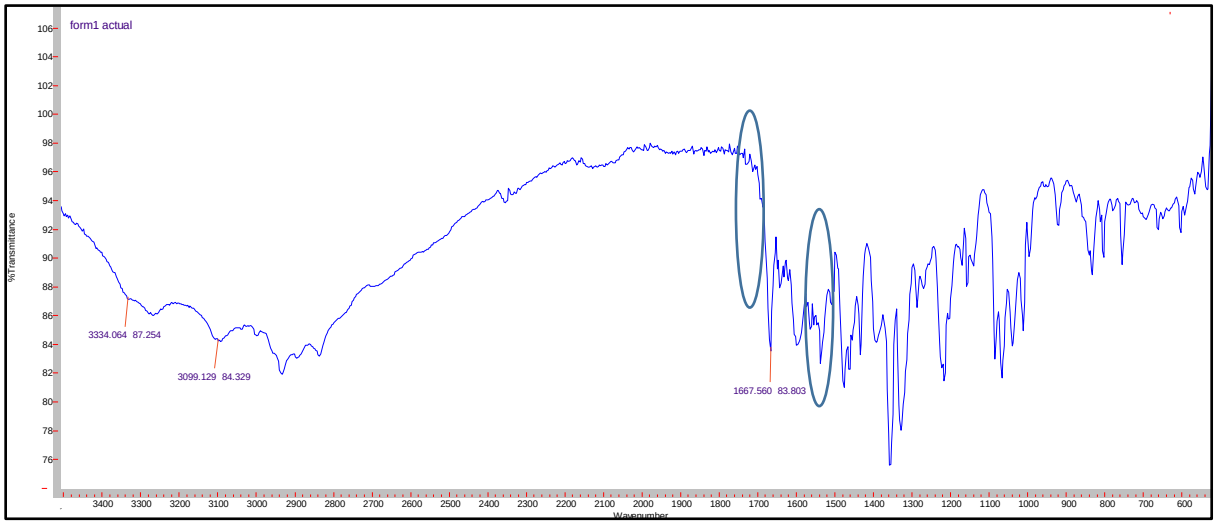

Figure 50 (B): FTIR spectra of Indo:Tro hot melt extrudate F-1

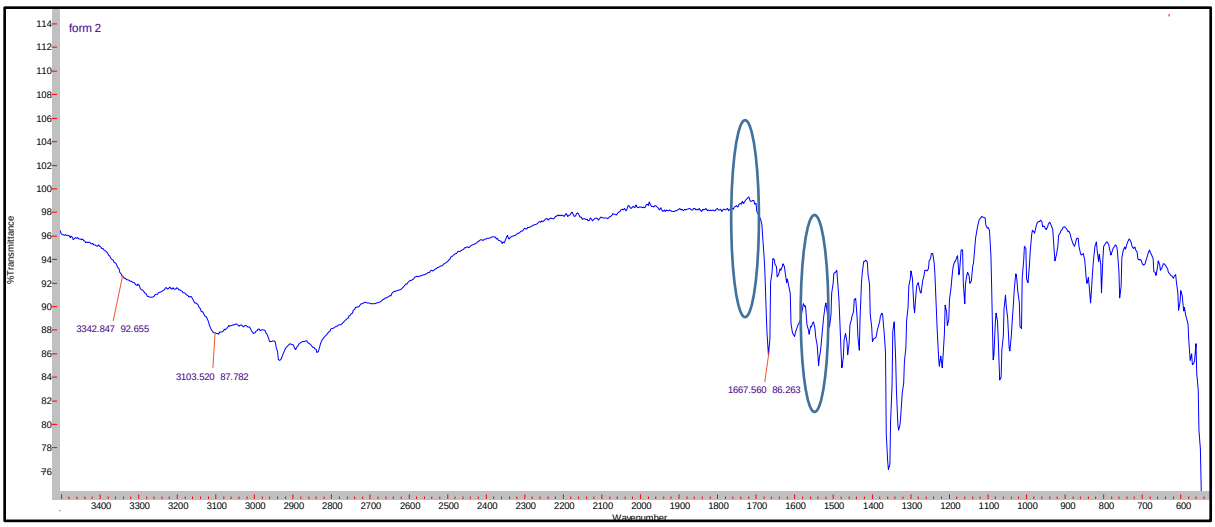

Figure 50 (C): FTIR spectra of Indo:Tro hot melt extrudate F-2

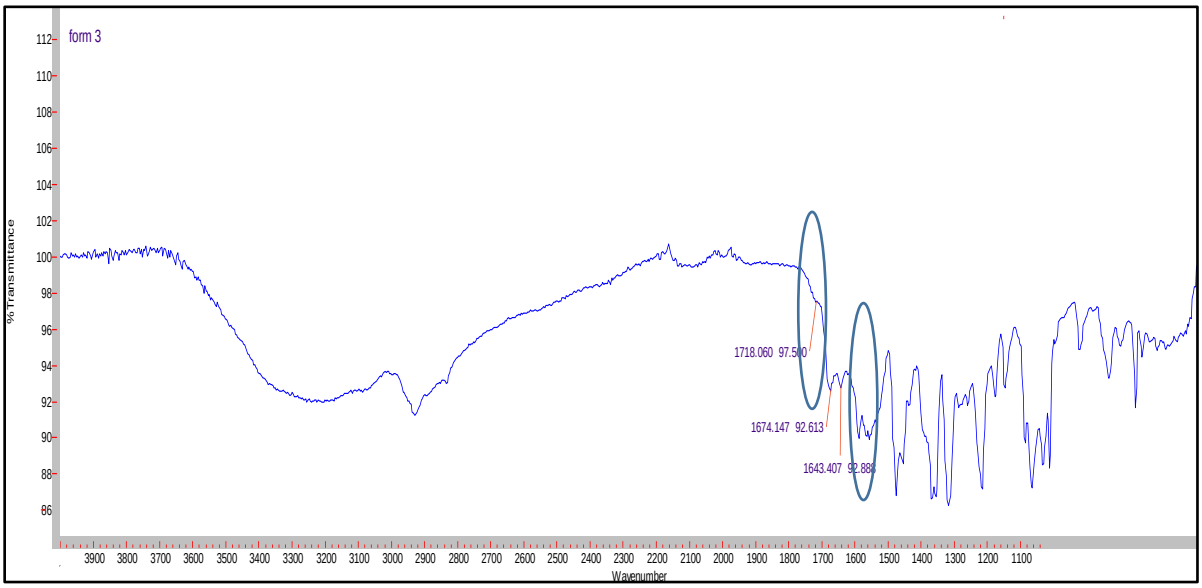

Figure 50 (D): FTIR spectra of Indo:Tro hot melt extrudate F-3

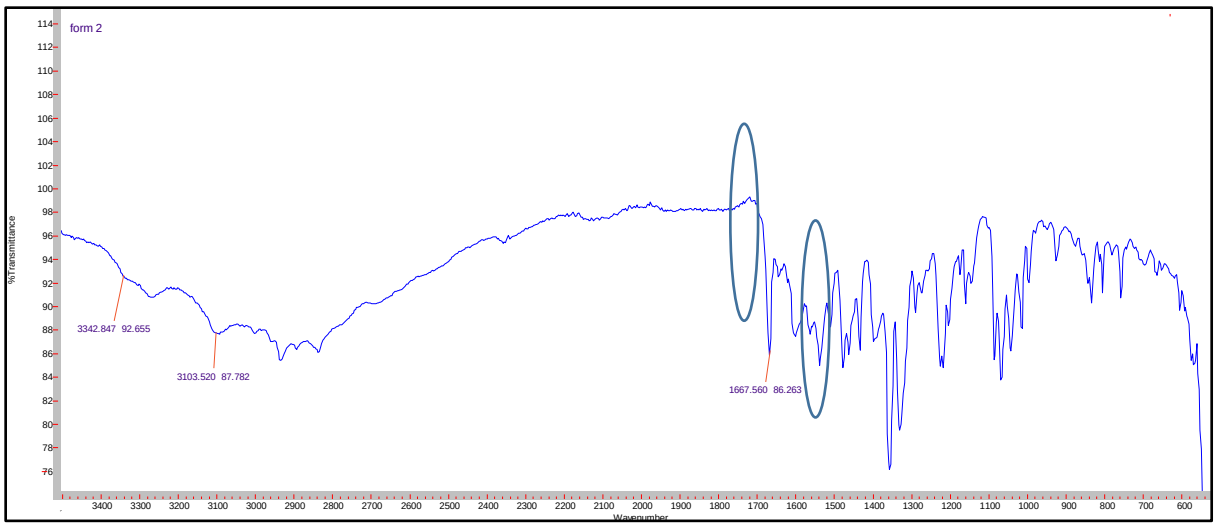

Figure 50 (E): FTIR spectra of Indo:Tro hot melt extrudate F-10

4.2 Differential Scanning Calorimetry

The DSC thermograms in Figure 51 (A) shows that Pure Indo melted at 160°C and pure TRO melted at 148 °C (metastable polymorph) and 174 °C, respectively. The Indo: Tro hot-melt extrudates, specifically F-1, F-2, F-10 showed endothermic melting events below the individual melting points. These low "eutectic-like" endothermic events were due to the suppression of Indo melting in the presence of Tro. The salt obtained by hot-melt extrusion had a melting point of 142 °C which was similar to the melting point of the salt prepared by solvent evaporation (SE). F-3 was observed to be amorphous due to extrusion above the melting temperature of the salt. It also showed small melting endotherm at 160°C (not seen in image due to overlay) which corresponds to Indo which might have precipitated out. Also, F-1 and F-2 had comparable enthalpy of melting compared to F-10 which had greater enthalpy of melting. Figure 51 (B) shows that F-4 was also crystalline sals of Indo:Tro having a melting point similar to the salt obtained from solvent evaporation. The lower enthalpy of F-4 compared to the SE salt, which indicates incomplete

crystallization. Thus it could be concluded that extrusion conditions of high feed rate (3.2g/min), low screw speed (100 rpm), low temperature (135 °C), low shear screw configuration were essential for formation of crystalline salt of Indo.

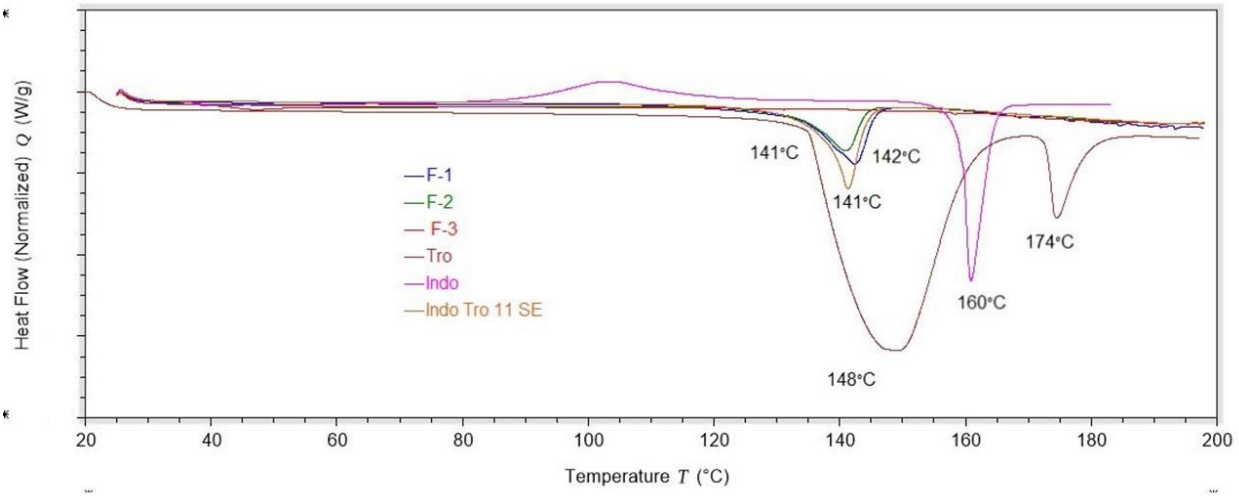

Figure 47 (A): DSC thermograms of Pure Indo, Pure Tro and 1:1 hot melt extrudates

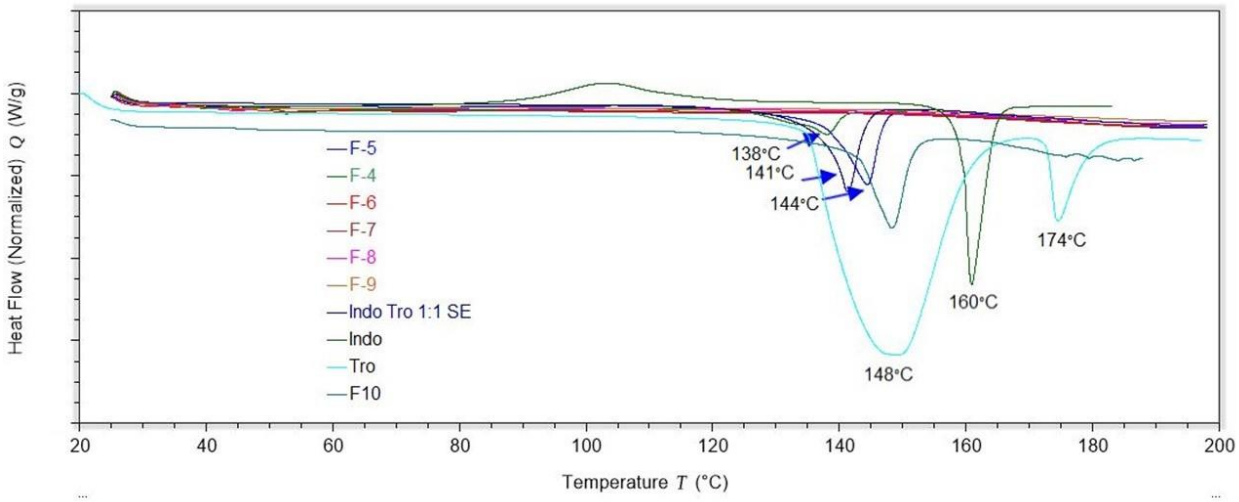

Figure 51 (B): DSC thermograms of Pure Indo, Pure Tro and 1:1 hot melt extrudates

4.3 X-ray Diffraction

Figure 52 (A) (B) depicts the X-ray diffractograms of crystalline (F-1, F-2, F-10, SE) and amorphous (F-3, F-4, F-5, F-6) formulations. It can be seen that the characteristic new 2θ peak at 13.6° for the F-1, F-2, F-10 salt which was not present in the pure components indicates formulation of a third crystal structure different from Indo and Tro. F-3, F-4, F-5 was observed to be amorphous due to no Braggs peaks present in the diffractogram. The minimal crystallinity of F-4 formulation observed in previous DSC data was not detected in XRD study. The maximum intensity peak was observed with F-10 which implies maximum new crystal content in the formulation. X-Ray diffraction study confirms with the observation of DSC study (Thakral & Suryanarayanan, 2015).

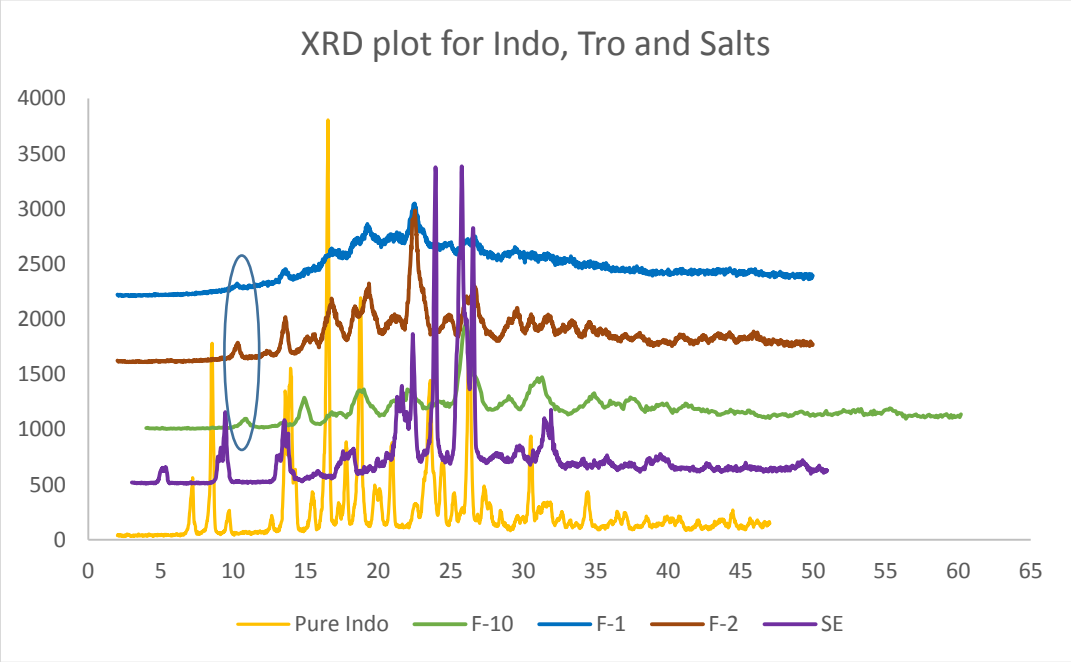

Figure 48 (A) XRD diffractograms of SE salt, F-1,F-2, F-10 crystalline formulation with pure components

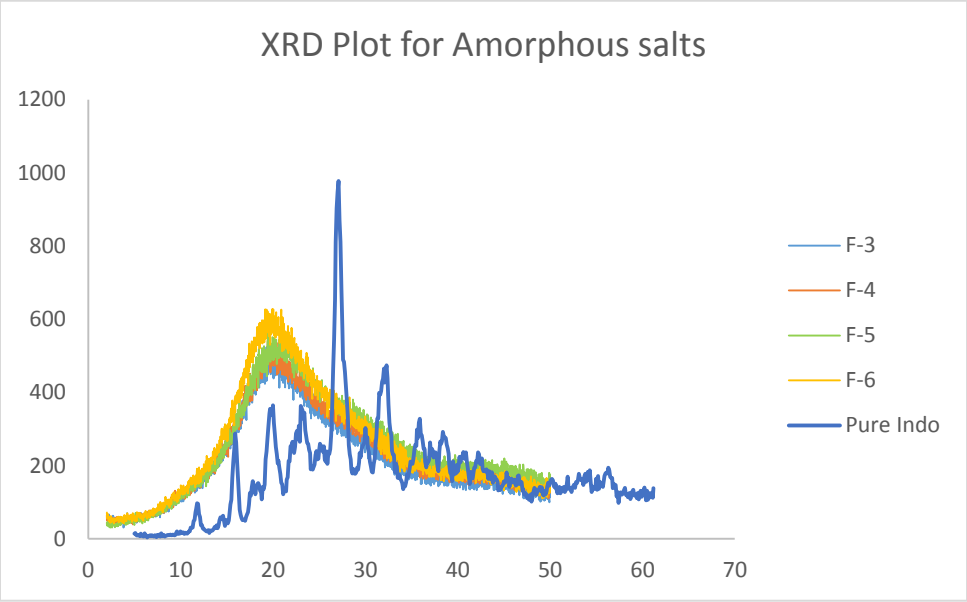

Figure 52 (B) XRD diffractograms of F-3, F-4, F-5, F-6 amorphous formulation with pure components

4.4 In-vitro dissolution

From figure 53 (A) and (B), formulations F1-F3 have >85% in-vitro drug release of in first 15 mins whereas pure Indo and physical mixture only had 5% and 52% release respectively. F-3 had lower drug release compared to F-1 due to small amount of crystalline indomethacin precipitated from amorphous salt. Formulations F-4 to F-10 also have >85% in-vitro drug release of in first 15 mins. F-10 had the highest drug release compared to other extruded formulations due to highest crystalline salt content in the formulation.

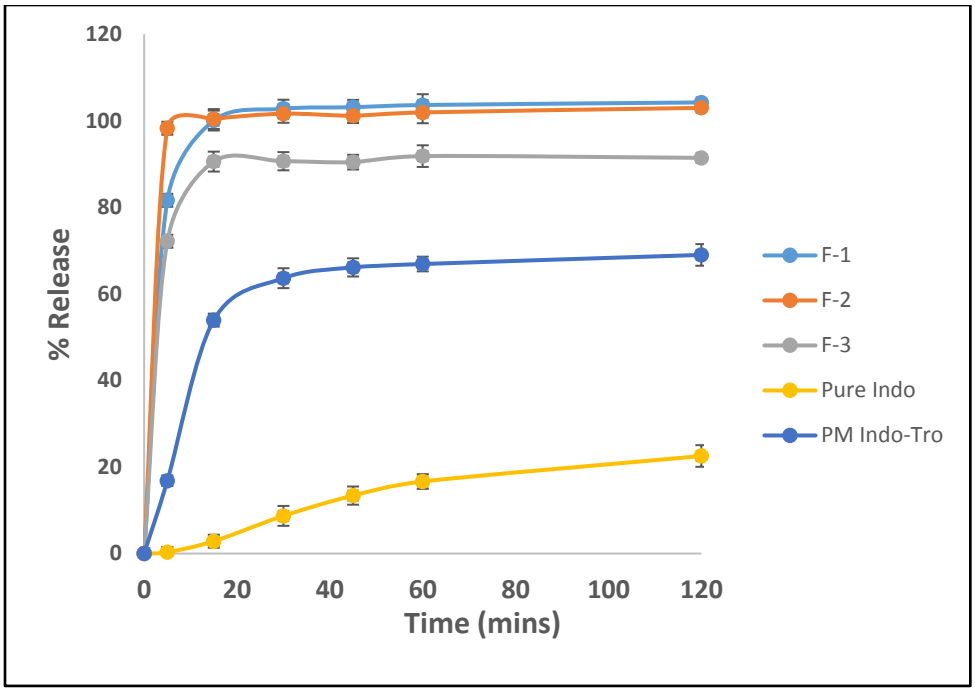

Figure 49 (A): In-vitro dissolution profile of F-1- F-3 extruded formulations

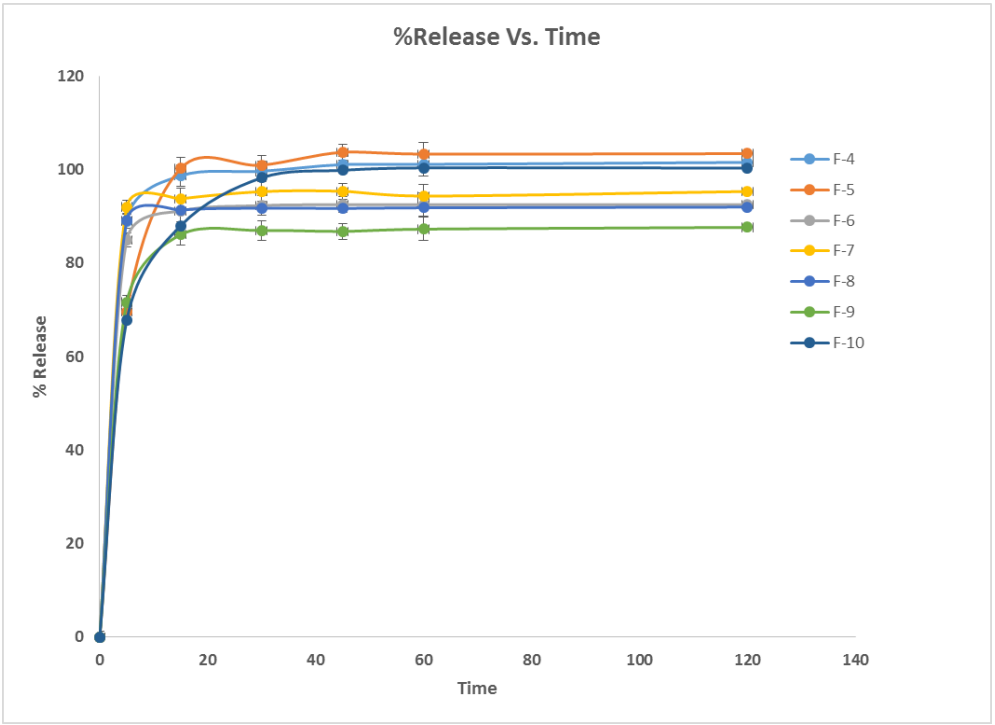

Figure 53 (B): In-vitro dissolution profile of F-4- F-10 extruded formulations

4.5 NMR spectroscopy

Figure 54 (A, B,C,D) depicts the ^{1}H- NMR spectra of Pure Indo, Pure Tro, SE salt formulation, F-2, F-10 and F-3 salt. It can be inferred from the plot that peak for –CH2 group beside the –COOH carboxylate (refer Figure 49 B) group in the F-1, F-3, SE salt shifts from 3.66 ppm to 3.45 ppm due to formation of $–COO^-$ ion. This indicates formation of salt in the extrudate as well as solvent evaporated formulation. The peaks for $–OCH_3$ and $–CH_3$ groups in Indo which occur at 3.7 ppm and 2.19ppm respectively stay constant in the formulations as well. The responses appearing between 6.5- 7.7 ppm, correspond to aromatic benzene –CH– groups of Indo which also stay constant in all the formulations. ^{13}C NMR was performed to check for the formation of salt which would be clearly depicted than ^{1}H- NMR study due to presence of single $–CH_2$ group that needs to be monitored. From Figure 55 (A, B) it can be observed that the $–CH_2$ and –C=O peak for the indomethacin which appeared at 29.5 ppm and 172.1ppm shifted to 32.8ppm and 174.4ppm respectively which indicated ionization of the carboxylic acid group and hence salt formation. Also 135 DEPT analysis was used to confirm the shift of $–CH_2$ group, as indomethacin converts to salt form (F-10). In 135 DEPT analysis all the $–CH_2$ peaks appear on the bottom of the baseline while the –CH peaks appear on the top of the baseline. As indomethacin has only one $–CH_2$ it was clearly depicted by the bottom position of the peak at 29.5ppm. The shift of bottom peak at 29.5ppm to top peak at 32.8ppm (due to shift of proton from $–CH_2$ to form –CH) was observed as hence salt formation via extrusion was confirmed.

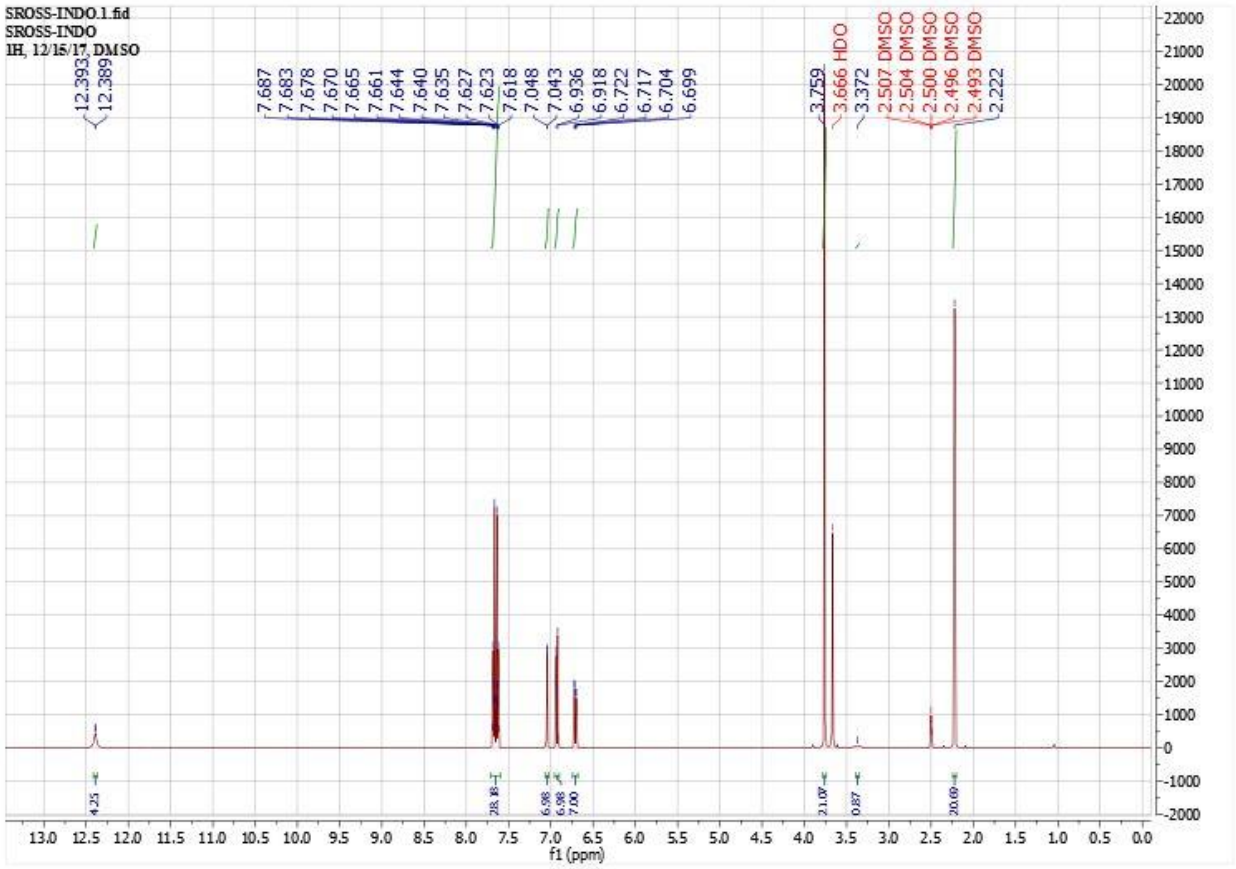

Figure 50 (A): ^{1}H- NMR spectroscopy of Pure Indomethacin in DMSO-d6 at 400 Mhz

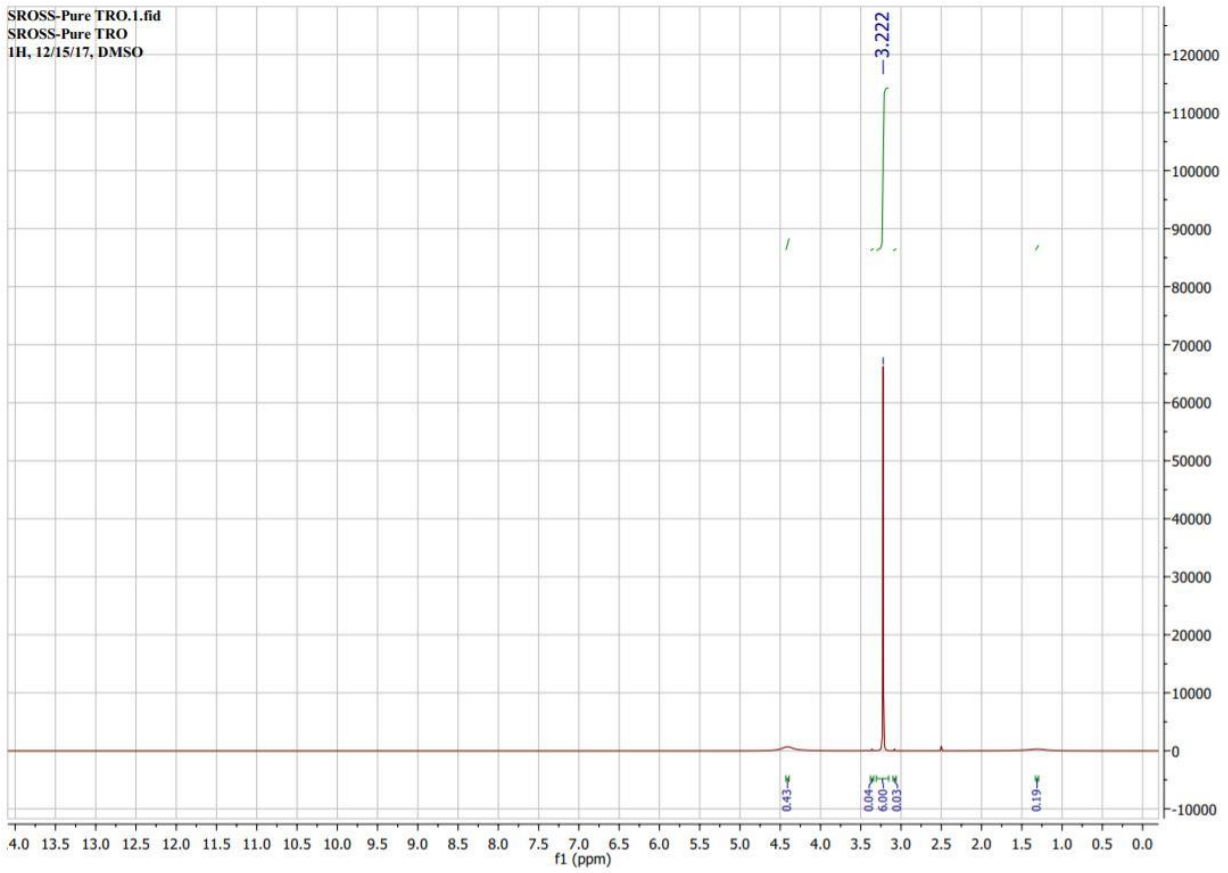

Figure 54 (B): ^{1}H- NMR spectroscopy of Pure Tromethamine in DMSO-d6 at 400 Mhz

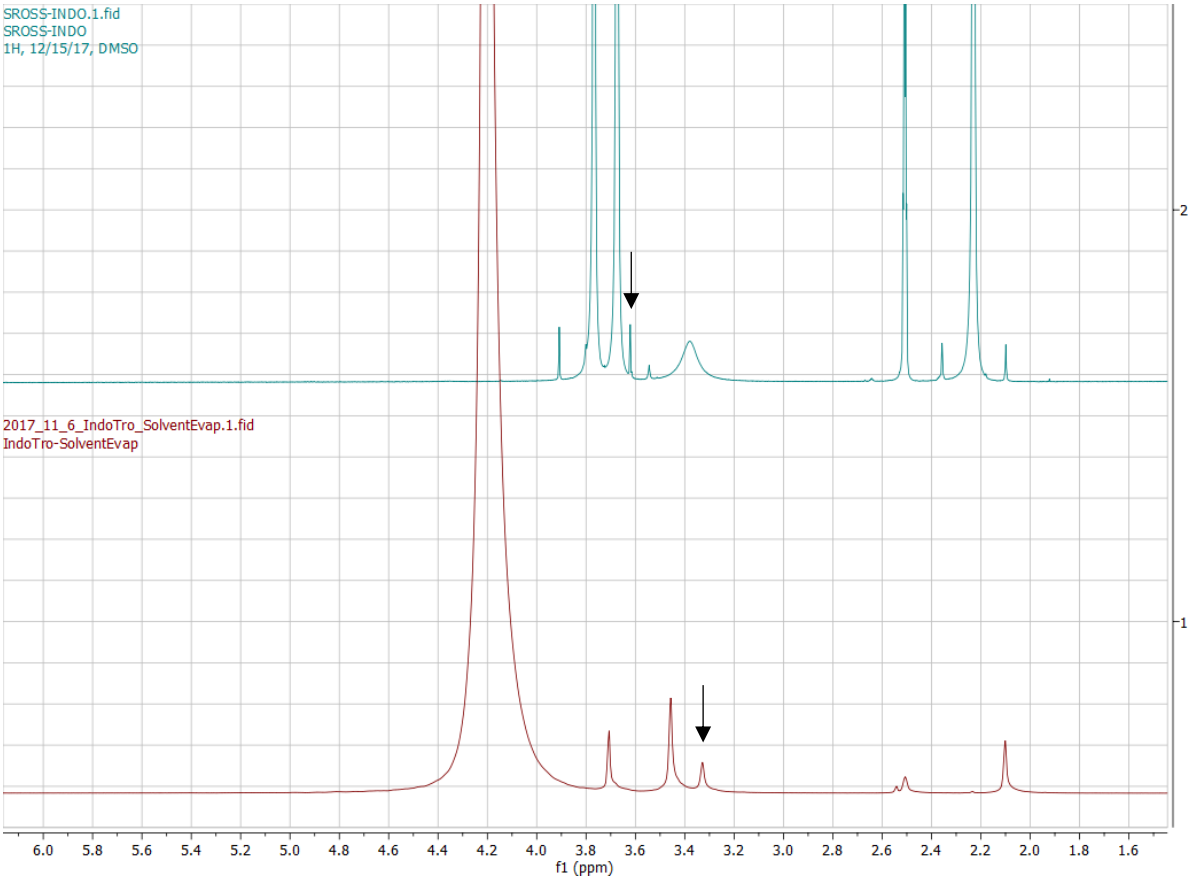

Figure 54 (C): ^{1}H- NMR spectroscopy of 1) Pure Indomethacin 2) SE salt in DMSO-d6 at 400 Mhz

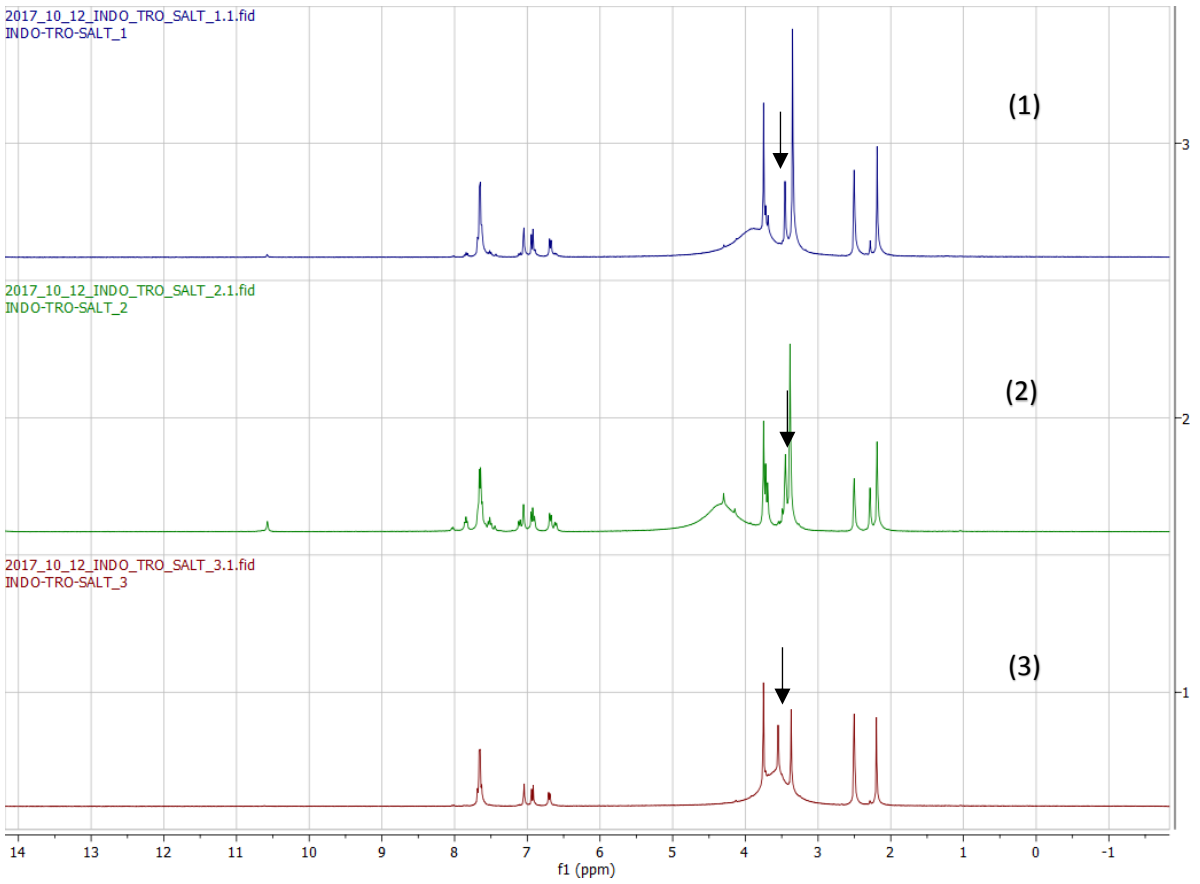

Figure 54 (D): ^{1}H- NMR spectroscopy of 1) F-2 salt 2) F-10 salt 3) F-3 salt in DMSO-d6 at 400 Mhz

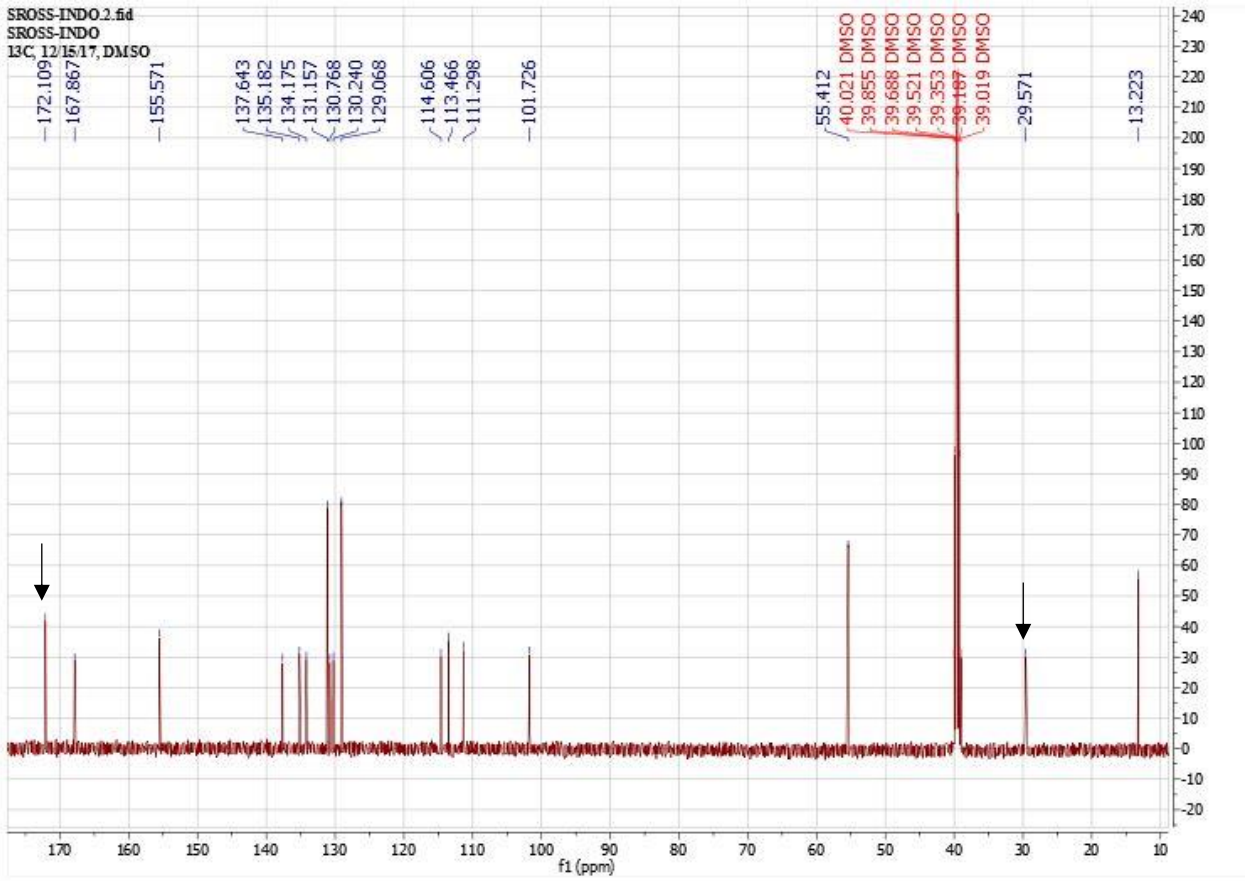

Figure 51 (A): ^{13}C- NMR spectroscopy of Pure Indomethacin in DMSO-d6

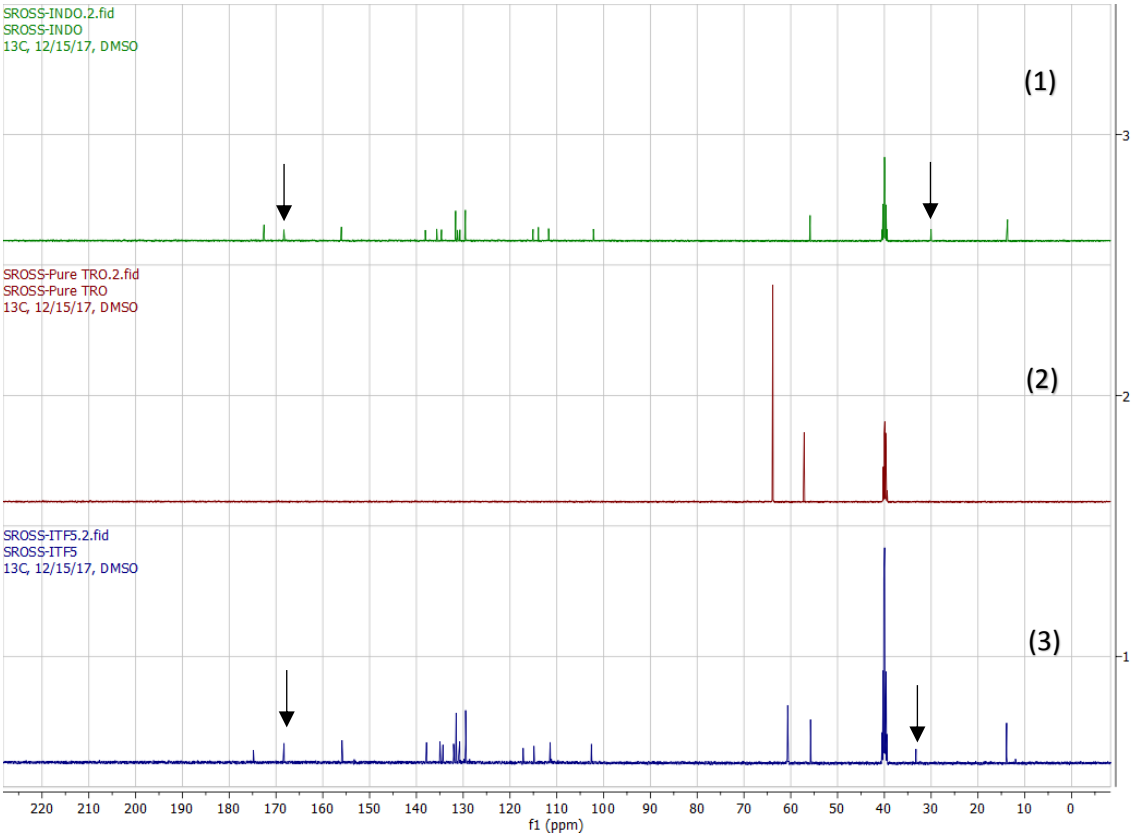

Figure 55 (B): ^{13}C- NMR spectroscopy(1) Pure Indo, (2) Pure Tro and (3) F-10 salt in DMSO-d6

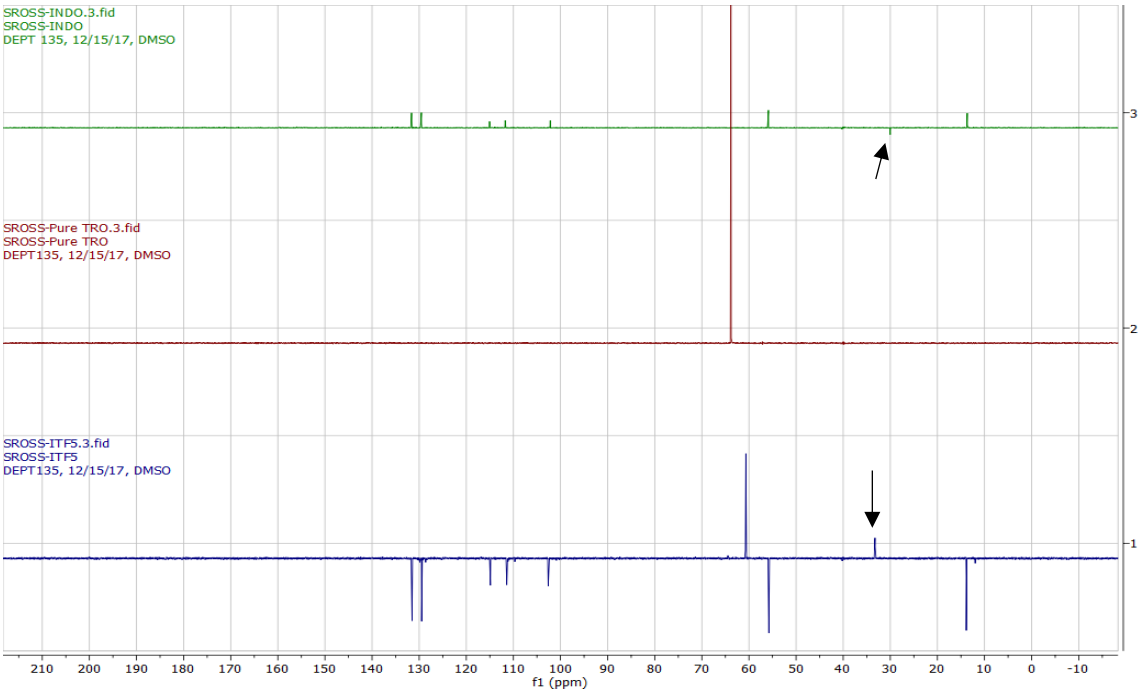

Figure 55 (C): 135 DEPT analysis of Pure Indomethacin, Pure Tromethamine and F-10 salt

4.6 FT-NIR study

Diffuse reflectance NIR spectra were continuously collected inline and non-invasively during hot-melt extrusion using a Fourier- Transform NIR spectrometer (Thermo Fisher Scientific, Antaris II near-IR analyzer) equipped with an InGaAs detector, a quartz halogen lamp, and a fibre-optic probe which was mounted in the extrusion die (Fig. 2). Spectra were collected every 16 s in the 9000–4500 cm^{-1} region with a resolution of 16 cm^{-1} and averaged over 8 scans. Data analysis was performed using the Result software (Version 3.0, Thermo Fisher Scientific) and TQ Analyst. Spectra collected in the diffuse reflectance mode mostly require spectral pre-treatment before analysis. The degree of scattering depends on the wavelength of the light and the refractive index of the sample, which causes a non-equal scatter over the whole spectrum. This can result in a baseline shift. Therefore, multiplicative signal correction (MSC) was used before chemometric analysis of the spectra. Using MSC, undesired scatter is removed from the raw spectra to prevent it from dominating over the chemical information within the spectra. The result of MSC pre-processing is that each corrected spectrum has the same offset and amplitude, eliminating the difference in light scatter in the spectra from the different samples, before developing the calibration model. Furthermore, second derivative pre-processing was done after MSC correction. Second derivatives of NIR spectra magnify differences in spectral features provide baseline normalization and remove data offsets due to scattering effects and pathlength variation (Saerens et al., 2012).

Figure 56 describes the FT-NIR spectra of pure indomethacin and pure tromethamine powders at room temperature. The peak at 6500 cm^{-1} is characteristic of the amine group of Tro and the peak at 5900 cm-1 is characteristic of the carboxylate group of Indo.

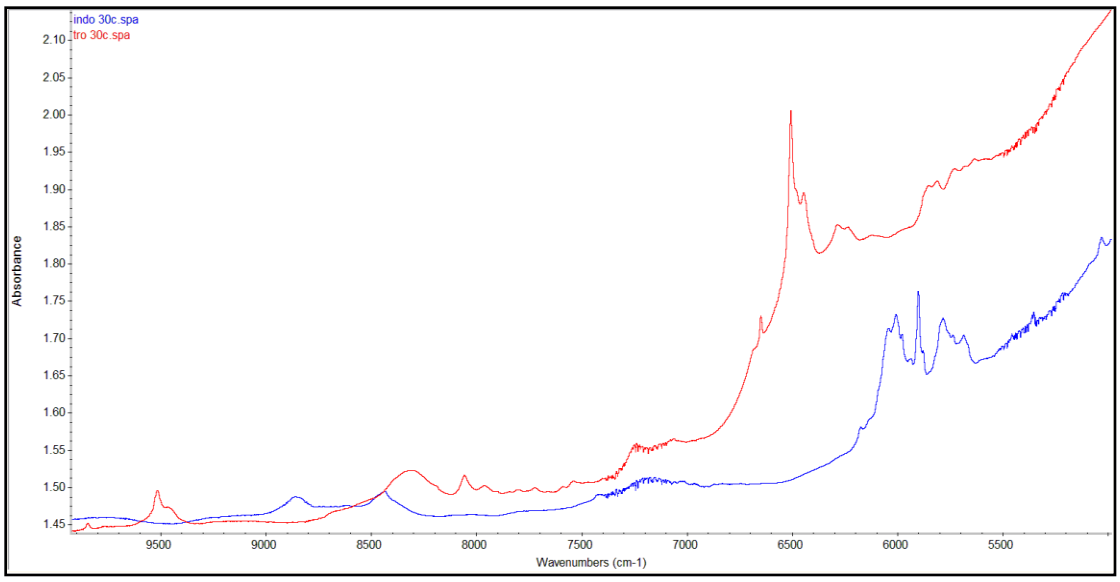

Figure 52: FT-NIR spectra of Indomethacin and tromethamine powders at room temperature

Figure 57 depicts the FT-NIR spectra of melting process of pure tromethamine. It can be noted that there is gradual increase in the intensity and sharp peak of amine group at 6500 cm^{-1}. Also there is gradual appearance of the –OH peak at 7000 cm^{-1} at the melting process proceeds, which might be due to breaking of intra-molecular H-bonding in the Tro salt and hence availability of –OH groups.

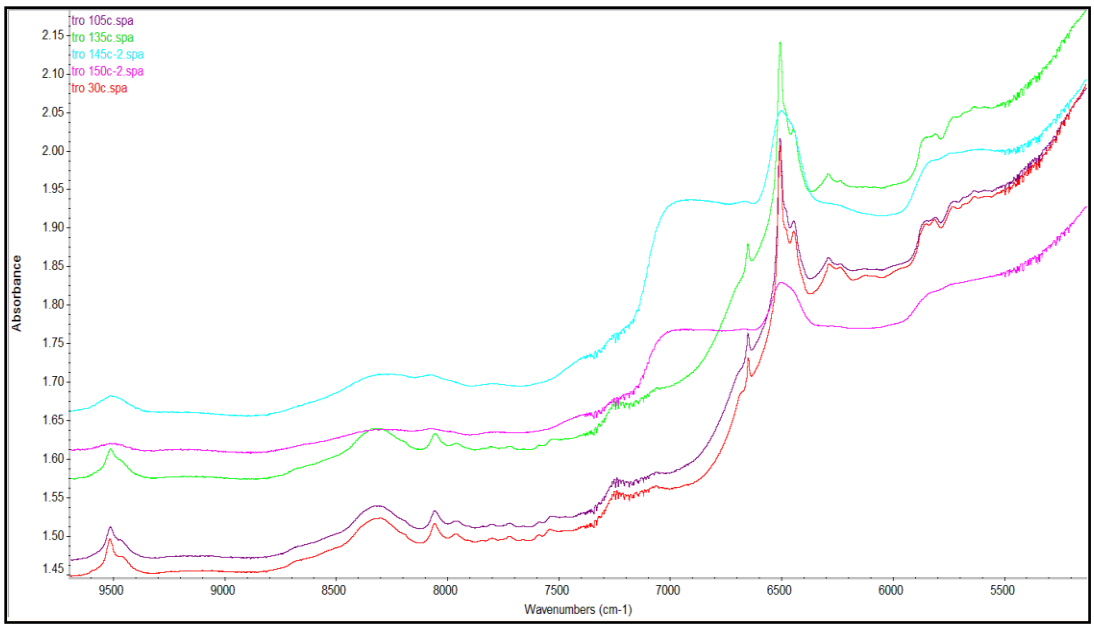

Figure 53: FT-NIR spectra of melting process of pure tromethamine

Figure 58 demonstrates the FT-NIR spectra of melting process of pure indomethacin. Here the peak corresponding to carboxylate group at 5900 cm^{-1} diminishes in size due to temporary amorphization in the melted state.

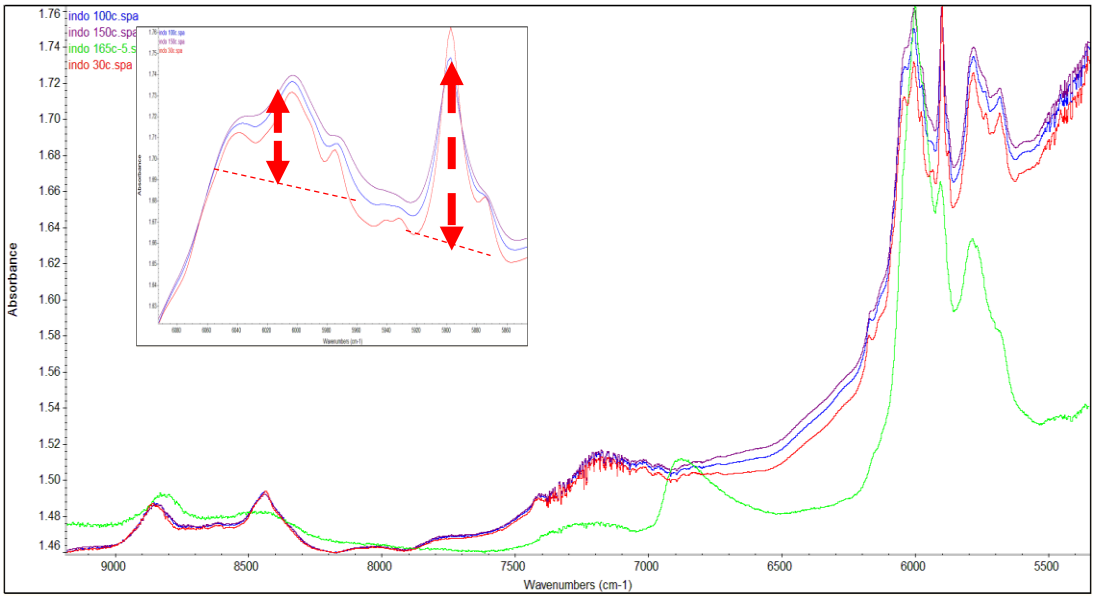

Figure 54: FT-NIR spectra of melting process of pure indomethacin

Figure 59 shows the overlay of the spectra of the melted forms of Indo and Tro respectively. Here it can be seen that the peaks of interest of Indo (5900cm^{-1}) and Tro (6500 cm^{-1}) can be selected for analyzing the salt formation as they do not overlap in the other spectra and hence characteristic to model interaction.

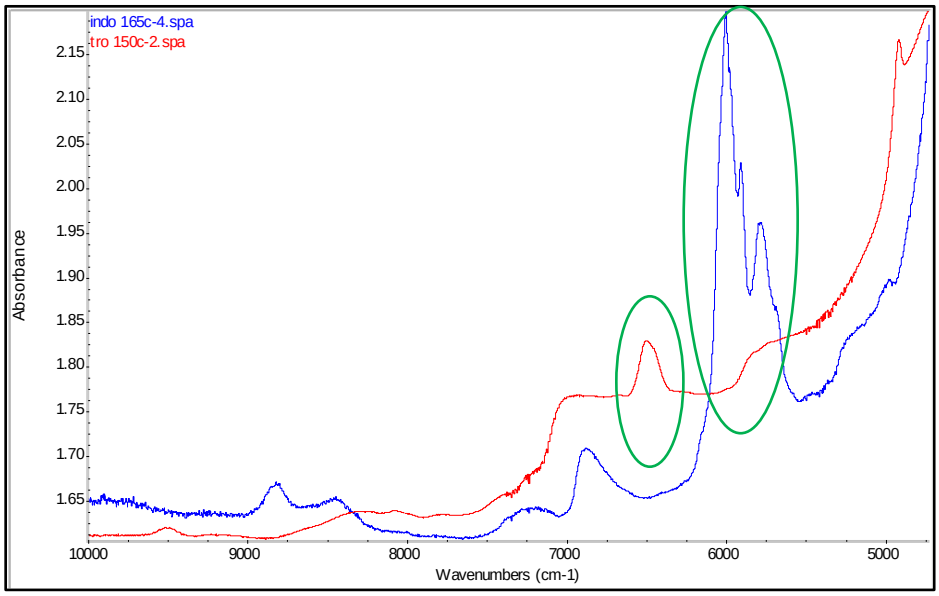

Figure 55: Comparison of Indomethacin and tromethamine hot-melts

Figure 60 shows the real time in-line data collected from the Antaris II probe. At 135^{o}C, the hot melt has opaque salt form of particles. The scattering from solid particles generated strong reflectance signal (low spectral baseline) and short penetration distance (low peak height). The hot melt became clear liquid at 145^{o}C and above, and the large baseline drift was the result of weak reflection signal.

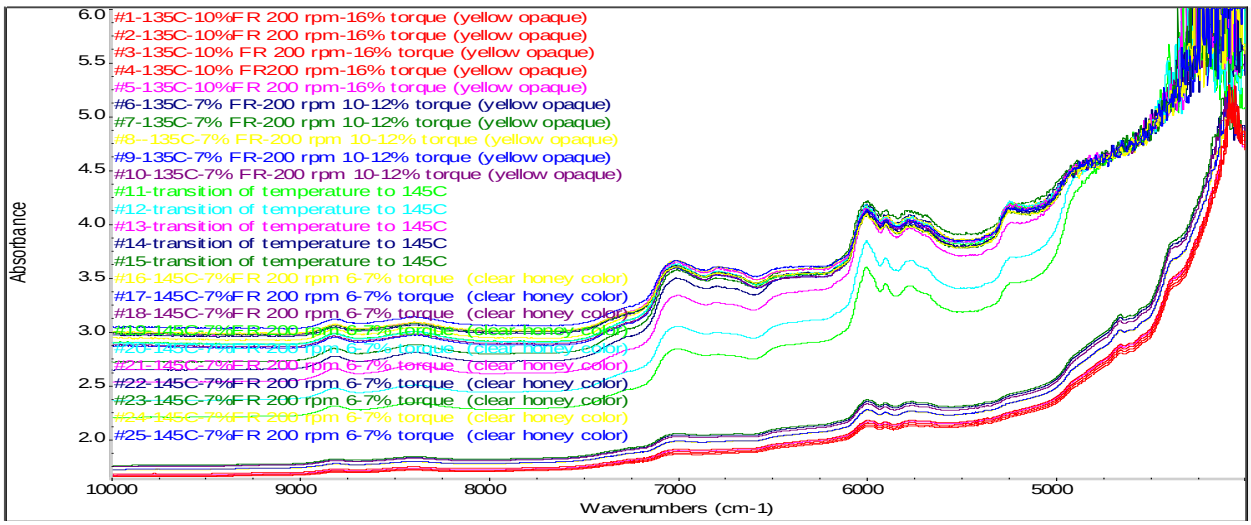

Figure 56: Absorption FT-NIR spectra collected during experiment of 1:1 Indomethacin:Tromethamine

In Figure 61, the spectral peak area at 5900 cm-1 was used for the penetration distance or pathlength correction. Since this peak is mainly the response from Indomethacin, the normalized spectra will more relate to per unit weight of Indomethacin.

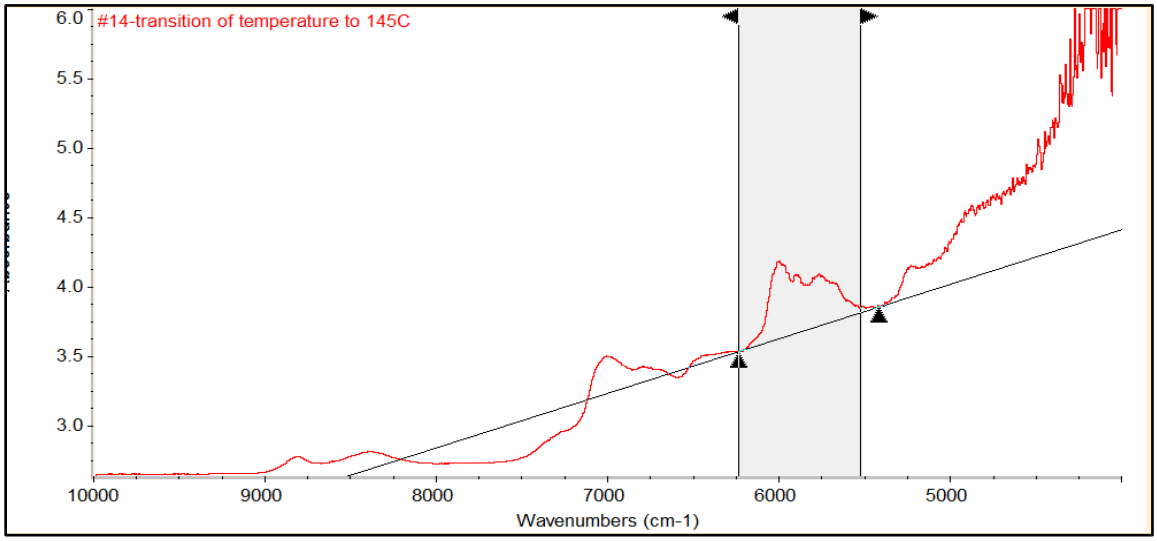

Figure 57: Spectral pathlength normalization

Figure 62 After application of Norris derivative to the spectral region of interest, the spectral variation in the intensity of the amine peak and the carboxylate group could be monitored. A statistical model is required to measure the difference in intensity of this signal.

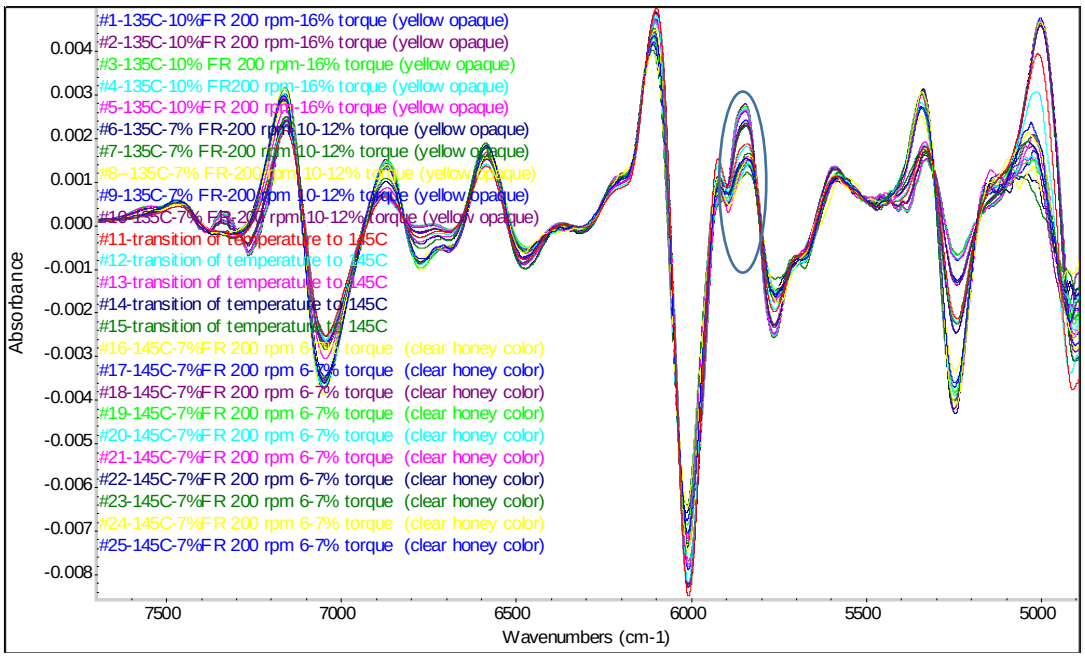

Figure 58: Second Norris derivative of complete FT-NIR spectra

Figure 63 depicts the calibration of the Partial Least Square (PLS) model used to determine the correlation between the % crystalline salt formation and peak intensity from 6100 cm^{-1} to 5800 cm^{-1}. The lesser intensity of carboxylate peak at lower temperature (135°C) implied greater crystalline salt formation reaction compared to higher temperature extrudates (145°C and above) where the interaction resulted in amorphous salt formation. From the calibration we could achieve a co-relation of greater than 95%. The crystalline salts achieved from F-1, F-2, F-4 and F-10 were analyzed and the % crystallinity mentioned in Table 10. F-10 was the formulation with greatest crystalline salt formation.

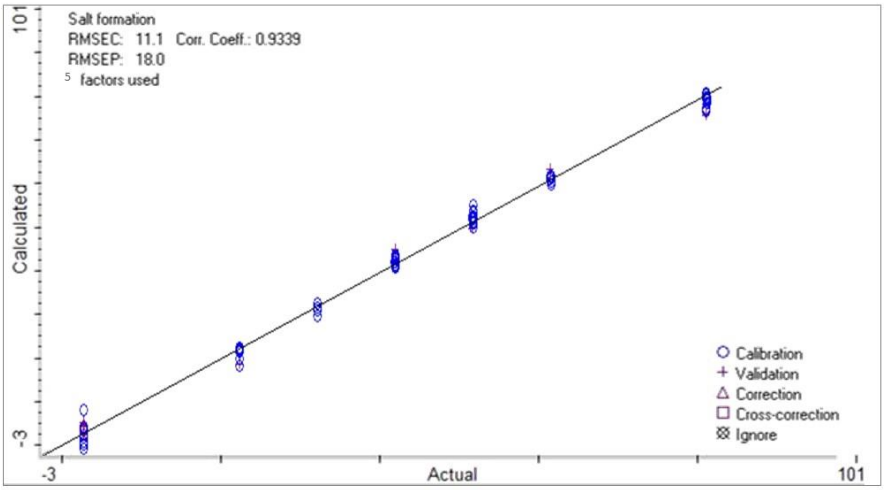

Figure 59: Calibration of the peak intensity from 6100 cm^{-1}- 5800 cm^{-1}

Formulation	Temperature (°C)	Screw speed (rpm)	Crystalline salt (%)	Feed rate (g/min)	Screw configuration
F-1	135	200	75.8	3.2	1
F-2	135	200	80.5	1.6	1
F-3	145	200	-	1.6	1
F-4	135	100	50.1	1.6	1
F-5	135	100	-	3.2	1
F-6	145	100	-	1.6	1
F-7	145	100	-	3.2	1
F-8	155	100	-	1.6	1
F-9	155	100	-	3.2	1
F-10	135	100	98.5	3.2	2

Table 10: % Crystalline salt formation of Indomethacin and Tromethamine at different extrusion conditions

5. Conclusion

Salt formation of a poorly water soluble compound was successfully achieved using hot-melt extrusion. The product characteristics were evaluated using in-line FT-NIR and other solid state characterization tools to better understand the influence of processing parameters. The extrusion condition of feed rate 3.2g/min, 100 rpm, 135 °C screw configuration 2 resulted in highest crystalline salt formation of 98.5% crystallinity. The extrusion at 145 °C and above resulted in amorphization of the API and resulting salt formulation. It could be concluded that temperature and shear stress were the two significant parameters to affect the product quality. At higher temperature and shear stress (by increasing kneading blocks in screw configuration and screw speed) resulted in breakdown of the possible crystalline nature of the salt. In-line FT-NIR was successfully applied as a PAT tool to detect the optimal processing conditions for salt formation using hot-melt extrusion process.

BIBLIOGRAPHY

Aakeröy, C. B., Fasulo, M. E., & Desper, J. (2007). Cocrystal or salt: does it really matter? *Molecular Pharmaceutics, 4*(3), 317-322.

Bahloul, B., Lassoued, M. A., & Sfar, S. (2014). A novel approach for the development and optimization of self emulsifying drug delivery system using HLB and response surface methodology: application to fenofibrate encapsulation. *International journal of pharmaceutics, 466*(1), 341-348.

Balakrishnan, P., Lee, B.-J., Oh, D. H., Kim, J. O., Hong, M. J., Jee, J.-P., . . . Yong, C. S. (2009). Enhanced oral bioavailability of dexibuprofen by a novel solid self-emulsifying drug delivery system (SEDDS). *European Journal of Pharmaceutics and Biopharmaceutics, 72*(3), 539-545.

Bari, H. C., Doijad, R. C., More, H. N., & Disouza, J. I. (2011). Design and optimization of chlordiazepoxide solid self-microemulsifying drug delivery system. *J Pharm Res, 4*(2), 369-372.

Berge, S. M., Bighley, L. D., & Monkhouse, D. C. (1977). Pharmaceutical salts. *Journal of pharmaceutical sciences, 66*(1), 1-19.

Bika, D., Tardos, G., Panmai, S., Farber, L., & Michaels, J. (2005). Strength and morphology of solid bridges in dry granules of pharmaceutical powders. *Powder Technology, 150*(2), 104-116.

Coates, J. (2000). Interpretation of infrared spectra, a practical approach. *Encyclopedia of analytical chemistry*.

Cole, E. T., Cadé, D., & Benameur, H. (2008). Challenges and opportunities in the encapsulation of liquid and semi-solid formulations into capsules for oral administration. *Advanced drug delivery reviews, 60*(6), 747-756.

Dixit, R. P., & Nagarsenker, M. (2010). Optimized microemulsions and solid microemulsion systems of simvastatin: characterization and in vivo evaluation. *Journal of pharmaceutical sciences, 99*(12), 4892-4902.

Gumaste, S. G., Pawlak, S. A., Dalrymple, D. M., Nider, C. J., Trombetta, L. D., & Serajuddin, A. T. (2013). Development of solid SEDDS, IV: effect of adsorbed lipid and surfactant on

tableting properties and surface structures of different silicates. *Pharmaceutical research, 30*(12), 3170-3185.

Gupta, V., Hwang, B. H., Doshi, N., & Mitragotri, S. (2013). A permeation enhancer for increasing transport of therapeutic macromolecules across the intestine. *Journal of controlled release, 172*(2), 541-549.

Kim, D. W., Kang, J. H., Oh, D. H., Yong, C. S., & Choi, H.-G. (2012). Development of novel flurbiprofen-loaded solid self-microemulsifying drug delivery system using gelatin as solid carrier. *Journal of microencapsulation, 29*(4), 323-330.

Kocbek, P., Baumgartner, S., & Kristl, J. (2006). Preparation and evaluation of nanosuspensions for enhancing the dissolution of poorly soluble drugs. *International journal of pharmaceutics, 312*(1), 179-186.

Lee, H. L., Vasoya, J. M., Cirqueira, M. d. L., Yeh, K. L., Lee, T., & Serajuddin, A. T. (2017). Continuous Preparation of 1: 1 Haloperidol–Maleic Acid Salt by a Novel Solvent-Free Method Using a Twin Screw Melt Extruder. *Molecular Pharmaceutics, 14*(4), 1278-1291.

Mu, B., & Thompson, M. (2012). Examining the mechanics of granulation with a hot melt binder in a twin-screw extruder. *Chemical engineering science, 81*, 46-56.

Nie, H., Xu, W., Ren, J., Taylor, L. S., Marsac, P. J., John, C. T., & Byrn, S. R. (2016). Impact of metallic stearates on disproportionation of hydrochloride salts of weak bases in solid-state formulations. *Molecular Pharmaceutics, 13*(10), 3541-3552.

Nováková, L., Matysová, L., Havlíková, L., & Solich, P. (2005). Development and validation of HPLC method for determination of indomethacin and its two degradation products in topical gel. *Journal of pharmaceutical and biomedical analysis, 37*(5), 899-905.

Park, J.-B., Lee, B.-J., Kang, C.-Y., Tiwari, R. V., & Repka, M. A. (2017). Process analytical quality control of tailored drug release formulation prepared via hot-melt extrusion technology. *Journal of Drug Delivery Science and Technology, 38*, 51-58.

Patel, D. P., Li, P., & Serajuddin, A. T. (2016). Enhanced microemulsion formation in lipid-based drug delivery systems by combining mono-esters of mediumchain fatty acids with di-or tri-esters. *Journal of Excipients and Food Chemicals, 3*(2).

Patil, H., Tiwari, R. V., Upadhye, S. B., Vladyka, R. S., & Repka, M. A. (2015). Formulation and development of pH-independent/dependent sustained release matrix tablets of ondansetron HCl by a continuous twin-screw melt granulation process. *International journal of pharmaceutics, 496*(1), 33-41.

Pudipeddi, M., Serajuddin, A., Grant, D., & Stahl, P. (2002). Solubility and dissolution of weak acids, bases, and salts. *Handbook of Pharmaceutical Salts, Properties, Selection, and Use. Zurich, Switzerland: Verlag Helvetica Chimica Acta and Weinheim, Wiley-VCH, Weinheim, Federal Republic of Germany: Wiley-VCH*, 19-39.

Pudlas, M., Kyerematen, S. O., Williams, L. A., Kimber, J. A., van Lishaut, H., Kazarian, S. G., & Woehrle, G. H. (2015). Analyzing the impact of different excipients on drug release behavior in hot-melt extrusion formulations using FTIR spectroscopic imaging. *European Journal of Pharmaceutical Sciences, 67*, 21-31.

Qian, F., Huang, J., & Hussain, M. A. (2010). Drug–polymer solubility and miscibility: stability consideration and practical challenges in amorphous solid dispersion development. *Journal of pharmaceutical sciences, 99*(7), 2941-2947.

Qiao, N., Wang, K., Schlindwein, W., Davies, A., & Li, M. (2013). In situ monitoring of carbamazepine–nicotinamide cocrystal intrinsic dissolution behaviour. *European Journal of Pharmaceutics and Biopharmaceutics, 83*(3), 415-426.

Rajput, L. (2014). Stable crystalline salts of haloperidol: A highly water-soluble mesylate salt. *Crystal Growth & Design, 14*(10), 5196-5205.

Saerens, L., Dierickx, L., Quinten, T., Adriaensens, P., Carleer, R., Vervaet, C., . . . De Beer, T. (2012). In-line NIR spectroscopy for the understanding of polymer–drug interaction during pharmaceutical hot-melt extrusion. *European Journal of Pharmaceutics and Biopharmaceutics, 81*(1), 230-237.

Saxena, V., & Hussain, M. D. (2012). Poloxamer 407/TPGS mixed micelles for delivery of gambogic acid to breast and multidrug-resistant cancer. *International journal of nanomedicine, 7*, 713.

Schilling, S. U., & McGinity, J. W. (2010). Novel application of hot-melt extrusion for the preparation of monolithic matrices containing enteric-coated particles. *International journal of pharmaceutics, 400*(1), 24-31.

Schmolka, I. R. (1977). A review of block polymer surfactants. *Journal of the American Oil Chemists' Society, 54*(3), 110-116.

Serajuddin, A. T. (1999). Solid dispersion of poorly water□soluble drugs: Early promises, subsequent problems, and recent breakthroughs. *Journal of pharmaceutical sciences, 88*(10), 1058-1066.

Sha, X., Yan, G., Wu, Y., Li, J., & Fang, X. (2005). Effect of self-microemulsifying drug delivery systems containing Labrasol on tight junctions in Caco-2 cells. *European Journal of Pharmaceutical Sciences, 24*(5), 477-486.

Shah, A. V., & Serajuddin, A. T. (2012). Development of solid self-emulsifying drug delivery system (SEDDS) I: use of poloxamer 188 as both solidifying and emulsifying agent for lipids. *Pharmaceutical research, 29*(10), 2817-2832.

Stephenson, G. A., Aburub, A., & Woods, T. A. (2011). Physical stability of salts of weak bases in the solid□state. *Journal of pharmaceutical sciences, 100*(5), 1607-1617.

Thakral, S., & Suryanarayanan, R. (2015). Salt formation during freeze-drying-an approach to enhance indomethacin dissolution. *Pharmaceutical research, 32*(11), 3722-3731.

Vasanthavada, M., Wang, Y., Haefele, T., Lakshman, J. P., Mone, M., Tong, W., . . . Abu, T. (2011). Application of melt granulation technology using twin□screw extruder in development of high□dose modified□release tablet formulation. *Journal of pharmaceutical sciences, 100*(5), 1923-1934.

Wahl, P. R., Treffer, D., Mohr, S., Roblegg, E., Koscher, G., & Khinast, J. G. (2013). Inline monitoring and a PAT strategy for pharmaceutical hot melt extrusion. *International journal of pharmaceutics, 455*(1), 159-168.

VITA

Priyanka Thipsay

EDUCATION

Doctor of Philosophy (Ph.D.) Pharmaceutics Aug 2018
University of Mississippi (UM), GPA: 3.92/4.0
Dissertation: *Application of Design of Experiments (DOE) and Process Analytical Technology (PAT) towards Pharmaceutical extrusion processes.* (Advisor: Dr. Michael Repka)

M.S. Industrial Pharmacy Aug 2013
St. John's University, NY, GPA: 3.8/4.0
Thesis: *Ionic Liquid: A Novel Approach for Improving the Dissolution Rate of a Poorly Water Soluble Drug*.

Bachelor of Science (B.S.) in Pharmacy May 2010
University of Mumbai, India, GPA: 3.7/4.0

PROFESSIONAL EXPERIENCE

Patheon Pharmaceuticals, OH, USA Apr 2018-current
Sr. Scientist I (Pharmaceutics & Process Technology)

AbbVie Inc., Lake county, IL, USA May 2016- Aug 2016
Graduate Summer Intern (Manufacturing Science & Technology, Oral drug products)

Hands-on course in tablet technology at University of Mississippi Sept 2014 – Dec 2017
Lab instructor

AWARDS AND HONORS

Travelship for 11th World meeting Pharmaceutics, Biopharm., Pham. Technology, Spain Mar 2018
Texture Technologies® sponsored scholarship, AAPS 2017-AM Oct 2017
Dissertation fellowship, Dept. of Pharmaceutics, University of Mississippi Nov 2017
Manufacturing Science & Engineering section Travelship Award for best poster, AAPS Aug 2016
Amgen sponsored Graduate Student Travelship Award for best poster, AAPS Oct 2015
Best Graduate Poster Award, 4th place Society of Plastic Engineering (SPE) conference Mar 2015
Honor Member, Rho-Chi Society, University of Mississippi Jan 2015
Astra Zeneca sponsored Graduate Student Travelship Award for best poster, AAPS Nov 2014
Scholarship for "Excellence in Academics" by Pfizer (I) Ltd, Mumbai Sept 2006

LEADERSHIP

University of Mississippi (UM)-AAPS student chapter Sept 2014- Sept 2017
Chairperson

AAPS Annual meeting 2013, San Antonio Nov 2013
Co-moderator

St. John's University -AAPS student chapter Sept 2010-Aug 2011
Treasurer

PROFESSIONAL PRESENTATIONS

- P.Thipsay, M.A.Repka; Effect of different HPMC grades and process parameters on physico-chemical properties of sustained release matrix granules prepared via twin screw melt granulation Nov 2017
- R. Lalge, P.Thipsay, M.A. Repka et.al. Cefuroxime Axetil Gastroretentive Floating Drug Delivery System Prepared by Hot-Melt Extrusion for Improved bioavailability Nov 2017
- P.Thipsay, M.A. Repka et al. "Formulation, evaluation and optimization of biodegradable polymeric implants prepared by hot-melt extrusion process" AAPS annual conference Oct 2015
- P.Thipsay, M.A. Repka et al. "Formulation of solid self-microemulsions using hot melt extrusion technology" at SPE annual technical conference, Orlando Mar 2015
- P.Thipsay, M.A. Repka et al. " Bioadhesive drug delivery system for enhancing bioavailability of BCS class III drug by hot-melt extrusion technology" at AAPS annual conference, Orlando Oct 2015
- P.Thipsay, M.A. Repka et al. " Hot melt extrusion technology for the formulation of Solid SMEDDS" at AAPS annual conference, San Diego Nov 2014
- P.Thipsay, E. Squillante et al. "Formulation of Ionic liquid to improve dissolution rate" at AAPS annual conference, San Antonio Nov 2013

PUBLICATIONS

- A. Bhagurkar, P. Thipsay, M.A. Repka; Effects of formulation composition on the characteristics of mucoadhesive films prepared by hot-melt extrusion technology, Journal of Pharmacy and Pharmacology, Nov 2018
- M. Bookwala, P.Thipsay, M.A.Repka; Preparation of a Crystalline Salt of Indomethacin and Tromethamine by Hot Melt Extrusion Technology, Eur. J. of Pharmaceutics and Biopharmaceutics, Aug 2018
- N. Mendonsa, P. Thipsay, M.A. Repka; Bioadhesive Drug Delivery System for Enhancing the Permeability of a BCS Class III Drug via Hot-Melt Extrusion Technology, AAPS Pharm Sci Tech Feb 2017
- A. Gandhi, B. Kirthivasan, P.Thipsay, E. Squillante; Adsorption on mesoporous silica using supercritical fluid technology improves dissolution rate of Carbamazepine: A poorly soluble compound, AAPS Pharm Sci Tech, Aug 2017.